GEORGIA DOT RESEARCH PROJECT 16-39

FINAL REPORT

EVALUATING THE PERFORMANCE OF GEORGIA'S CRCPS USING GROUND PENETRATING RADAR (GPR)

OFFICE OF PERFORMANCE-BASED MANAGEMENT AND RESEARCH
15 KENNEDY DRIVE
FOREST PARK, GA 30297-2534

TECHNICAL REPORT STANDARD TITLE PAGE

1. Report No.: FHWA-GA-1639	2. Government Accession No.:	3. Recipient's Catalog No.:
4. Title and Subtitle: Evaluating the Performance of Georgia's CRCPs Using Ground Penetrating Radar (GPR)		5. Report Date: September 2018
		6. Performing Organization Code:
7. Author(s): Stephan A. Durham, Ph.D., P.E., Mi G. Chorzepa, Ph.D., P.E., S. Sonny Kim, Ph.D., P.E., and Nazik Citir		8. Performing Organization Report No.:
9. Performing Organization Name and Address: University of Georgia College of Engineering Driftmier Engineering Center, Athens, GA 30602 Phone: (706) 542-9480 Email: sdurham@uga.edu		10. Work Unit No.:
		11. Contract or Grant No.: PI#0015304
12. Sponsoring Agency Name and Address: Georgia Department of Transportation Office of Performance-Based Management and Research 15 Kennedy Drive Forest Park, GA 30297-2534		13. Type of Report and Period Covered: Final; December 2016 –September 2018
		14. Sponsoring Agency Code:
15. Supplementary Notes: Prepared in cooperation with the U.S. Department of Transportation, Federal Highway Administration.		

16. Abstract:
In an effort to provide reliable decisions regarding highway pavements, condition assessment is often conducted to evaluate pavement performance. For Continuously Reinforced Concrete Pavements (CRCP) evaluated in this study, pavement distress is classified as having transverse and longitudinal cracks and/or punchouts. This report evaluated the influence of reinforcement placement and concrete cover on distresses through the use of non-destructive testing methods that included Ground Penetrating Radar (GPR) and eddy current technology. In addition, this research evaluated whether an eddy current technology could be used in the absence of a cored sample for the calibration process of GPR in the field. Ultimately, information on pavement distress type and severity, reinforcement location, and cover depth was collected for six CRCP sites on major interstates in Georgia. This study confirmed that the location and depth of reinforcements affect the performance of CRCPs in terms of cluster cracking and punchouts.

17. Keywords: Continuously Reinforced Concrete Pavement, Ground Penetration Radar, Eddy Current Technique, Condition Assessment	18. Distribution Statement:		
19. Security Classification (of this report): Unclassified	20. Security Classification (of this page): Unclassified	21. No. of Pages: 158	22. Price:

Form DOT 1700.7 (8-69)

GDOT Research Project No. 16-39

EVALUATING THE PERFORMANCE OF GEORGIA'S CRCPS USING GROUND PENETRATING RADAR (GPR)

Final Report

By

Stephan A. Durham, Ph.D., P.E.
Associate Professor of Civil Engineering

Mi G. Chorzepa, Ph.D., P.E.
Associate Professor of Civil Engineering

S. Sonny Kim, Ph.D., P.E.
Associate Professor of Civil Engineering

Nazik Citir
Graduate Student

University of Georgia
College of Engineering

Contract with

Georgia Department of Transportation

In cooperation with

U.S. Department of Transportation
Federal Highway Administration

September 2018

TABLE OF CONTENTS

LIST OF TABLES

LIST OF FIGURES

Figure Page

EXECUTIVE SUMMARY

This study evaluated distress levels for Continuously Reinforced Concrete Pavements (CRCP) throughout Georgia. Specifically, pavement distress including transverse and longitudinal cracks and punchouts was investigated in this research. There are many contributing factors affecting these types of structural distresses such as pavement design, load, temperature, pavement materials, and construction. The primary objective of this research study is to evaluate CRCPs throughout the state of Georgia to identify common characteristics between CRCPs having a long history of good performance, and those with repetitive significant distresses such as punchout. To accomplish this objective, an analysis was performed relating influences of longitudinal reinforcement placement, concrete cover, and pavement thickness with the severity of distresses found on Georgia's CRCP interstates and highways. This study evaluated the influence of reinforcement placement and concrete cover on distresses through the use of non-destructive testing methods that included Ground Penetrating Radar (GPR) and eddy current technology. In addition, this research evaluated whether eddy current technology could be used in the absence of a cored sample for calibrating the GPR unit in the field. Ultimately, six site investigations on Interstate 20, Interstate 75, and State Route 6 in Georgia were performed by collecting data that included documentation of pavement distress type and severity, reinforcement location, and cover depth. This study confirmed that the location and depth of reinforcement affects the performance of CRCPs in terms of cluster cracking and punchouts. Results from this study indicate that the lower the placement of the transverse and longitudinal reinforcements within the pavement cross-section, the more transverse cracks occur. Ultimately, reinforcement placed lower within the pavement cross-section results in wider crack widths and presents the potential for water intrusion and steel reinforcement corrosion. Based on these

findings, if the reinforcement is placed close to mid-depth of the pavement thickness or deeper, pavement distresses increase. Therefore, this study recommends placing longitudinal reinforcement at the top-third of the total concrete thickness, rather than within a specified range of 3.50-4.25in (89-108mm), because reinforcement could be located outside the top third for thinner pavement slabs. Findings also revealed that increased transverse cracking occurred when the transverse reinforcing steel was spaced less than 3.5ft (1.1m) apart.

Condition assessment is often conducted to evaluate pavement performance in order to make informed decisions regarding the repair or replacement of highway pavements. This assessment can be performed using destructive or non-destructive methods, with this study investigating the use of the latter in the field investigation of CRCP. GPR is an effective technology for measuring the concrete cover depth in the field. While field calibration is necessary with known concrete cover depth, calibration of the GPR unit can be performed through measurement of cored specimens or by employing eddy current technology (i.e., cover meter). This research study found eddy current technology to be a practicable technique for easily calibrating the GPR unit in the field. The technology gives estimated cover depth values close to cored specimens. However, the accuracy of the technology decreases as the concrete cover depth increases. Based on the field test results and analysis, eddy current technology is preferred when the concrete cover depth is not deep and where spacing between reinforcements is not small.

The GPR system and procedure were primarily used in this study to determine depth and alignment of reinforcement in pavements. GPR scans were used to identify defects (e.g., weak bonds and/or voids between pavement layers) beneath the pavement layer and within the pavement layers, and to determine the density of concrete/asphalt layers and material properties.

Conducting GPR scans in conjunction with a rebar cover meter (e.g., Profometer) has the advantage of being rapid, efficient, and cost-effective compared to conducting corings to assess existing pavement conditions. Continuous monitoring of the pavement performance is recommended to better understand the causes of distresses and crack development on the CRCP.

ACKNOWLEDGEMENTS

The University of Georgia would like to acknowledge the financial support for this work provided by the Georgia Department of Transportation. The authors would like to thank the many GDOT personnel who assisted with this study. A special thanks to Mr. David Jared, P.E., Mr. Binh Bui, Mr. Peter Wu, Ph.D., P.E., Mr. Gary Wood, Mr. Ian Rish, P.E., Mr. JT Rabun, and Ms. Supriya Kamatkar for their research support and valuable input. Special thanks also to Mr. Brennan Roney, who advised the research team in successfully performing the study and assisted with the coordination of the field site visits and testing. Additionally, the authors would like to thank Dennis Kehres from Proceq Inc. for his assistance with training for the eddy current technology device.

1. INTRODUCTION

1.1 Overview

Forensic investigations of pavement failures are needed to diagnose the major causal effects that result in pavement distress. The primary concern in the operation and maintenance of pavement is cracking as a result of structural and functional failures. Cracks form because of inadequacies in the pavement properties or from the design and construction of pavement.

Although the specifications, equipment, and construction processes have improved in recent years, variables still exist that may impact the long-term durability of constructed pavements. These variables result from "the low bid process, lack of experienced inspectors and project managers, poor selection of construction materials, lack of knowledge of the existing pavement conditions, unfamiliar construction methods and procedure and other issues unforeseen during design and construction phases" (Chen and Scullion 2008).

This report examines the existing and potential distresses in Continuously Reinforced Concrete Pavement (CRCP) sections in Georgia. The causes of distress include, but are not limited to: poor construction practices involving concrete placement, traffic loading, environment or climate influences, and materials. Additionally, this study diagnosed inconsistencies in longitudinal reinforcement placement in the evaluated CRCP sections. Specifically, this study investigated the variation in longitudinal and transverse reinforcement placement height by mobilizing a Ground Penetrating Radar (GPR) unit over areas of cluster cracking, severe punchout, and patching to identify the cause of serious and repeated distress. Finally, a recommended GDT non-destructive test method for the utilization of GPR for CRCPs has been developed as a result of this study.

1.2 Study Objectives

The objective of this study was to evaluate CRCPs throughout the state of Georgia to identify common characteristics between CRCPs having good performance with a long history and those with repetitive significant distresses such as punchouts and excessive transverse and longitudinal cracking. Specifically, the following primary tasks were accomplished through the completion of this study:

1. Determine the influence of reinforcement placement and concrete cover on the punchout of CRCPs.
2. Identify and discuss the factors that affect the location and extent of distresses and punchouts.
3. Investigate the effect pavement profile has on the CRCP performance (if any).
4. Evaluate whether eddy current technology can be used in the absence of a cored sample for the calibration process of GPR in the field.
5. Create a standard procedure for the evaluation of pavements utilizing GPR technology.

Non-destructive test methods (NDTs), GPR, and eddy current technique (Profometer 600), were selected for this study to investigate the existing conditions and determine reinforcement placement at distressed and patched CRCP locations on Georgia highways.

1.3 Project Scope

A review of previous research involving the forensic investigation of CRCPs in Georgia is included in Chapter 2. Furthermore, a literature summary of work related to CRCPs and the utilization of GPR and Profometer as the non-destructive testing methods for pavement investigations is provided in Chapter 3. The literature review includes discussion on the design,

construction, and performance of CRCPs, as well as common distresses found in this pavement type. In addition, a description of the development and utilization of GPR technology is provided. Chapter 4 details the significance and benefit of this study, in addition to the overall goals of the project. Chapter 5 details the experimental work plan for this research study. Chapter 6 presents the experimental results obtained from the site investigations and post-processing. Chapter 7 provides the research conclusions, along with recommendations for future studies.

2. BACKGROUND

2.1 CRCP History in Georgia

Built in 1967, Interstate 75 (I-75) consisted of 13.0mi (20.9km) of State Route 42 (SR-42) between Forsyth and Macon, GA, which became the southbound lanes of I-75. In 1971, the first CRCP overlay in Georgia was designed and built on top of the existing State Route 42 (SR-42) jointed concrete pavement. The thickness of this CRCP overlay was 8.00in (203mm) throughout 10.0mi (16.1 km) and 7.00in (178mm) throughout the remaining miles of the project. For 8.00in (203mm) and 7.00in (178mm) thick sections, #5 reinforcing bars spaced 6.00in (152mm) apart were used on center with 0.6 and 0.7 percent steel, respectively. In 1989, GDOT built four new lanes in each direction on I-75 -- two northbound and two southbound lanes -- to reinforce it against heavy traffic load. The two new southbound lanes were designed with 8.00in (203mm) -thick full-depth CRCP, with #6 longitudinal and #4 transverse reinforcing bars spaced 6.00in (152mm) on-center. Between 1990 and 2002, the vehicular load increased by 64% for traffic on I-75 in Forsyth, GA. After 2001, GDOT stated that the three lanes of I-75 needed rehabilitation, and the outside lane of I-75 needed to be replaced since it showed transverse cracking (CRSI 2003).

Gulden (1980) evaluated the conditions of the six CRCP sections on Interstate 95 (I-95). The I-95-1 (32) section is 12.6mi (20.3km) in length, running from US-17 in Bryan County to Interstate 16 (I-16) in Chatham County. The pavement structure has an 8.50in (216mm) continuous reinforced concrete (CRC) slab with a 6.00in (152mm) soil-cement base. The majority of the project was in good condition and included some cluster cracking and wide cracks with spalling. The northbound lane (NBL) between MP 94 and MP 96 had three punchouts due to poor base or subgrade support. These locations had been patched. Another

distressed area located at the MP 91 southbound lane (SBL) had a longitudinal crack about 40.0ft (12.2m) in length, which was located approximately 3.0ft (0.9m) from the centerline. This distress indicated that the pavement had subsided in this area. The average crack spacing was determined as a range from 6.3-9.8ft (1.9-3.0m), with a great amount of cluster cracking and Y cracking.

One project, I-95-1 (27), was conducted on the 10.5mi (16.8km) length section located from the end of the asphalt section north of SR-38 south to US-17. The pavement structure has 9.00in (229mm) of CRC with a 6.00in (152mm) base including 1.00in (25mm) of asphaltic-concrete and 5.00in (127mm) of soil-cement. The project was in excellent condition, with a few tight cracks. The average crack spacing ranged from 2.8-6.1ft (0.9-1.9m) in the NBL and from 4.2-9.2ft (1.3-2.8m) in the SBL.

The I-95-1 (36) section runs between US-17 at South Newport River and SR-99 near Eulonia with a 9.1mi (14.6km) length. The pavement structure has 8.50in (216mm) of CRC with a 6.00in (152mm) soil-cement base. The project was in good condition. Since this section is located in a marsh area, most problems resulted from settlement and poor concrete quality. Longitudinal cracking, which could lead to significant problems in the future, was detected between MP 58 and MP 59 in the NBL. In addition, two punchouts were observed in the inside wheel path of the outside lane at MP 58 SBL. The average crack spacing ranged from 4.4-7.1ft (1.3-2.2m) in the NBL and from 4.8-8.6ft (1.5-2.6m) in the SBL.

Another project, I-95-1 (41) Glynn-McIntosh section, is located from SR-251 near Darien to US-25 close to Brunswick, with a distance of 13.3mi (21.4km). The pavement structure has 9.00in (229mm) of CRC and a 6.00in (152mm) soil-cement base with a 3.00in (76mm) asphaltic-concrete drainage layer under shoulder at the base pavement interface. The

project was in good condition with the major problems being longitudinal cracking. The average crack spacing ranged from 3.8-6.1ft (1.2-1.9m) except for one section with 8.2ft. (2.5m) crack spacing.

I-95-1 (29) Camden from SR-40 near Kingsland to the Satilla River Bridge near Woodbine with 10.6mi (17.1km)-length has a tined texture, which was in excellent condition. The average crack spacing ranged from 5.3-8.9ft (1.6-2.7m). The last project, I-95-1 (38) Camden, is 4.1mi (6.6km) from SR-40 near Kingsland to the Florida-Georgia State Line. The project was in excellent condition with a few cluster cracks. The average crack spacing ranged from 7.2-10.1ft (2.2-3.1m).

Based on the recommendations in Gulden's study, the existing cracks should not necessarily be used for the boundary of the patch when patching punchouts. The boundaries of the patch should be determined by considering the location of distress caused by a loss of support, such as an edge punchout. Generally, the poor support extends beyond the boundaries of the punchout. Thus, NCHRP Report 60 "Failure and Repair of Continuous Reinforced Concrete Pavement" includes the suggested practices for the repair of CRCP (Gulden 1980).

In 2006, State Route 6 was reconstructed with CRCP as a major pavement type. The rebuilt section has two lanes each in each direction consisting of 12.00in (305mm) CRCP throughout the 6.2mi (9.7km). In 2007, other CRCP projects were undertaken, including three sections of I-20, four sections of I-75, four sections of I-85, and at least two projects on I-95 (CMC 2007). Based on a book that published an overview of Georgia's pavement history, information on the original construction of each of the Interstates in Georgia (GGfGA Engineering 2016) was found for use in this study. CRCP placed in 1974 on I-75 Cobb County was presented in Figure 1 by a photo in the 1990s. In addition, CRCP was placed on I-95 in

Georgia; however, settlement from hydraulic fills on the coast was observed. Therefore, the pavers simultaneously had to feed the steel reinforcements, which caused a shorter than normal service life for some of the CRCP sections during testing. Around 2000, GDOT began to carry out maintenance on portland cement concrete (PCC) for both concrete pavement rehabilitation (CPR) of the inside lane, and full lane replacement of the outside lane.

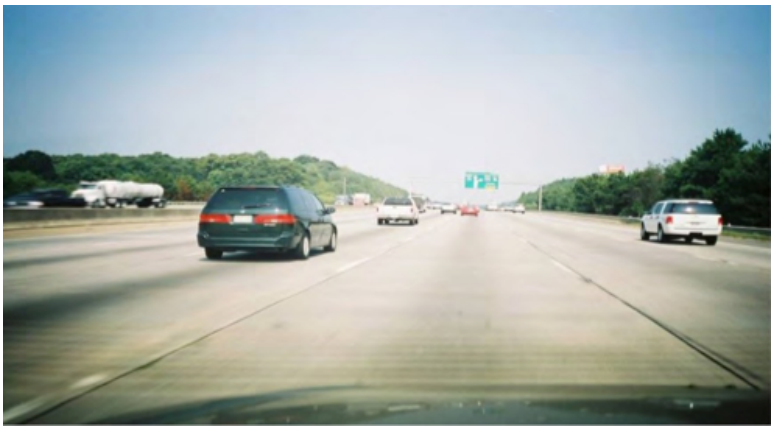

Figure 1 - I-75 Cobb County (CRCP) in 1974 (GGfGA Engineering 2016)

Approximately 100 lane miles (161 lane kilometers) of full lane were replaced on I-20, I-75, and I-85. Along with the use of CRCP again, the pavements on I-75 in Cook, Tift, Crisp, and Dooly Counties below Macon were replaced with Jointed Plain Concrete Pavement (JPCP). In order to provide a proper method for maintenance of traffic, the traffic was first diverted to one side of the interstate. After the construction of the pavement, the traffic was switched to be able to construct the new pavement. Georgia preferred the use of 13.0ft (4.0m) outside lanes instead of 14.0ft (4.3m) lanes, since pavement with 14.0ft (4.3m) lanes in other states had developed longitudinal cracks.

The 1972 AASHTO Pavement Design Guide is currently the governing document for pavement design (GGfGA Engineering 2016). GDOT is currently in the implementation stage of the most recent pavement software -- AASHTO Pavement ME -- which utilizes the new

Mechanistic-Empirical Pavement Design Guide. This software required local calibration because due to concerns that the asphalt pavement was too conservative in the estimation of depth. One of the problems with the existing software is that it provides consistent PCC thicknesses that are unrealistic for interstates. For this reason, GDOT has been limiting PCC thicknesses of up to 12.00in (305mm) since 2000. Therefore, current typical GDOT Interstate pavement design for rigid pavements includes 11.00in (279mm) or 12.00in (305mm) thickness for CRCP with a 3.00in (76mm) hot-mix asphalt (HMA) interlayer used as a separator between Graded Aggregate Base (GAB) and PCC.

Based on the original typical sections for the 15 Interstate sections in Georgia, some information about pavement was obtained from various sources and projects in the 1990s. The typical CRCP sections and their locations were listed as the following (GGfGA Engineering 2016);

1. I-20-1(21)24 710140
    - 1975 in Douglas County
    - 9.00in (229mm) CRCP, 1.00in (25mm) HMA, 5.00in (127mm) GABCS, 6.00in (152mm) Aggregate Stabilized Soil
    - From MP 23 to MP 35
2. I-75 -3(35)280 710003
    - 1974 in Cobb County
    - 9.00in (229mm) CRCP, 1.00in (25mm) 'H' mix, 6.00in (152mm) GABCS, 5.00in (127mm) crushed aggregate ends at MP 270
    - From MP 265 to MP 270
3. I-95-1(38)00 H007219 and I-95-1(29)04 H007252
    - 1973 in Camden County
    - 8.50in (216mm) CRCP, 6.00in (152mm) premixed soil cement stabilized sub-base course

- From MP 0 to MP 4 and from MP 4 to MP 15

4. I-95-1(41)36 H007221
   - 1973 in Glynn/McIntosh Counties
   - 9.00in (229mm) CRCP, 6.00in (152mm) premixed soil cement stabilized sub-base course
   - From MP 35 to MP 49
5. I-95-1(36)59 H007217
   - 1973 in McIntosh/Liberty Counties
   - 8.50in (216mm) CRCP, 6.00in (152mm) premixed soil cement stabilized sub-base course
   - From MP 58 to MP 68
6. I-95-1(27)36 510017-
   - 1975 in Liberty Counties
   - 9.00in (229mm) CRCP, 1.00in (25.4mm) 'H', 5.00in (127mm) premixed soil cement
   - From MP 67 to MP 78
7. I-95-1(32)84 H007257
   - 1971 in Bryan/Chatham Counties
   - 8.50in (216mm) CRCP, 6.00in (152mm) premixed soil cement sub-base
   - From MP 86 to MP 99

2.2 Overview of the Related Research Project

Research conducted by Johnson at the University of Georgia evaluated three pavement types, Jointed Plain Concrete (JPC), CRC, and Hot Mix Asphalt (HMA), to present recommendations for forensic investigations of pavements. The National Cooperative Highway Research Program (NCHRP) Report 747 was used as a guide in this study to conduct forensic investigations of highway pavements for use in Georgia. Based on the recommendations of the guide, Johnson's research included destructive and on-site field/non-destructive testing using Ground Penetrating Radar (GPR) and a Falling Weight Deflectometer (FWD).

In Johnson's study, the selected CRCP sites included two pavement sections on Interstate I-85 through Coweta County, Georgia. I-85 was composed of three lanes in one direction. The pavement at distance of 10 miles apart was in fair performance; the other pavement was in poor performance. A forensic site investigation was conducted with non-destructive, destructive, and laboratory testing.

The first site showed fair performance from MP 45 to MP 44, called MP 45 in this study. MP 45 consisted of 11.50in (292mm) PCC, 3.50in (89mm) Asphalt-Concrete (AC), and 12.00in (305mm) of GAB. The second pavement, in poor performance, was located between MP 55 and MP 54, called MP 55. MP 55 consisted of 12.00in (305mm) PCC, 3.00in (76mm) AC, and 12.00in (30 mm) of GAB.

The transverse cracks varied from 0.7-3.0ft (0.2-0.9m) in length and were observed throughout all three lanes in both sites. According to the Federal Highway Administration (FHWA 2012), crack spacing shall be between 2.0-8.0ft (0.6-2.4m). Another source notes that the recommended crack spacing is between 1.8-7.0ft (0.5-2.1m) (Caltrans, 2007). In MP 45, the depth and width of cracks were measured as about 3.50in (89mm) and 0.02-0.04in (0.5-1mm), respectively. In addition, this site had 3.0ft (0.9m) transverse reinforcement spacing and 2-3 longitudinal cracks. Similar to MP 45, the MP 55 site included cracks spaced a distance from 3.50in (89mm) to 13.00in (330mm).

2.2.1 Non-Destructive Testing Methods

In this study, non-destructive testing was performed on CRCPs by using GPR and FWD. The GPR testing results showed the pavement layers. When the GPR unit includes the reinforcing steel in its pavement scans, the image becomes distorted at the reinforcement area. The GPR

images are shown in Figure 2. Therefore, transverse rebar spacing was detected as 30ft (0.9m) on center. Other design parameters are presented in Table 1.

Table 1 - CRCP Non-Destructive Testing Results and Design Parameters (Johnson 2016)

	Parameters	I-85 MP 45-44 (Fair)		I-85 MP 55-54 (Fair/ Poor)	
		Outside	Inside	Outside	Inside
	Average ISM (kip/in)	9400	3800	3600	4100
	Back-calculated subgrade reaction (pci)	460	221	--	--
CRC Design Parameters	Surface Texture	Transverse Tining		Transverse Tining	
	Epoxy Coated Rebar	No	No	No	No
	Longitudinal Rebar Depth (Clear Cover) (in.)	3.75	3.75	3.25	4.5
	Longitudinal Rebar Diameter (No.)	0.75" (#6)	0.75" (#6)	0.75" (#6)	0.75" (#6)
	Transverse Rebar Depth (Clear Cover) (in.)	4.25	4.25	4	5.75
	Transverse Rebar Diameter (No.)	0.5" (#4)	0.5" (#4)	0.5" (#4)	0.5" (#4)
	Longitudinal Rebar Spacing (ft.)	0.45 to 0.5	0.45 to 0.5	0.42 to 0.46	0.42 to 0.46
	Transverse Rebar Spacing (ft.)	3	3	3	3

2.2.2 Destructive Testing Methods

2.2.2.1 Coring and Field Testing

Cores were extracted on the I-85 sections. A 4.00in (102mm) core drill was used for the laboratory test. To detect the pavement thickness and reinforcement size and location, a 6.00in (152mm) core bit was utilized. For the carbonation and alkali-silica reaction (ASR) testing, one core (C8M-TR) was taken from MP 45 and two cores were extracted from the MP 55 outside and inside lanes. The test results showed a negative reaction for both sections.

The core sample taken from the MP 45 outside lane indicated consistent longitudinal reinforcement depth, although this depth varied by as much as 0.75in (19mm) in the inside lane.

Numerous transverse cracks were observed on the MP 55 section. It was noted that both longitudinal and transverse reinforcements were not epoxy-coated for MP 45 and MP 55.

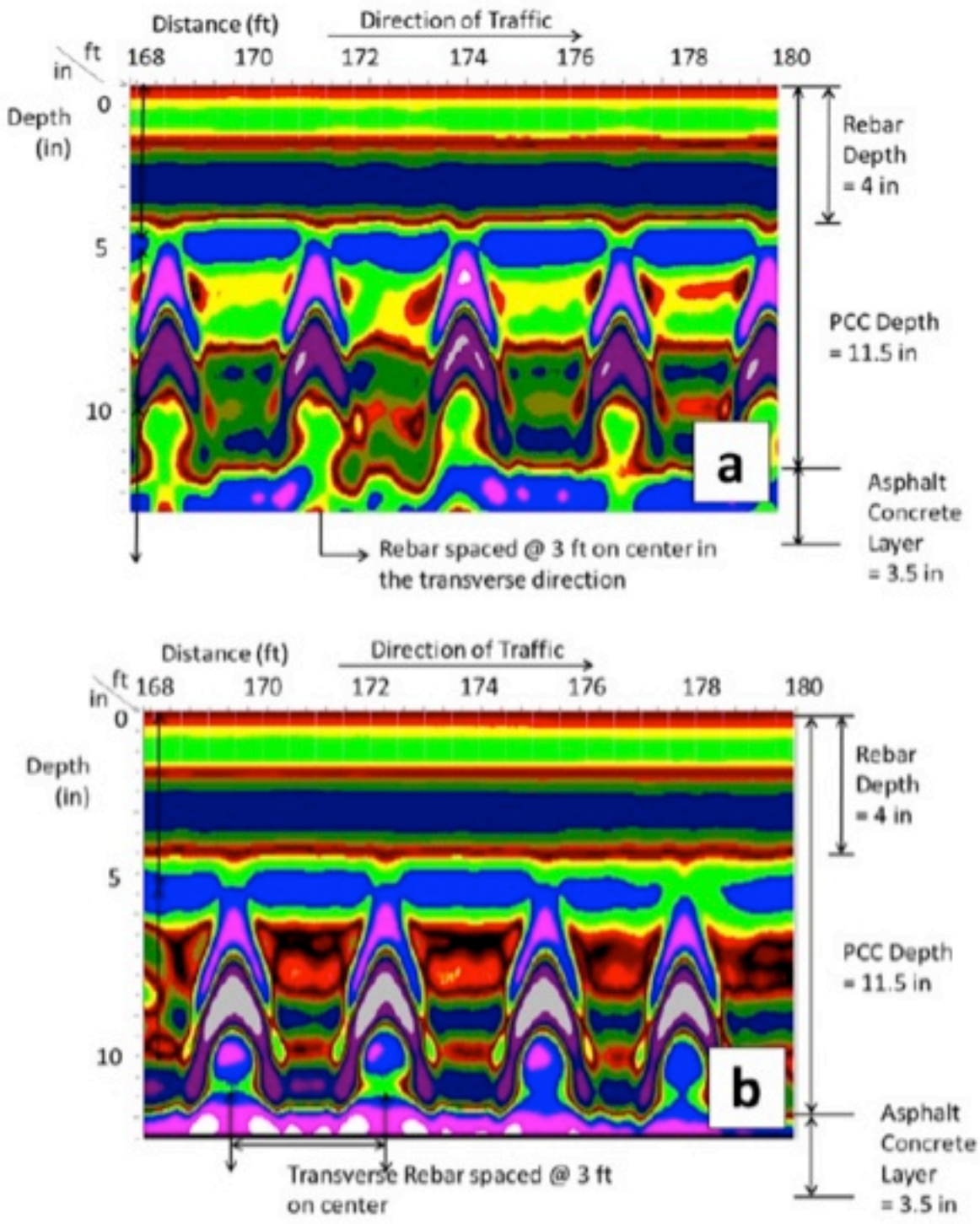

Figure 2 – GPR Scans in the Direction of Traffic (Johnson, 2016)

2.2.2.2 Laboratory Testing

Laboratory tests including coefficient of thermal expansion (CTE), rapid chloride penetrability (RCP), and modulus of elasticity (MOE) were conducted for the cored specimens in accordance with AASHTO T 336 (2011), ASTM C1202-12, and ASTM C469, respectively. Results from these tests are presented in Table 2. The CTE values of MP 45 and MP 55 were measured as 4.73 and 4.60 microstrain/°F, respectively. These values were considered acceptable because the range for the CTE of PCC is between 4.4 to 5.5 microstrains/°F. The RCP values seen in Table 2 were evaluated as reasonable. The average MOE for MP 45 was 3550ksi (24,776MPa). The MOE for MP 55 was lower than MP 45 with a value of 2790ksi (19,236MPa).

2.2.2.3 Petrographic Analysis

Two cores (C3W-LR and C8M-LR from I-85 from MP 55) were selected for petrographic analysis. The outside lane of MP 55 had a similar concrete mixture to MP 45; therefore, no cores were taken from MP 45. Based on the analysis, the MP 55 outside lane included a crushed nominal maximum aggregate size (NMAS) of 0.75in (19mm). See Table 2. The selected section with Class C fly ash had a water-to-cement ratio ranging from 0.40 and 0.45 and an entrained air content of 5.0-7.0%. The concrete did not include slag. The material properties of MP 55 outside lane may meet the GDOT acceptance criteria (GDOT 430.3.06, 2013).

The sample analyzed from the MP 55 inside lane showed that the crushed granite and amphibolite had a NMAS of 0.38in (10mm). Natural quartz was used as coarse and fine aggregate, respectively. The selected section without Class C fly ash was identified as fair quality with a water-to-cement ratio of 0.40 and 0.45 and an air content of 3%. Taking into account GDOT acceptance criteria, this water-to-cement ratio is acceptable, although the air

content is not in the required range (4.0-5.5%). Therefore, the material properties of MP 55 inside lane do not meet the current design requirements (GDOT 430.3.06, 2013).

Table 2 - CRCP Destructive Testing Results and Design Parameters (Johnson 2016)

	Parameters	I-85 MP 45-44 (Fair)		I-85 MP 55-54 (Poor)	
		Outside	Inside	Outside	Inside
Condition	Good/Fair/ Poor	Fair	Fair	Fair	Poor
On-site Field Testing	ASR	No	No	No	No
	Carbonation	No	No	No	No
Laboratory Testing	MOE (ksi)	3687	3417	3125	2450
	f'c (psi)	7,400	7,300	7,700	7,900
	RCP (Coulomb)	2085	3058	3382	3909
	CTE (in/in/°F)	4.73	4.6	5.25	5.34
Petrographic Analysis	Coarse Aggregate	See I-85 MP 55-54 Inside Lane		Crushed Granite and Amphibolite	Crushed Granite
	Maximum Aggregate Size			3/8"	3/4"; Segregation at the surface
	Fine Aggregate			Natural quarts; The max sand particle size s 3mm.	Natural quartzite and gray quartz; The maximum sand particle size is 1/5".
	W/C ratio			0.4-0.45	0.4-0.45
	Fly ash			Class C fly ash and no slag in the cement.	Class C fly ash and no slag in the cement.
	Paste			The paste is of fair quality.	The paste is of fair quality. The paste is somewhat soft as it is scratched by a Mohs 3 hardness point.
	Air entrained			No	Yes
	Air content			Approximately 3% air consisting of mostly entrapped voids.; The air is not evenly distributed as there is more air in the middle of the core.	Approximately 5-7%. Mostly air entrained air voids. There is frequent ettringite in the voids.
	Cracks			Rare microcracks in the paste.	There are occasionally internal cracks in the aggregate. These cracks could present durability issues but do not appear to be presently detrimental.
	Other distresses to note			No corrosion is present at the periphery of the rebar. It has 3and3/4 inches of top surface concrete cover.	

3. LITERATURE REVIEW

3.1 Portland Cement Concrete Pavement

PCC is exposed to volumetric changes as a result of moisture loss and temperature variations. In PCC pavement, those volume changes are controlled by concrete self-weight, reinforcement, and friction between the concrete and the sub-base. Concrete stresses within the pavement increase during traffic flow because of wheel loading. Together with this physical loading and volume change, cracks might occur if the total applied stress exceeds the maximum allowable stress capacity of the PCC pavement. Therefore, PCC pavement is separated into two types based on the effects of cracking potential on the durableness of the pavement type: JPC or CRCP (Ha et al. 2012). This study focused entirely on CRCPs.

3.1.1 Continuously Reinforced Concrete Pavement (CRCP)

In this study, only selected CRCP sections in Georgia were investigated to determine the vertical location of the reinforcement within the pavement section at selected punchout locations. In 1921, the Bureau of Public Roads built the first experimental CRCPs on Columbia Pike in Arlington, Virginia. In 1938, the State of Indiana constructed the first significant length of CRCP (Highway Research Board 1973). CRCP was first used for the construction of the Interstate Highway System in the United States during the 1960s and 1970s (American Iron and Steel Institute 2014). Folliard and Prozzi (2005) reported that utilization of CRCP increased throughout the U.S. during the construction of the Interstate Highway System in the 1960s, 1970s, and 1980s. Historically, Texas and Illinois have used CRCP more often than other states. Based on GDOT design practice for full-depth (12.00in [305mm]) or overlay (11.00in [280mm]) CRCP, the cover depth is required to range between 3.50-4.25in (89-108mm). However, the previous work conducted by Johnson (2016) indicated that the thickness of CRCP in some

sections of I-85 is greater than 12.00in (305mm), and longitudinal rebar depth varies in I-85 CRCP sections.

3.1.1.1 CRCP Design

CRCP contains continuous longitudinal reinforcement and does not employ the use of transverse contraction joints at intermediate locations. The pavement is allowed to crack at random locations, with the cracks held tightly together by the longitudinal reinforcing steel. Transverse cracks are allowed to free concrete stresses in the transverse direction, which typically form at intervals of 1.5-6.0ft (0.5-1.8m). In addition, the cracks are held together with continuous longitudinal reinforcing steel, as shown in Figure 3. The percentage of reinforcing steel for CRCP is commonly 0.6-0.7% of the pavement cross-sectional area (ACPA CRCP 2016). The minimum recommended percentage of steel content to keep the crack spacing between 3.5-8.0ft (1.1-2.4m) is 0.6%. The minimum (3.5ft [1.1m]) and maximum (8.0ft [2.4m]) criteria are recommended by FHWA to be able to control the formation of punchouts and spalling, respectively (Tsai and Wang 2014). If the crack spacing is greater than 8.0ft (2.4m), it causes the joint opening to become vulnerable to spalling. In addition, the large crack spacing causes wider crack width, which creates the loss of load-transfer efficiency (LTE) across transverse cracks and results in punchouts and faulting (ARA, Inc. 2004). The Mechanistic-Emperical Pavement Design Guide (MEPDG) recommends 3.0-6.0ft (0.9-1.8m) for the mean crack spacing range (Tsai and Wang 2014).

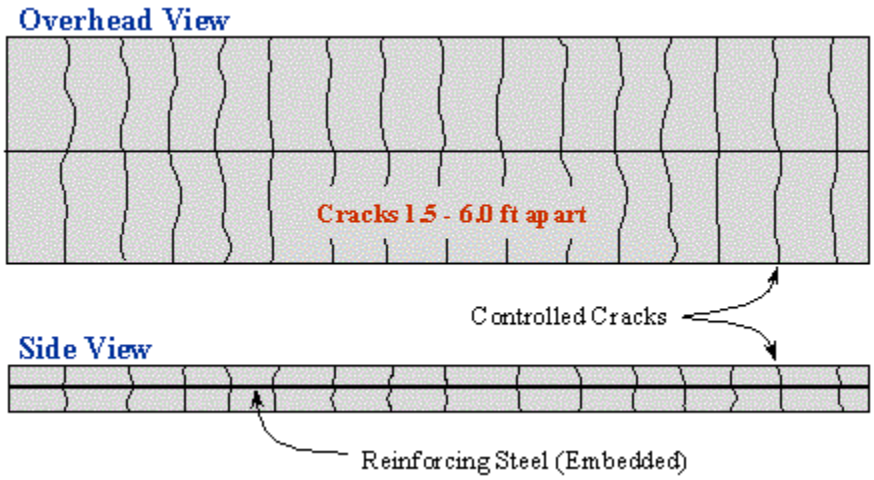

Figure 3 – Overhead and Side Views of CRCP (ACPA CRCP 2016)

The crack width of CRCP is almost always smaller than 0.04in (1mm), and typically less than 0.02in (0.5mm) (Kohler and Roesler 2005). It has been suggested that the maximum crack width at the pavement surface should be 0.04in (1mm) to prevent water infiltration (AASHTO 1986, 1993). If the crack width is 0.03in (0.6mm) or less, water penetration in temperatures below freezing is reduced, resulting in a reduction in the corrosion of the steel and a higher sustained load transfer efficiency (Ren 2015). The essential difference between JPCP and CRCP is that while the behavior of cracks is accepted as a distress in JPCP, it is not considered a distress in CRCP (Ha et al. 2012). Distresses including punchouts, crack spalling, and steel rupture might occur from traffic and environmental loadings. Engineers working on CRCP designs manage the cracking that develops to reduce this distress. Therefore, CRCP can be constructed for many miles without joints (FHWA 2012). According to the performance factors mentioned in Topic 622 in the California Department of Transportation guide, CRCP design should have at most 10 punchouts per mile at the end of its design life under worst-case conditions (Caltrans 2015).

Kohler and Roesler (2006) analyzed crack width (CW) and crack spacing (CS) data from full-scale CRCP sections. The authors utilized CRCP CW and CS models with the new Mechanistic-Empirical Pavement Design Guide (MEPDG) to compare measured CS and CW data collected under different temperature conditions throughout five test sections. Based on the results, the CW model was calibrated to standardize the measurements. Instead of using MEPDG software, CS and CW were calculated with MEPDG formulas. Figure 4 presents the predicted CS compared with the measured CS for sections located at the center of the CRCP test strip. According to Figure 4, the CS prediction model based on MEPDG closely matched the actual CS, as illustrated by the cluster of data points along the line of equality.

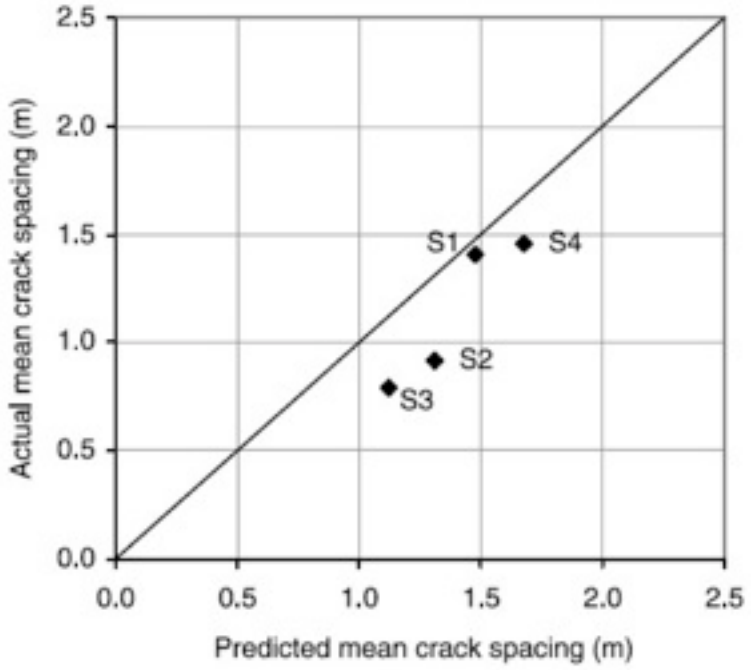

Figure 4 – Predicted and Measured Crack Spacing (Kohler and Roesler 2006)

Kohler and Roesler defend the notion that CW plays a key role in affecting the performance of CRCP. CW affects the aggregate interlock and shear load transfer capabilities between adjacent concrete sections. In the presented research, a CW-predicted model was

calibrated by using a defined factor to represent the model correctly and obtain a reasonable prediction of actual CW. According to the results, using high steel reinforcement content reduced the average CW on the selected sections.

Figure 5 shows a CRCP section typical of those specified by GDOT. The CRCP slab thickness ranges between 11.00-12.00in (280-305mm) on top of a 3.00in (76mm) asphalt cement concrete (ACC) layer with a 12.00in (305mm) graded aggregate base (GAB) below that is no less than 8.00in (203mm) in thickness. Longitudinal reinforcement typically utilized for CRCPs is a #6 steel reinforcing bar. The #4 reinforcing bar used in the transverse direction supports the longitudinal steel. Steel reinforcement is placed no less than 3.50in (89mm) and no more than 4.25in (108mm) below the top surface of the slab (Tsai and Wang 2014). This distance provides adequate concrete cover while positioning the steel reinforcement such that it prevents cracks from widening.

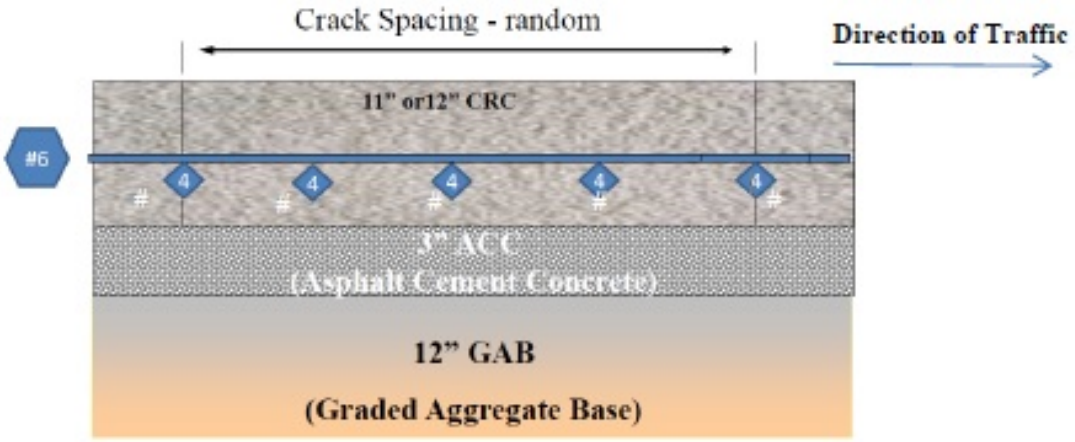

Figure 5 – GDOT CRCP Section (Tsai and Wang 2014)

3.1.1.2 CRCP Performance

CRCP performs well when appropriately designed and constructed for local conditions. According to Topic 612 in the California Department of Transportation guide (Caltrans 2015),

pavement design life is defined as the optimum number of years that CRCP will properly provide service without any major recovery or restoration. CRCP performance is contingent upon materials, design, construction, and environmental factors as follows (Folliard and Prozzi 2005):

- PCC properties that include elastic modulus, tensile strength, coefficient of thermal expansion, and drying shrinkage
- Steel properties that include steel bar diameter and location, percent reinforcement
- Slab and sub-base resistance
- Size and geometry of pavement (i.e., thickness)
- Environmental loads that include ambient air temperature, wind speed, and humidity
- Traffic loads that include static wheel load and mobile dynamic load

3.1.1.3 Distress Types of CRCP

Distress types of CRCP are categorized in two main groups, defined as *structural distress* and *functional distress*. Yoder et al. (1975) made a further distinction between two different types of failure. The first type includes a collapse of the pavement structure or pavement components, and is defined as structural failure. The second type, functional failure, occurs when the pavement will not perform its intended function without causing discomfort to passengers or high stress in vehicles crossing over it due to its excessive roughness. Thus, the differences between these two types of failure must be analyzed properly since they require different types of maintenance or repair. Functional failure requires minimal and regular maintenance such as resurfacing to re-establish smooth-riding qualities to the pavement; however; structural failure might require a complete removal and replacement of the pavement section (Yoder and Witczak 1975).

Many factors contribute to structural and functional distresses, as listed in Table 3. This table shows the possible causes and the primary, contributing, and negligible factors for the types of distresses (Rada et.al 2013). FHWA (2013) indicated that punchouts, wide transverse cracks, and longitudinal cracks are the most detrimental structural distresses. Other types of distresses that occur in concrete pavement include spalling, patch deterioration, faulting, and blowup. Table 4 provides supporting information from Rada et.al (2013) that shows severity of distress types caused by traffic loading, climate, and materials.

3.1.1.3.1 Cracking

Cracks in the transverse direction in CRCP are allowed to remain tight. Therefore, this type of cracking is not considered distress. However, wide transverse cracks and longitudinal cracks might require rehabilitation (FHWA 2013).

3.1.1.3.1.1 Wide Transverse Cracks

Wide transverse cracks are perpendicular to the pavement centerline and occur due to inadequate and/or defective structural design and loss of support. In addition, large crack spacing formed due to low levels of reinforcement can make the transverse cracks widen, increasing increases tensile stress in the reinforcement. When the reinforcement ruptures, the transverse cracks will not transfer load. Medium and high severity cracks ranging between 0.12-0.24in (3-6mm) should be quickly rehabilitated (FHWA 2013).

Table 3 - Types of Distress and Possible Causes (Rada et.al 2013)

Structural Distress	Contributing Factors[1]					
	Pavement Design	Load	Water	Temp.	Pavement Materials	Construct.
Structural Distress						
Cracking[2]						
Transverse	P	P	N	C	C	P
Longitudinal	P	P	N	C	C	P
Corner	C	P	C	C	N	N
Intersecting	C	P	C	N	C	N
Possible causes of cracking: Fatigue, joint spacing too long, shallow or late joint sawing, base or edge restraint, loss of support, freeze-thaw and moisture-related settlement/heave, dowel bar lock-up, curling, and warping.						
Joint/Crack Deterioration						
Spalling	C	C	N	C	P	C
Pumping[2]	C	P	P	N	C	N
Blowups	C	N	N	P	C	N
Joint Seal Damage[2]	C	C	C	C	P	C
Possible causes of joint/crack deterioration: Incompressibles in joint/crack, material durability problems, subbase pumping, dowel socketing or corrosion, keyway failure, metal or plastic inserts, rupture and corrosion of steel in JRCP, high reinforcing steel.						
Punchouts[2]	P	P	C	N	C	N
Possible causes of punchouts: Loss of support, low steel content, inadequate concrete slab thickness, poor construction procedures.						
Durability						
D-cracking	N	N	P	C	P	N
Alkali-Silica Reactivity (ASR)	N	N	P	C	P	N
Freeze-thaw damage	N	N	P	P	P	C
Possible causes of durability distresses: Poor aggregate quality, poor concentrate mixture quality, water in the pavement structure.						
Functional Distress						
Roughness						
Faulting[2]	P	P	P	C	C	N
Heave/swell[2]	C	N	P	P	C	N
Settlement[2]	C	C	C	N	N	C
Patch deterioration	C	C	C	C	C	C
Possible causes of roughness: Poor load transfer, loss of support, subbase pumping, backfill settlement, freeze-thaw, and moisture-related settlement/heave, curling and warping, and poor construction practices.						
Surface Polishing	N	C	N	N	P	N
Possible causes of surface polishing: High volumes of traffic, poor surface texture, wide uniform tine spacing, wide joint reservoirs, and wheel path abrasion because of studded tires or chains.						
Noise	P	C	N	N	C	P
Possible causes of noise: High volumes of traffic, poor surface texture, wide uniform tine spacing, wide joint reservoirs, and wheel path abrasion because of studded tires or chains.						
Surface Defects						
Scaling	N	N	C	C	P	P
Popouts	N	N	C	C	P	C
Crazing	N	N	N	C	C	P
Plastic shrinkage cracks	N	N	N	C	C	P
Possible causes of surface defects: Over-finishing the surface, poor concrete mixture, reactive aggregates, and poor curing practices.						

[1] P= Primary Factor C= Contributing Factor N= Negligible Factor

[2] Loss of support is an intermediary phase between the contributing factors and these distresses. Loss of support is affected by load, water, and design factors.

Table 4 – Common Distress Types and Their Severities Formed by Causes (FHWA 2013)

Distress Type	Caused by Traffic Loading	Caused by Climate / Materials
Punchout	X	
Cracking		
Wide transverse cracks	X (M,H)	X (L)
Longitudinal cracks		X
Spalling	X	X
Faulting		
Longitudinal joint faulting	X	X
Lane/Shoulder dropoff or heave		X
Erodibility		
Pumping and water bleeding	X (M,H)	X (L)
Joint distress		
Construction joint distress	X	X
Lane/shoulder joint separation		X
Materials-related distresses		
D-cracking		X
Alkali–silica reactivity		X
Popouts		X
Scaling, map cracking, and crazing		X
Corrosión		X
Swell		X
Depression		X
Localized distress		X
Blowup		X
Patch deterioration		
Asphalt patch deterioration	X	
Concrete patch deterioration	X (M,H)	X (L)
Adjacent slab deterioration	X	X

Note: L = low severity, M = medium severity, and H = high severity.

The severity levels of the transverse cracks are separated into three primary groups: low, moderate, and high (FHWA 2003). In low severity, the cracks are either not spalled or have spalling formed from less than 10% of the crack length. Moderate severity is classified by cracks

with spalling formed between 10-50% of the crack length. Where spalling has developed along more than 50% of the crack length, a high severity case exists, as seen in Figure 6.

a. Low Severity **b. Moderate Severity** **c. High Severity**

Figure 6 – Examples of Severity Levels of Transverse Cracks (FHWA 2003)

3.1.1.3.1.2 Longitudinal Cracks

Longitudinal cracks occur due to poor construction techniques or settlement, and are parallel to the pavement centerline. As long as repeated loadings exist on the pavement, these cracks typically expand and allow water to enter the pavement structure (FHWA 2013). According to FHWA (2012), the longitudinal reinforcement shall be placed no less than 3.50in (89mm) and no more than 4.25in (108mm) beneath the top of the slab.

Roesler et.al (2005) conducted research that showed a failure investigation on longitudinal cracking distress for CRCPs in Illinois. The aim of his study was to determine the distress mechanisms causing premature longitudinal cracking on CRCP. The longitudinal cracking occurred over the driving and passing lanes embedded with reinforcement steel. The results showed cracking was not triggered by steel corrosion, damaging reactions in the concrete materials, or insufficient constructional design. Instead, cracking was linked to the settlement of reinforcing steel in the concrete pavement. Settlement cracking typically occurs in concrete slabs with high slump and reduced concrete cover depth. However, the team found that the

longitudinal reinforcing steel in CRCP settled within the concrete due to the large cover depth, low slump concrete, and the technique of placing the steel reinforcing bars in the fresh concrete (tube-feeding). This led to the formation of longitudinal cracks.

Longitudinal cracks are categorized into three different severity levels (low, moderate, and high) (FHWA 2003). Cracks at low severity have no spalling or faulting and crack widths less than 0.12in (3mm). At moderate severity level, cracks range from 0.12in (3mm) to 0.52in (13mm) in width with spalling or faulting less than 3.00in (75mm) and 0.52in (13mm), respectively. High-severity cracks are more than 0.50in (13mm) in width, with spalling greater than 2.95in (75mm) or faulting of more than 0.50in (13mm), as shown in Figure 7.

a. **Low Severity** **b. High Severity**

Figure 7 – Examples of Severity Levels of Longitudinal Cracks (FHWA 2003)

3.1.1.3.2 Spalling

FHWA (2013) reported that spalling -- defined as the cracking, breaking, chipping or fraying of the slab edges -- develops up to 2.40in (60mm) of a crack or joint. The spalling of CRCP might be related to weak surface concrete, corrosion of reinforcing steel, inadequate concrete cover, poor structural design, misaligned reinforcement, and/or extensive pressures. Figure 8 shows spalling forming at transverse cracks and joints.

a. Spalling at Transverse Cracks **b. Spalling at a Transverse Joint**

Figure 8 – Examples of Spalling at Cracks and Joints (FHWA 2013; NCHRP 2001)

3.1.1.3.3 Punchouts

Punchouts and longitudinal cracking are considered major structural distresses in CRCPs (NCHRP 2001). A study by Sub and McCullough (1992) describe a punchout as a major structural failure in which a small segment of pavement is broken loose from the main body and dislocated downward under traffic. The punchout is usually bounded by two closely spaced transverse cracks, a longitudinal crack, and the pavement edge (Sub and McCullough 1992). Punchouts are defined as a form of cracking that develops between two closely spaced transverse cracks in CRCP (ARA, Inc. 2003). Punchout occurs when a short longitudinal crack links together two closely spaced transverse cracks. The longitudinal crack develops as a result of the large deflections and high stresses under traffic wheel loads across the pavement area between the transverse cracks.

Punchouts affect the long-term performance of CRCP, resulting in pavement failure and negative impacts on ride quality and safety. In order to estimate pavement life, the severity levels of punchouts must be determined. Severity levels are categorized as low, moderate, or high, as shown in Figure 9. In low severity, the transverse and longitudinal cracks are tight and might have spalling less than 2.95in (75mm) or faulting less than 0.24in (6mm) without loss of

material. There are no ‘Y’ cracks at this level. In moderate severity, spalling might be more than 2.95in (75mm), or faulting might be between 0.24-0.51in (6-13mm). In high severity, spalling might be more than 5.91in (150mm). In addition, the punchouts might be pushed down by 0.51in (13mm) and/or broken into pieces due to traffic flow. Figure 10 illustrates pavement at each of these three severity levels. The number of punchouts is recorded at each level (FHWA 2003).

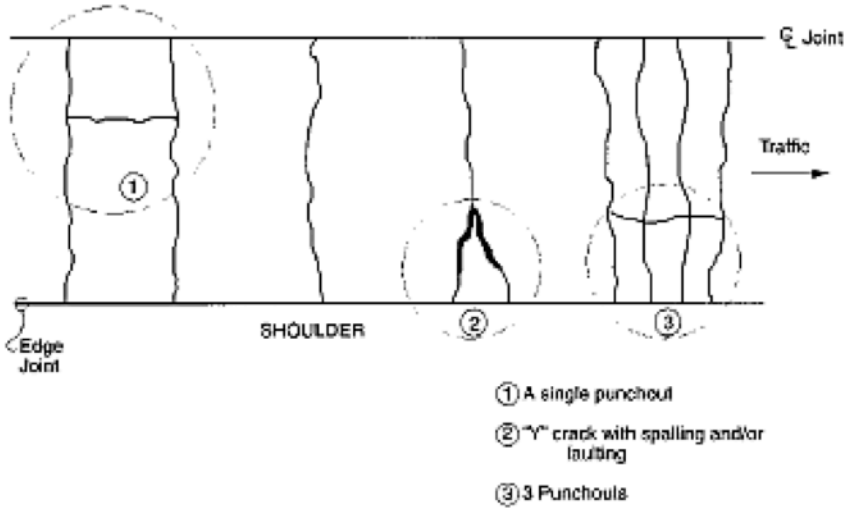

Figure 9 – Severity Levels of Punchouts (FHWA 2003)

Kohler and Roesler (2004) investigated crack spacing and crack width by conducting experiments on CRCP sections. The authors found that punchouts and spalling distresses, which are unwanted crack patterns on the pavement, had formed in the presence of small crack spacing, cluster cracks, divided cracks, and Y-cracks (Figure 11). Based on Kohler and Roesler (2004) study, cluster cracking was described as the moving average of five cracks spaced less than 2.0ft (0.6m). Other research mentioned in the study proved that if the depth of reinforcement increased, Y-cracking decreased. However, this increase in depth developed more cluster

cracking. Likewise, the increase in cluster cracking, together with concrete shrinkage, decreased Y-cracking (Kohler and Roesler 2004).

a. Low Severity **b. Moderate Severity** **c. High Severity**

Figure 10 – Example Severity Levels of Punchouts (FHWA 2003)

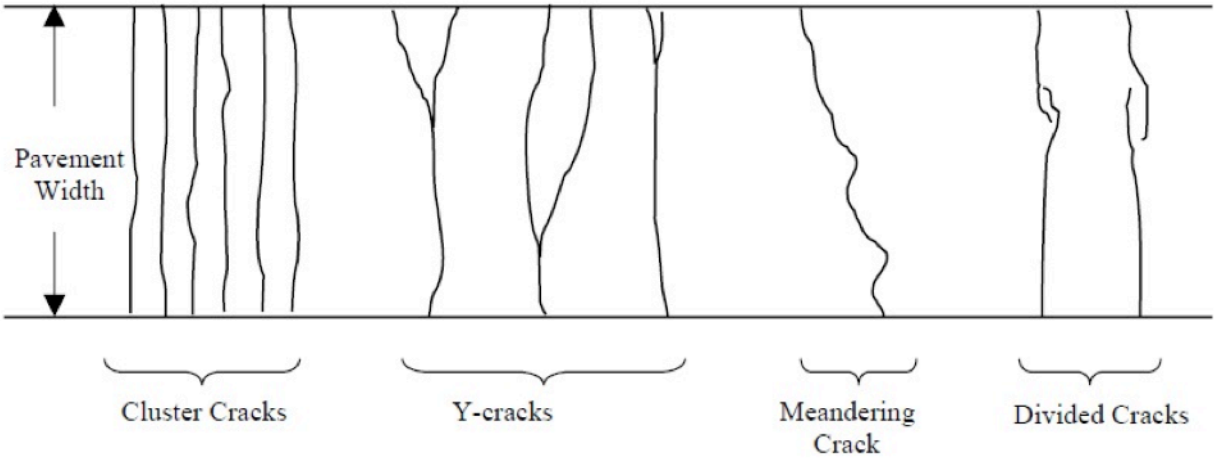

Figure 11 – Crack Shapes and Patterns (Kohler and Roesler 2004)

Kohler and Roesler's research showed that the cluster of transverse cracks was defined as the group of three or more transverse cracks having a spacing of 2.0ft (0.6m) or less. It was accepted that if two consecutive transverse cracks were spaced at more than 3.0ft (0.9m) apart, the cluster cracking ended and the next cluster cracking (or single transverse crack) began at the next transverse crack (McGhee 1998).

In a study referenced by Kohler and Roesler (2004), the average crack spacing in CRCP was in the range of 1.0-6.0ft (0.3-1.8m) based on data obtained from approximately 80

test sections. They noted the ideal spacing between cracks was within the range of 3.0-5.0ft (0.9-1.5m). In addition, the authors stated that more variability in the crack spacing increases the likelihood of punchout growth (Kohler and Roesler 2004). The punchouts often formed between two transverse cracks spaced at 2.0ft (0.6m) or less (ARA, Inc. 2003).

According to previous AASHTO pavement design guides, the two most important factors causing punchouts were crack spacing and width, although punchouts were not taken into account during design calculations. In addition, these guides indicated that ideal crack spacing is at intervals of 3.5-8.0ft (1.1-2.4m). Narrowly spaced cracks are undesirable (AASHTO 1986, 1993). Based on prior research, another structural casual factor is weak support of the concrete slab. Due to sub-base erosion, crack failure might occur because of poor support (ARA, Inc. 2004). The National Cooperative Highway Research Program (NCRHP) states that the number and magnitude of applied wheel loads, slab thickness and stiffness, base stiffness, steel reinforcement, drainage conditions, and erosion of slab support are factors affecting punchout development (NCHRP 2001).

In a study examining the effect of reinforcement cover on punchouts, the lower the reinforcement was placed in the pavement section, the more punchouts occurred over time, as illustrated in Figure 12. Ultimately, as reinforcement is placed closer to the pavement surface, crack openings will remain relatively small, as the reinforcing steel holds the crack together. Therefore, the number of cracks will be reduced (ARA, Inc. 2003).

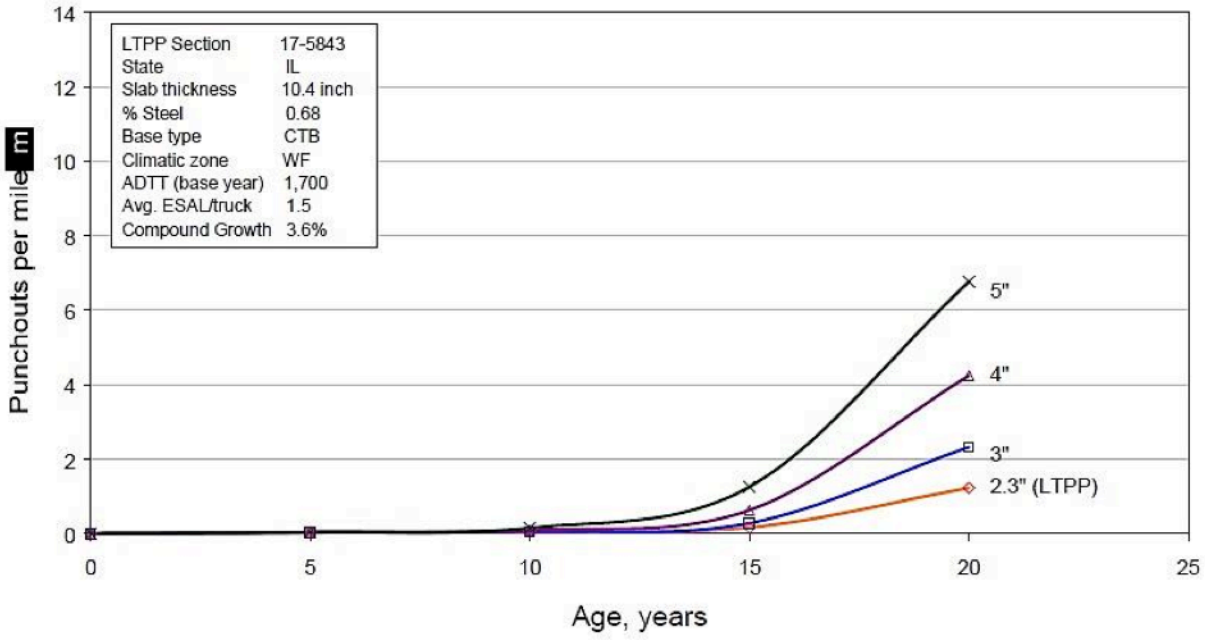

Figure 12 – Effect of Cover Depth on Punchouts Over Time (ARA, Inc. 2003)

An experimental project that supports the theory mentioned above regarding the relationship between cover depth and punchouts was conducted in 1963 in Illinois (Gharaibeh et al. 1999). Reinforcing steel was placed in varying depths, and as Table 5 indicates, the closer the steel was placed to the slab surface, the tighter the transverse cracks remained, and the fewer punchouts occurred. Conclusions from the study showed that proper depth of steel reinforcement should be at least 3.00in. (76mm). With consideration of factors that include construction and steel reinforcing protection from chlorides, steel reinforcement is placed at a depth of about 3.50in (89mm) within a 10.00-12.00in (254-305mm) CRCP in the State of Illinois.

Table 5 – Effect of Reinforcement Depth on CRCP Performance (Gharaibeh et al. 1999)

Reinforcement Depth, in (mm)	Crack Width in Winter, in (mm) (pavement age = 9 years)	Patching, $ft^2/1000\ ft^2$ ($m^2/1000\ m^2$) (pavement age = 14 years)
2.00 (51)	0.0187 (0.48)	7.0 (7.0)
3.00 (76)	0.0312 (0.79)	12.7 (12.7)
4.00 (102)	0.0327 (0.83)	30.9 (30.9)

A report prepared for NCRHP referenced investigations that show the causes and factors of punchouts in CRCPs (ARA, Inc. 2003). Studies by LaCourserie et al. (1978) and Darter et al. (1979) explain the mechanism of edge punchout based on the field investigations of punchout distress in CRCP in Illinois. The development of high tensile stresses occurred at the top of the slab approximately 3.3-6.6ft (1.0-2.0m) from the longitudinal edge of the slab. The results demonstrated poor load transfer across the transverse cracks. In addition, crack spacing was defined as a significant factor impacting the magnitude of the critical tensile lateral stresses on the slab top. Selezneva (2001, 2002) affirmed these conclusions by observing Long-Term Pavement Performance (LTPP) sections located in 22 states. Approximately 90 percent of all punchouts observed were on CRCP sections surrounded by two transverse cracks spaced at 2.0ft (0.6m) or less. Findings from these studies identify the following factors as affecting the development of punchouts (ARA, Inc. 2003):

- Narrow transverse crack spacing (2.0ft [0.6m] or less) existing in the crack spacing distribution
- Loss of LTE along the transverse cracks due to aggregate intertwined from heavy crack opening and repetitive loads
- Base erosion due to the support loss along the sidewalk

- An increase in bending stresses due to the negative temperature above the slab thickness and shrinkage at the slab drying
- The repeated cycles of heavy tensile bending stresses formed from heavy axles, causing the longitudinal fatigue cracking defined as punchout.

The computation of the total number of failures per 1.0mi (1.6km) consists of the sum of punchouts, existing repairs, transverse cracks, and sectional failures. In this case, factors such as steel reinforcement percentage and slab thickness, steel placement method, and base type affect pavement failure. An increase in slab thickness or percentage of steel (or both) reduces the number of pavement failures. In addition, steel placement methods affect CRCP performance. This includes placing steel on a chair or through the use of tubes. When comparing both methods, the use of chairs provides a slightly better performance than tubes at high traffic load locations.

In order to evaluate the effect of pavement base type on punchout, CRCP pavement with a slab thickness of 8.00in (203mm), 0.62 steel reinforcement percentage, and reinforcement placed on chairs was constructed and evaluated utilizing different base types, including no base, cement-aggregate mixture (CAM), granular mixture (GRAN), and bituminous-aggregate mixture (BAM). The results showed that BAM, GRAN, CAM, and no base type performance ranked from good to poor, respectively (Gharaibeh et al. 1999). Tsai and Wang (2014) reported solutions to reduce or control the development of punchouts as (ARA, Inc. 2004):

- Increased longitudinal steel reinforcement content
- Increased load transfer efficiency (LTE)
- Increased slab thickness
- Increased PCC strength,

- Decreased PCC coefficient of thermal expansion (CTE) to lower the thermal causing tensile stresses
- Decreased bending after placement
- The placement of reinforcing steel above the mid-section of slab thickness which satisfies the minimum cover
- The use of a stabilized base,
- The use of a connected PCC shoulder to prevent the movement of the CRCP slab.

3.2 Ground Penetrating Radar (GPR)

The most common types of Non-Destructive Testing (NDT) equipment for evaluating pavement performance are GPR, Falling Weight Deflectometer (FWD), friction testers, and profilometers. FWD equipment measures the deflection responses by applying an impulsive load to a pavement surface to evaluate structural issues. The impact load, loading duration, and area are set to correspond to the actual loading by a standard truck carried on a service load (Sharma and Das 2008).

Friction testers determine the frictional resistance by using a two-wheeled trailer and water. The trailer sprays a measured amount of water on the pavement. After spraying, the trailer is locked by braking. Friction is then generated between the tire and the pavement surface when the tire slides over the wet surface. As a result, a torque develops on the trailer axle and is then measured resulting in friction numbers (FN) showing the frictional properties of the pavement (IDOT 2005).

Another method, profile-measuring equipment, evaluates ride quality issues. Lasers in customized vehicles are used to measure profiles by collecting data including longitudinal and transverse profile, crack pattern, and micro and macro textures. GPR effectively assesses the

layer thickness of the slab and identifies certain problem areas in the pavement "such as debonding, presence of moisture, voids under concrete slabs, and other issues that are typically assessed through coring" (Rada et.al 2013). This report focuses on the utilization of GPR to investigate causes of punchouts in Georgia's CRCPs. Recently, GPR has gained widespread acceptance as a geophysical technique. The GPR method has been particularly practical form imaging certain sediments and soils that are located approximately 0.7-16.4ft (0.2-5.0m) below the ground surface (Conyers 1995).

In 1929, the first attempt at a non-destructive testing system, a precursor to modern GPR, was used to determine the depth of ice in a glacier in Austria (Conyers 1998). Researchers working with electromagnetic energy transmitting within a medium other than air pioneered this technique. In 1930, the U.S. military realized that an airplane flying overhead interrupted radio communication. The military initiated work to detect objects using radio waves. In 1934, the word "RADAR", an acronym for Radio Detection and Ranging, was coined. The use of radar to determine ice, underground water table, and subsoil properties began during this time (Lohonyai 2015). In 1972, The National Aeronautics and Space Administration (NASA) built a prototype GPR system and sent it on Apollo 17 to the moon to investigate the electrical and geological properties of the lunar subsurface (Conyers 1998). GPR has been successfully used in a number of areas for non-destructive underground measuring applications, "including detecting buried explosives, locating possible archaeological dig sites, buried pipes, and embedded reinforcing steel, inspecting pavements, mapping soil strata, contaminant plumes, groundwater levels, and ice thicknesses" (Lohonyai 2015).

A GPR system is comprised of three main components: an antenna, a control unit, and a power supply, as shown in Figure 13. The control unit includes electronics stimulating a pulse of

energy waves that are sent into the ground by the antenna. The system contains a computer and hard disk to store data for analysis once testing has been completed (GSSI 2016). GPR uses the antenna placed on the ground surface to penetrate high-frequency electromagnetic (EM) waves through pavement, structures or other media and identify the various layers beneath the subsurface. Data is typically received via the antenna (ASTM-D6432 2011).

Because the radio waves need to penetrate to the desired depth of the structure, the selection of the antenna frequency is one of the most significant factors when using the GPR system. The frequency of GPR antennas commonly ranges from approximately 10 to 1,200 megahertz (MHz) (Conyers 1998). When the frequency of the antenna is higher, the penetration into the ground will be superficial (GSSI 2016).

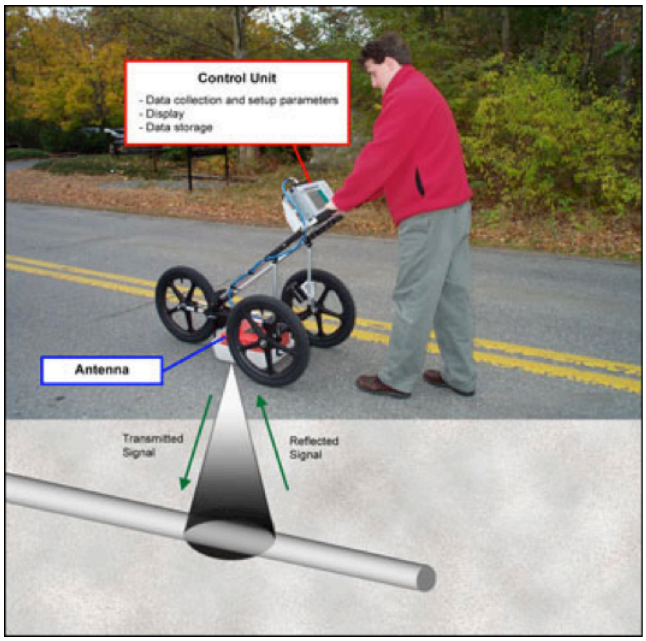

Figure 13 – GPR Unit (GSSI 2016)

In a forensic investigation performed by Chen and Scullion (2008), GPR was used for pavement evaluation with a 1.0 GHz antenna through approximately the top 2.0ft (6.1m) of the

pavement. The authors note that GPR has become a practical test method for exploring cracks through asphalt layers, and has been found to provide comprehensive results of underground conditions. Due to the large number of GPR traces for each GPR test, a color coding scheme was used to convert the variations of dielectric signals from these traces to subsurface images. An example of the color coding for a hot-mix asphalt pavement is presented in Figure 14 and Figure 15. Figure 14 represents the reflections of well-compacted pavement without defects. GPR reflection indicates that the two reflections in the color-map are a red line at the top of the figure that is the pavement surface, and a yellow area located between 16.00-17.00in (406-432mm) depth that is the top of the base layer. The right and bottom axes show the depth and distance scales, respectively. When the pavement section has a weak structure, a GPR unit registers strong reflections (blue and red signs), as shown in Figure 15. The primary aim of the study conducted by Chen and Scullion (2008) was to evaluate the rehabilitation for pavements with stripping. One of the sections investigated was approximately 18.0mi (29.0km) of US281. This site has 6.00in (150mm) of AC and 12.00in (300mm) of granular caliche, sedimentary rock, base. Using GPR, the authors determine that many locations had stripping problems at various depths. In addition, FWD test results showed that the structure of the pavement was inadequate. Based on both test results, the bases were found to be wet and very weak. The other objective conducted by the team was to determine causes of distress. The selected area was US69. A porous layer causing debonding was detected at 2.00-4.00in (50-100mm) by GPR, FWD, and coring. The results showed that the presence of the porous layer resulted in surface distress.

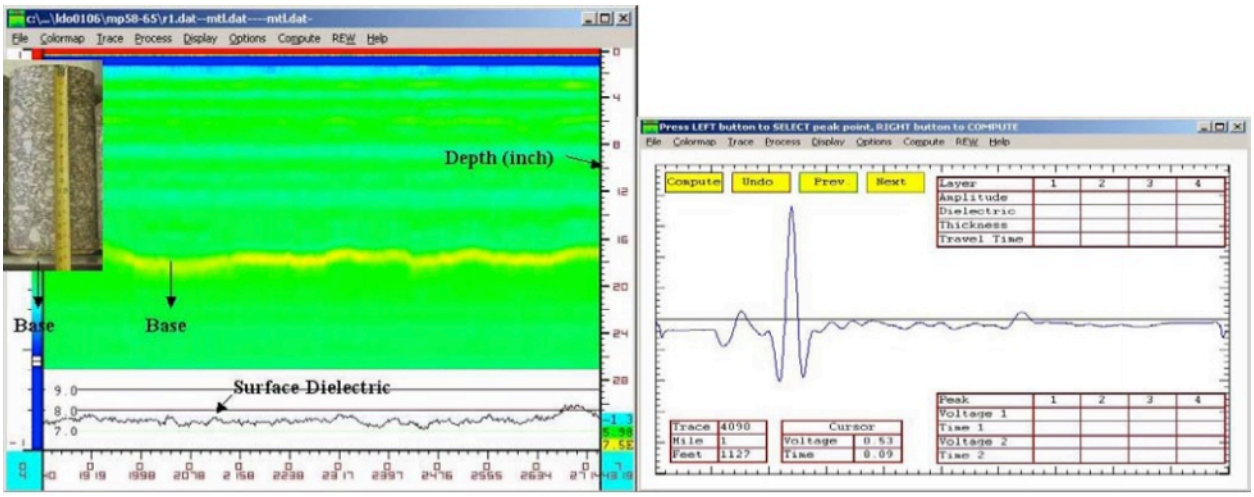

Figure 14 – 18 inch (450 mm) Thick Asphalt Pavement with No Defects (Chen and Scullion 2008)

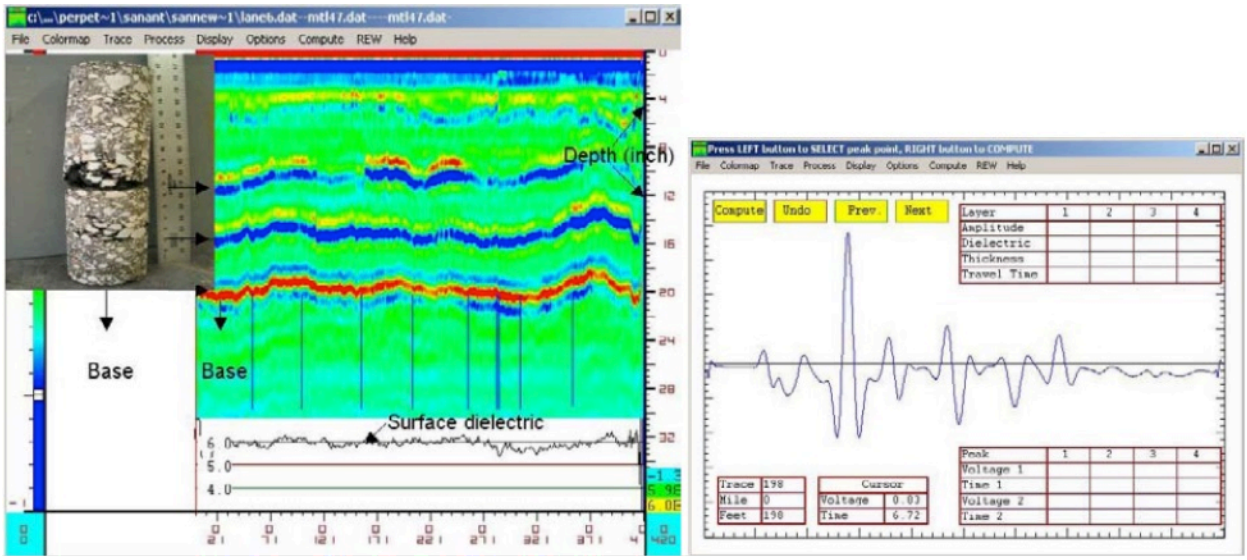

Figure 15 – 20 inch (500 mm) Thick Asphalt Pavement with Defects (Chen and Scullion 2008)

A survey conducted by Annan (2004) was applied to the floor of a one-story slab by using GPR system with 1200 MHz antennas. The results showed rebar located at a depth of 3.20-6.00in (81-152mm) and the condition of rebar as bent during construction.

Diamanti and Redman explored two different topics related to GPR and concrete pavements. First, they observed reflective cracking in the asphalt layer located over contraction joints in the PCC layer below. The results indicated that the strongest reflection in GPR energy develops at the intersection area between the bottom of the crack and the asphalt pavement because of the presence of a granular layer. The other conclusion reached by Diamanti and Redman was that by using the GPR system with different antenna frequencies (250 and 1000 MHz) GPR could be effectively used to investigate asphalt pavements over a granular layer. The results indicated that the 250 MHz GPR was more efficient than the 1000 MHz GPR at detecting cracks due to the roughness of crack and waveguide issues (Diamanti and Redman 2012).

Several studies have demonstrated the various functions of GPR. In some investigations, GPR test results have been verified with coring tests. This has demonstrated the reliability of the GPR test. GPR is used to determine the locations of the punchouts and the structural properties of the material being tested. The resulting images of the GPR test provide accurate results to interpret the layers of a pavement.

3.3 Eddy Current Technology (Profometer 600)

Detection of the rebar location for reinforced concrete pavement is a desired activity for site investigations. Investigators performing pavement evaluations are often tasked with locating the reinforcing steel prior to drilling, cutting, and coring the concrete pavement. The utilization of non-destructive testing technologies such as eddy current pulse induction provides a unique method to aid investigators. The principle of eddy current pulse induction is to provide an image that is not affected by moisture and concrete composition, resulting in a high accuracy for determining concrete cover under all circumstances (Proceq 2017).

Szymanik et al. (2016) studied the detection of steel rebar in reinforced concrete structures using two different methods: active infrared thermography with microwave excitation and eddy current sensors. The authors noted that the multi-frequency eddy current technique may be used for both the detection of the location of reinforcements and the diagnosis of some properties of the structures. It was found that the massive multi-frequency method can be used as a complementary technique to the standard single-frequency eddy current method.

The Profometer, one of the eddy current techniques, is known as a rebar locator (Figure 16). The working principle of this instrument is based on detection of the change in the electromagnetic field in the reinforced concrete. The device is relatively easy to operate. In order to obtain accurate data, the unit must be calibrated prior to beginning field measuring applications. The accuracy of the calibration is checked by comparing readings against a test block that includes reinforcement. The location and size of reinforcement in the test block are measured at different sections on the block. The block is then scanned using the Profometer. The results should be similar (Lokesh et al. 2014).

Figure 16 – The Covermeter - Profometer 600 (Impact Test Equipment 2017)

The reinforcement bar diameter can be detected by Pachometer or Profometer, which are two different commercial brand names of eddy current techniques. The most recent generation of Pachometer is the Profometer, and both techniques work using the pulse induction measuring method. The Profometer provides more accuracy due to its sensitivity to external influences such as adjacent parallel bars (Mihai et al. 2010). One research team used a Profometer 4 to focus on identifying the limitations and capabilities of utilizing it in high strength concrete (Sivasubramanian et al. 2013). The team found that spacing between reinforcement bars is significant in order to obtain more accurate data using the Profometer. When this spacing is small, the measurement of bar diameter is affected by external influences such as adjacent bars. In addition, the smaller probe showed more accurate results if the clear concrete covers were less than 2.75in (70mm), as the manufacturer claimed. This meant that as the concrete cover depth increased, the accuracy of the Profometer decreased.

Barnes and Zheng (2008) conducted research on detecting the factors affecting the accuracy of concrete cover measurement. The authors found that British Standard 1881 Part 204, entitled 'Recommendations on the use of electromagnetic covermeters', states that the concrete cover detected by a calibrated covermeter shall be accurate to ±5% or ±0.08in (2mm), (whichever is the greater) in the operating range given by the manufacturer. In addition, they noted that this specification mentions that when the size of reinforcement is known, the concrete cover can be measured to an approximate accuracy obtained in the laboratory. The accuracy of measurement for reinforcements having less than 3.94in (100mm) concrete cover depth is within (the greater of) 15% or 0.20in (5mm). Based on these findings, the cover measurement was affected by many factors, such as bar diameter settings, existence of neighboring bars under and

parallel to the bar being measured, and whether probe settings for concrete cover were shallow or deep.

4. PROBLEM STATEMENT

The primary goal of this project is to evaluate CRCPs throughout the state of Georgia to identify common characteristics between CRCPs having good performance with a long history, and those with repetitive significant distresses such as punchouts.

To achieve this primary goal, the overall objectives of this study were twofold. First, this study analyzed the correlation between the depth of longitudinal reinforcement, concrete cover depth, and the formation of distresses, while evaluating the severity and crack density on the pavement surface. Second, this study examined the utility of eddy current technology in the calibration process of the GPR unit in the field without taking any core specimens from the sites.

Some CRCPs result in significant structural distress such as punchout, while others perform exceptionally well. Based on previous work, it is suspected that the location of the longitudinal reinforcing steel is associated with the distresses such as cluster cracking and punchout. Therefore, the evaluation of the reinforcement placement height at the location of distresses provides a definitive answer to this hypothesis, and may identify the cause for punchout distress being experienced on CRCP sections in Georgia.

Six sites on major interstates and highway in Georgia were selected for the investigations. A preliminary site investigation revealed that each consisted of different structural conditions in terms of the density and severity of cluster cracking, the existence of punchouts and patched areas, and material problems when compared to one another. This project provides supportive information on distress problems. The previous study (Johnson 2016) determined that the CRCP on I-85 had different reinforcement depths. Therefore, the purpose of this study is to investigate the effect of reinforcing steel placed at different depths on transverse cracks and punchouts. To determine the causes of this repetitive and severe distress, severe clusters of single transverse

cracks, punchouts, and patching areas were identified. The selected sections in Georgia were investigated using a GPR unit and Profometer over the damaged and non-damaged areas.

A GDT-GPR standard has been developed and recommended based on the outcomes obtained from these site investigations. This standard procedure may aid future investigations in detecting other factors affecting punchouts when evaluating the pavement performance utilizing GPR technology. The GPR method provides significant benefits for the long-term monitoring plan of Georgia CRCP.

5. EXPERIMENTAL PLAN

To successfully accomplish the objectives of this project, the proposed research program takes the steps discussed in 5.1 and 5.2.

5.1 Calibration of Ground Penetrating Radar (GPR) Unit

Ground Penetrating Radar (GPR) is a common non-destructive testing system for evaluating pavement performance and subsurface features. To secure accurate data with the results obtained from the GPR unit, equipment, principal components, the frequencies for appropriate pavement type and depth, and calibration must occur, as discussed in Section 3. In this section, a few related terms will be defined before discussing how to calibrate a GPR unit based on pavement type and profile.

All material is governed by two physical properties: electrical conductivity and dielectric constant. Since GPR uses electromagnetic (EM) energy, the depth of scan is measured by the electrical conductivity of the material. When a material has low conductivity – e.g., dry sand, dry concrete, or ice -- the radar will penetrate deeper. Thus, as the water content of a material decreases, conductivity decreases, resulting in deeper ground penetration. The other physical property, dielectric constant, illustrates how fast GPR energy travels over a material by means of descriptive numbers. These numbers range from 1 for air, through which radar energy propagates easily, to 81 for water, through which radar energy does not propagate continuously. Wet material will slow the radar signal due to an increase in the dielectric constant of the material. In other words, the higher the dielectric constant number, the slower GPR energy travels through the medium (GSSI 2006).

Amplitude, frequency, and velocity are terms used to describe a reflected GPR wave. Amplitude is defined as the maximum extent of a vibration or oscillation as is seen in Figure 5.1. Larger amplitudes generate brighter images on a GPR screen. The greater the difference between the dielectrics of varying materials, the larger the amplitude of the reflections. Frequency is described as the total number of oscillations per a given amount of time, as shown in Figure 17. Velocity is typically determined by the dielectric constant and used to detect the depth of the material. Lower velocity indicates higher dielectric number, and vice versa (Penhall 2017).

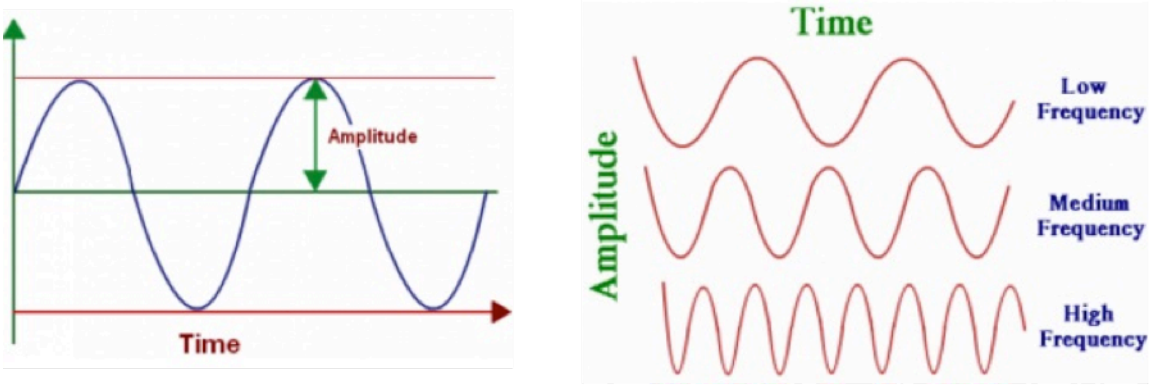

a. Amplitude **b. Frequency**

Figure 17 –Terms Describing a Reflecting GPR Wave (Penhall 2017)

This research was conducted using a GSSI TerraSIRch SIR System-3000 technology referred to as SIR-3000. The SIR-3000 is preferred for a wide variety of applications due to it being a lightweight, portable, and single channel ground penetrating radar system (GSSI 2003). It consists of six modes: TerraSIRch, Concrete, Structure, Utility, Geology Scans and Quick 3D. TerraSIRch mode was used to detect shallow structural features and locations in concrete. GSSI TerraSIRch system includes four subsections: Collect Playback, Output, and System as shown in Figure 18. The Collect mode consists of Radar, Scan, Gain, Position, and Filters.

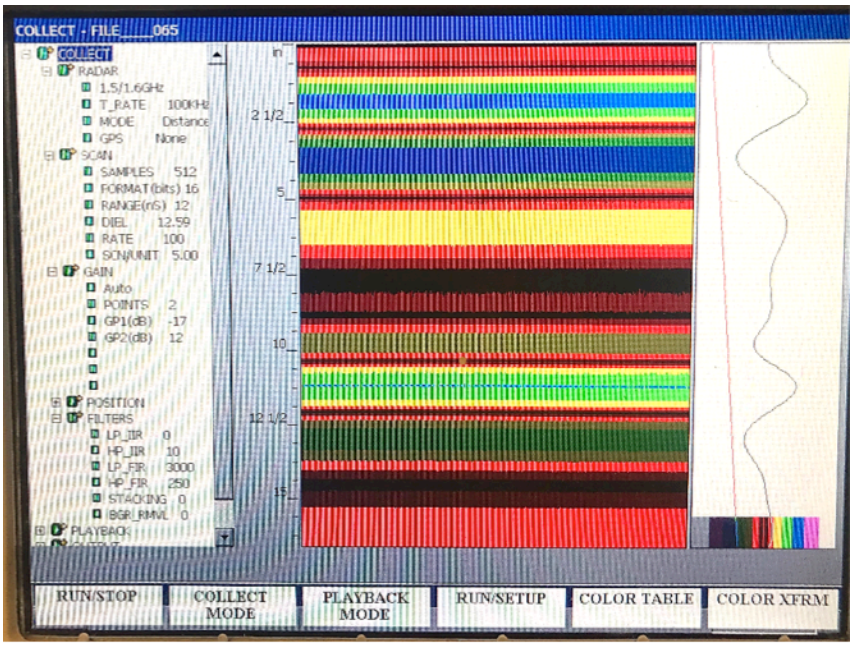

Figure 18 – GSSI ConcreteScan System Submenus (GSSI 2003)

5.1.1 Radar

5.1.1.1 Antenna Choice

The frequency under the Radar submenu allows the SIR-3000 to carry out the auto-surface operation (GSSI 2003). The lower frequencies penetrate the subsurface deeper than higher frequencies. The frequency of the antenna determines the maximum theoretical distance to which the GPR unit can penetrate (Penhall 2017). This depth depends on the properties of the applications listed in Table 6. For this study, the frequency selected was 1.5/1.6 GHz because the material was CRC pavement, as shown in Table 6. With this antenna, the scanned depth was 1.5ft (0.5m), deep enough for the selected sites.

5.1.1.2 T_RATE

The T_RATE is set for the antenna transmit rate in KHz. The maximum rate is 100 KHz. A GPR unit with a higher transmit rate collects data faster (GSSI 2003). In this survey, the T_RATE was set as 100 KHz.

Table 6 – Antennas by Applications (GSSI 2003)

Frequency	Sample Applications	Typical Max Depth Feet (meters)	Typical Range (ns)
1.5 GHz	Structural Concrete, Roadways, Bridge Decks	1.5 (0.5)	10-15
900 MHz	Concrete, Shallow Soils, Archaeology	3 (1)	10-20
400 MHz	Shallow Geology, Utility, Environmental, Archaeology	12 (4)	20-100
200 MHz	Geology, Environmental	25 (8)	70-300
100 MHz	Geology, Environmental	60 (20)	300-500

5.1.1.3 Mode

The Mode provides three different options to collect data. These options are point, time, and distance-based. *Point data collection* is typically used for very deep investigations. Once the mark is pressed, the system will record one scan every time. Then, when the antenna is moved to the next location, the next scan will be recorded. *Time based data collection* records a certain number of scans per second. The survey speed plays a key role in terms of the data density over ground. *Distance based data collection* is carried out with a survey wheel. A certain number of scans are recorded per unit distance. This mode is recommended because it gives the most accurate data (GSSI 2003). In this study, distance-based data collection was selected for more accurate results and reporting.

When distance-based data collection is selected, the survey wheel must be calibrated to local conditions at each different site. For difficult terrain, the calibration can be performed manually. A measured line must be prepared on the survey surface. The longer the measured line, the more accurate the survey wheel calibration. The calibration distance, taken from the

measured line, is entered, and the position of the antenna is set for the beginning of the line as front, center, or rear of the antenna. Next, the antenna is moved the survey distance. If this process is done several times and the average of the results is taken, the calibration will be more accurate. With this method, the GPR unit is calibrated for the survey wheel (GSSI 2003).

5.1.1.4 GPS

The GPS selection provides an option to connect the GPS during collecting data. The GPS capability can be set as 'on' or 'off' (GSSI 2003). In this project, this selection was selected as 'off (none)' because the GPS was not used.

5.1.2 Scan

5.1.2.1 Samples

Each scan curve is formed by data points. A set number of data points is termed *samples*. The more samples that are collected, the better the vertical resolution and the smoother the scan curve. When the number of samples increases, the file size increases. This selection presents six options: 256, 512, 1024, 2048, 4096, and 8192. GSSI recommends using 512 or 1024 samples per scan (GSSI 2003). In addition, the option of 512 samples per scan is recommended within the use of 1.5 GHz frequency. Therefore, in this study, the 512 option was chosen.

5.1.2.2 Format (bits)

This selection is set for the resolution of the outputs. There are two options that include 8-bit and 16-bit format. The 16-bit data format was used in this project and recommended due to its dynamic range being greater than 8-bit. As the format size increases, the data profiles occupy more place in the computer storage (GSSI 2003).

5.1.2.3 Range (nS)

The Range selection is to set time in nanoseconds (nS) for the recording of reflections from a single pulse. It depends on depth. In other words, the longer the range, the deeper the ground penetration; therefore, the GPR unit provides reflections from deeper sections in the ground (GSSI 2003). The 12-nS range was selected in this survey.

5.1.2.4 Dielectric Constant (Diel)

This selection indicates the dielectric constant value of the material and, relatedly, the velocity that the radar can move through a material. A higher dielectric value results in a slower survey speed. The dielectric values for common materials are presented in Table 7. If this value is known, it can be entered directly under this submenu (GSSI 2003). If the dielectric value of material is not known exactly, it can be determined through calibration in the field. This part of the survey plays a key role in the site investigations.

The calibration process of the GPR unit in this study began by considering a dielectric value between 5 and 8 for concrete material (Table 7). At the beginning of the site investigation, a short scan was performed in the longitudinal direction (the direction of traffic) through the GPR unit to be able to see where the transverse reinforcements were located. After designating the locations of transverse reinforcements, a single bar was selected. On the selected transverse reinforcement, both GPR and Profometer units were used to scan the pavement in the transverse direction, from shoulder to the inner lane. Thus, the locations of the longitudinal reinforcements were determined. For confirmation of the depth and size of reinforcements and layer thicknesses, a core 6.00in (152mm) in diameter was taken from each site. The core location was marked on the ground by selecting one of the longitudinal reinforcements (Figure 19).

Table 7 – Dielectric values for common materials (GSSI 2003)

Material	Dielectric	Velocity (mm/ns)
Air	1	300
Water (fresh)	81	33
Water (sea)	81	33
Polar snow	1.4 – 3	194 - 252
Polar ice	3 - 3.15	168
Temperate ice	3.2	167
Pure ice	3.2	167
Freshwater lake ice	4	150
Sea ice	2.5 – 8	78 – 157
Permafrost	1 – 8	106 – 300
Coastal sand (dry)	10	95
Sand (dry)	3 – 6	120 - 170
Sand (wet)	25 – 30	55 – 60
Silt (wet)	10	95
Clay (wet)	8 – 15	86 – 110
Clay soil (dry)	3	173
Marsh	12	86
Agricultural land	15	77
Pastoral land	13	83
"Average soil"	16	75
Granite	5 – 8	106 – 120
Limestone	7 – 9	100 – 113
Dolomite	6.8 – 8	106 – 115
Basalt (wet)	8	106
Shale (wet)	7	113
Sandstone (wet)	6	112
Coal	4 – 5	134 – 150
Quartz	4.3	145
Concrete	5 – 8	55 – 120
Asphalt	3 – 5	134 – 173
PVC	3	173

After obtaining a core, information for the reinforcements and layers was confirmed. For instance, if the concrete cover (the depth to the longitudinal reinforcement from the pavement surface) was measured as 3.70in (94mm) from the core and the GPR image produced a differing cover value, then the concrete cover shown on the GPR screen was corrected to 3.70in (94mm). This calibration process was used at each site. Calibrating the depth of the GPR unit affects the dielectric constant values. Thus, the last step of the calibration process should be saved in the system so as to use the same dielectric value throughout the same site.

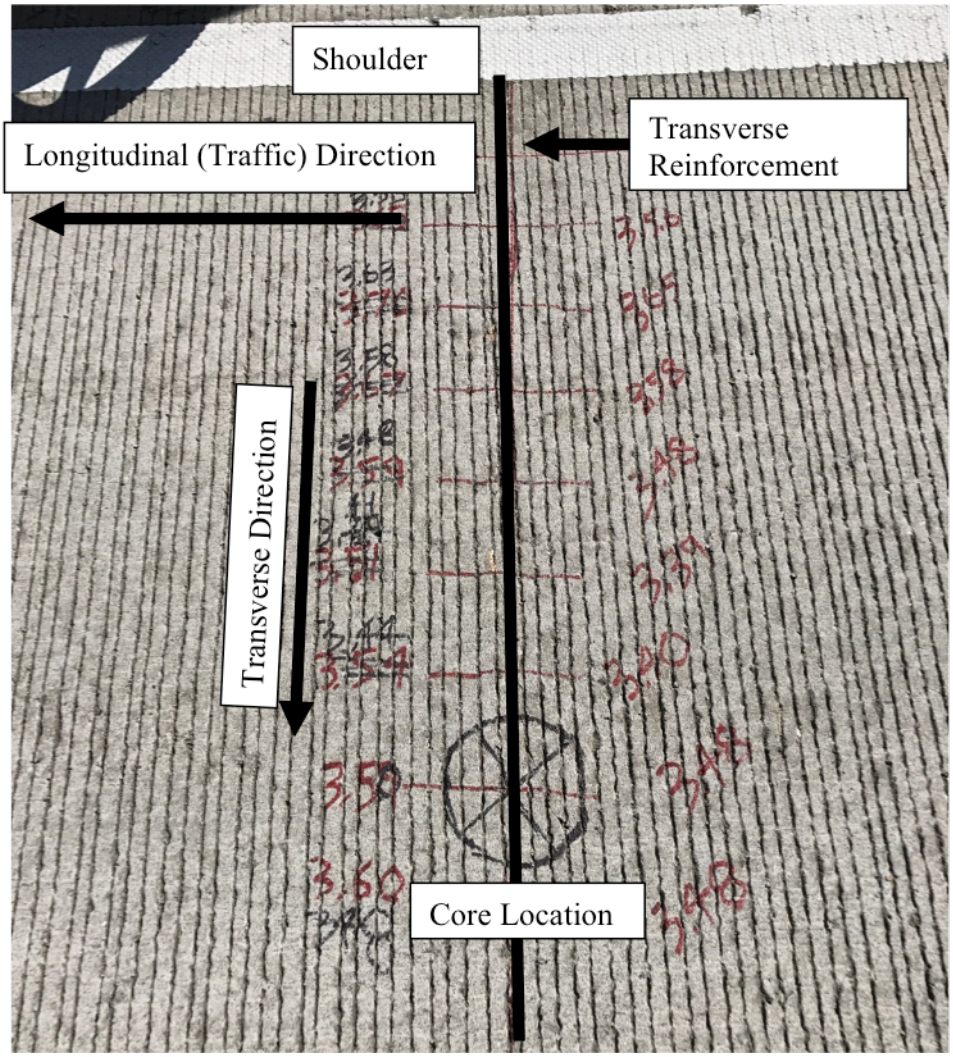

Figure 19 – The Designation of the Core Location at the site (Tift County)

5.1.2.5 Rate

This selection indicates the number of scans per second. If the distance-based data collection mode is selected, this number should be set very high, because the system holds the number of scans in its memory per second. If the number of scans is not enough to collect data for the defined distance per second, the data collection will not be successful. It is recommended that if the transmit rate is set to 100 KHz, the scan rate should be set to 100 scans per second (GSSI 2003), which was used in this project.

5.1.2.6 Scan/Unit

The scans per unit of horizontal distance detect how detailed the survey will be along lines. In other words, the more scans per unit, the slower the survey speed. Figure 20 shows the effects of scans per unit, including 5/in (2/cm), 7.5/in (3/cm), and 10/in (5/cm) (GSSI 2006). In addition, the smaller the scan spacing, the higher the resolution in data, which results in a larger file size. The unit is set to English feet as a default property. Thus, the unit used is scans per foot or inch. It is recommended that 60 scans/foot or 5 scans/inch, the densest scan spacing, should be set for shallow structures, in the case of using the 1.5 GHz antenna (GSSI 2003). In this study, this recommended value, 60 scans/foot or 5 scans/inch, was set for the scan/unit selection.

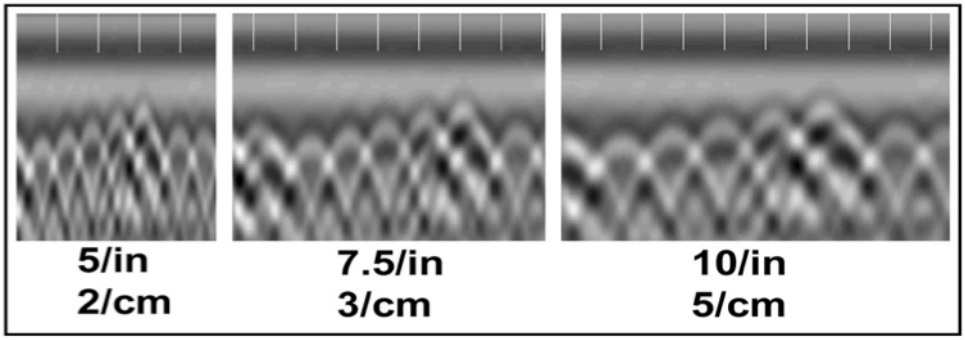

Figure 20 – Scans per unit and effects (GSSI 2006)

5.1.3 Gain

The gain selection neutralizes the effects of attenuation. When a radar scan unit travels on the ground, some of the scans are reflected and the rest of them are absorbed. In addition, deeper scans cause weaker reflections. At this point, the gain selection provides the artificial addition of signal to make the subtle sections more visible (GSSI 2003). The 2 gain points were added to the system in these site investigations.

5.1.4 Filters

Filters allow the user to remove noise in the ground. This selection includes six subsections: LP_IIR, HP_IIR, LP_FIR, HP_FIR, Stacking, and BGR_Removal. LP stands for low-pass, which allows the system to pass any frequency which is lower than one entered in this section. HP stands for high-pass, which has the opposite meaning of LP. The first four subsections, vertical filters, are the frequency filters; their values are in MHz. Stacking technique reduces the noise. BGR_Removal, standing for background removal filter, is a horizontal high pass, which removes low frequency noise. In this study, the HP_IIR, LP_FIR, and HP_FIR filters were set 10 MHz, 3000 MHz, and 250 MHz, respectively.

Based on the preloaded setups for the SIR-3000 (GSSI 2003), the system's data collection parameters and filters, mentioned above, are listed in Table 8. These parameters are recommended for a 1.5 GHz antenna to view approximately 18.00in (457mm) depth in concrete (GSSI 2003).

Table 8 – Data Collection Parameters and Filters (GSSI 2003)

Frequency	**1.5 GHz (Model 5100)**
Transmit Rate (T_RATE)	100 KHz
Samples per Scan	512
Format (Resolution, bits)	16 bits
Range (nS)	12 nS
Scan per Unit	5/inch (2/cm)
Number of Gain Points	2
Vertical IIR High Pass (HP_IIR)	10 MHz
Vertical Low Pass Filter (LP_FIR)	3000 MHz
Vertical High Pass Filter (HP_FIR)	250 MHz

5.2 Calibration of the Cover Meter (Profometer 600)

A project objective was to confirm the results regarding the location and position of the

reinforcements placed into the concrete pavement obtained from GPR technology by employing Profometer, one of the eddy current techniques. This concept is rare in the literature, especially for this instrument. It served to determine the locations of cores fast and accurately for this project. Ultimately, it contributed to the calibration process of the GPR unit during the field investigations.

The Profometer 600 detects rebar locations by using electromagnetic pulse induction. A magnetic field is produced through coils charged by current pulses in the probe (Figure 21). Eddy currents are generated on the surface of any conductive material in the magnetic field and induce this magnetic field in the opposite direction. At the end of this action, the voltage undergoes change, which is used for the measurement of concrete covers (Proceq 2017).

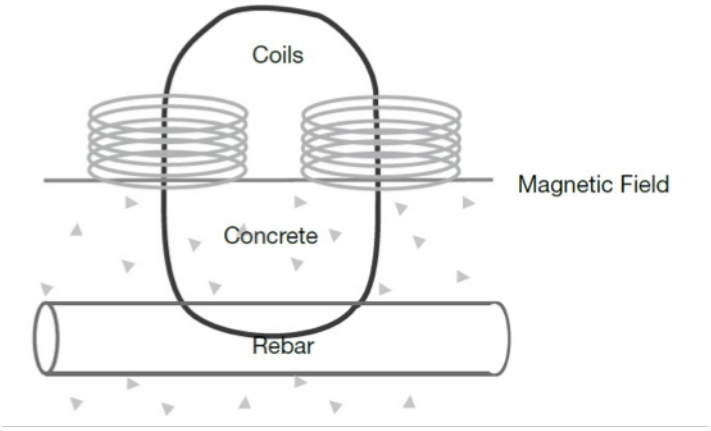

Figure 21 – The Measuring Principle of Profometer (Proceq 2017)

The Profometer 600 has only 'Locating Mode', which can measure the concrete cover. The measuring range setting has four different selections capable of measuring the full range of concrete covers: standard, large, auto, and spot probe range. The standard range (default) setting provides the most accurate data. The large range setting should be selected if the concrete cover is deeper and cannot be detected with the standard range setting. The spot range setting is appropriate if the measured area is small, such as between close reinforcements. In addition, the

auto range setting provides the automatic switch option between standard and large range settings. Figure 22 indicates that the expected accuracy of the concrete cover measurement depends on the reinforcement size (Proceq 2017). In this project, the auto range setting was used to measure sites accurately for any case.

There are minimum limits for the spacing between reinforcements such that the Profometer can detect reinforcement location accurately. These minimum limits of rebar spacing depend on the rebar diameter and cover depth. If the limits (curves indicated in Figure 23) are exceeded, the reinforcements cannot be detected (Proceq 2017).

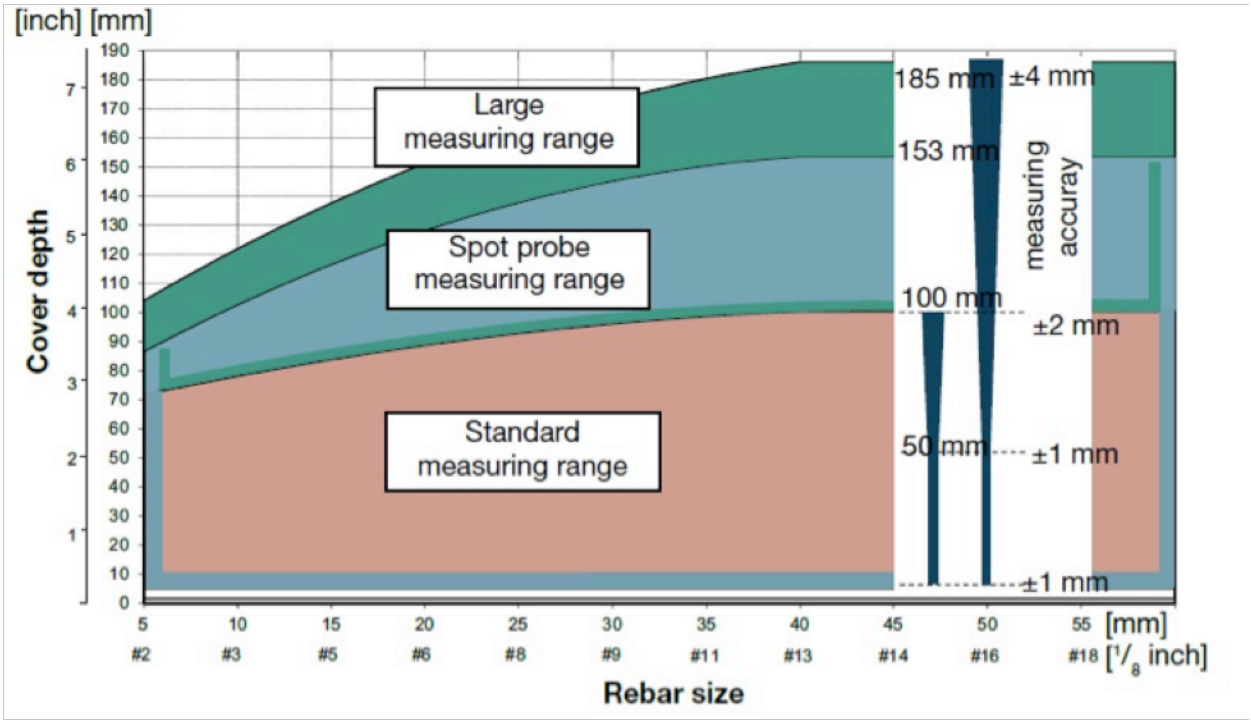

Figure 22 – The Measuring Range and Accuracy of Cover Depth (Proceq 2017)

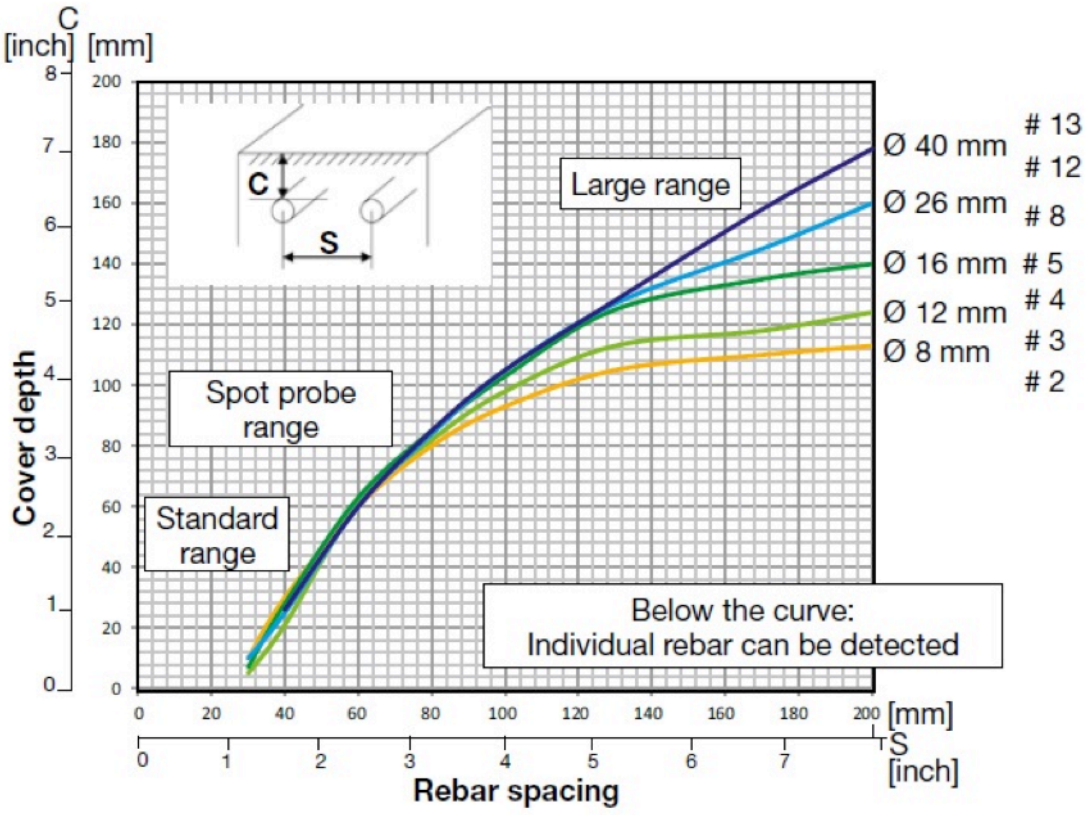

Figure 23 – The Minimum Limits for Spacing of Reinforcements (Proceq 2017)

Overall, the calibration process of GPR requires several preparations and settings prior to operation. The flowchart in Figure 24 presents a summary of how to calibrate GPR in the field. Based on the process explained in Section 5.1 and 5.2, GPR must first be prepared for the site investigation by adjusting its settings in compliance with the specifics of the pavement section. The location of longitudinal and transverse reinforcements should be determined by GPR together with Profometer. Next, a core is taken to confirm the concrete cover depth value and layer thicknesses. In the final step of the calibration process, the GPR unit is corrected using the measured data from the core or the predicted data from Profometer.

In a site investigation, there is no requirement to simultaneously perform the Profometer along with the operation of taking a core to calibrate GPR. For this project, both techniques were used in order to be able to evaluate the results predicted by Profometer. In the

general process, either a Profometer or a core might be utilized to calibrate the GPR unit. In the flowchart (Figure 24), all steps to calibrate GPR were indicated in the case that both Profometer and a core would be used. However, for this chart, each method used for this aim was determined to be optional.

5.3 Project Locations

In this task, a site survey including six different sites was conducted to evaluate CRCPs throughout the state of Georgia to identify characteristics indicative of reliable performance, and to determine the potential reasons for significant CRCP distresses such as punchouts. The GPR unit and Profometer recorded the placement of steel reinforcing bars within the CRC pavement slab. GPR images, which showed the location of the transverse cracks, punchout, and adjacent areas over four segments throughout 1.0mi (1.6km) were obtained for each site. This task was completed with relatively high frequency for the improved resolution of images required to identify the reinforcement height.

After selecting the project locations, including a review of CRCPs in Georgia that incorporated location, historical information, and pavement condition, a Geographic Information Systems (GIS) database was developed (Figure 25). CRCP locations were confirmed through the use of satellite imagery. Through this imagery, specific sections (MPs) were identified for testing. The six sites were selected based on condition and proximity, and were evaluated as being in good/fair or poor condition. Historical information for many of these sites was found and confirmed through a review of the pavement design/drawings found on Project Search (GeoPI). Based on the original typical sections for some CRCP sections of Interstates in Georgia, information about pavement was obtained from various sources and projects from the 1990s.

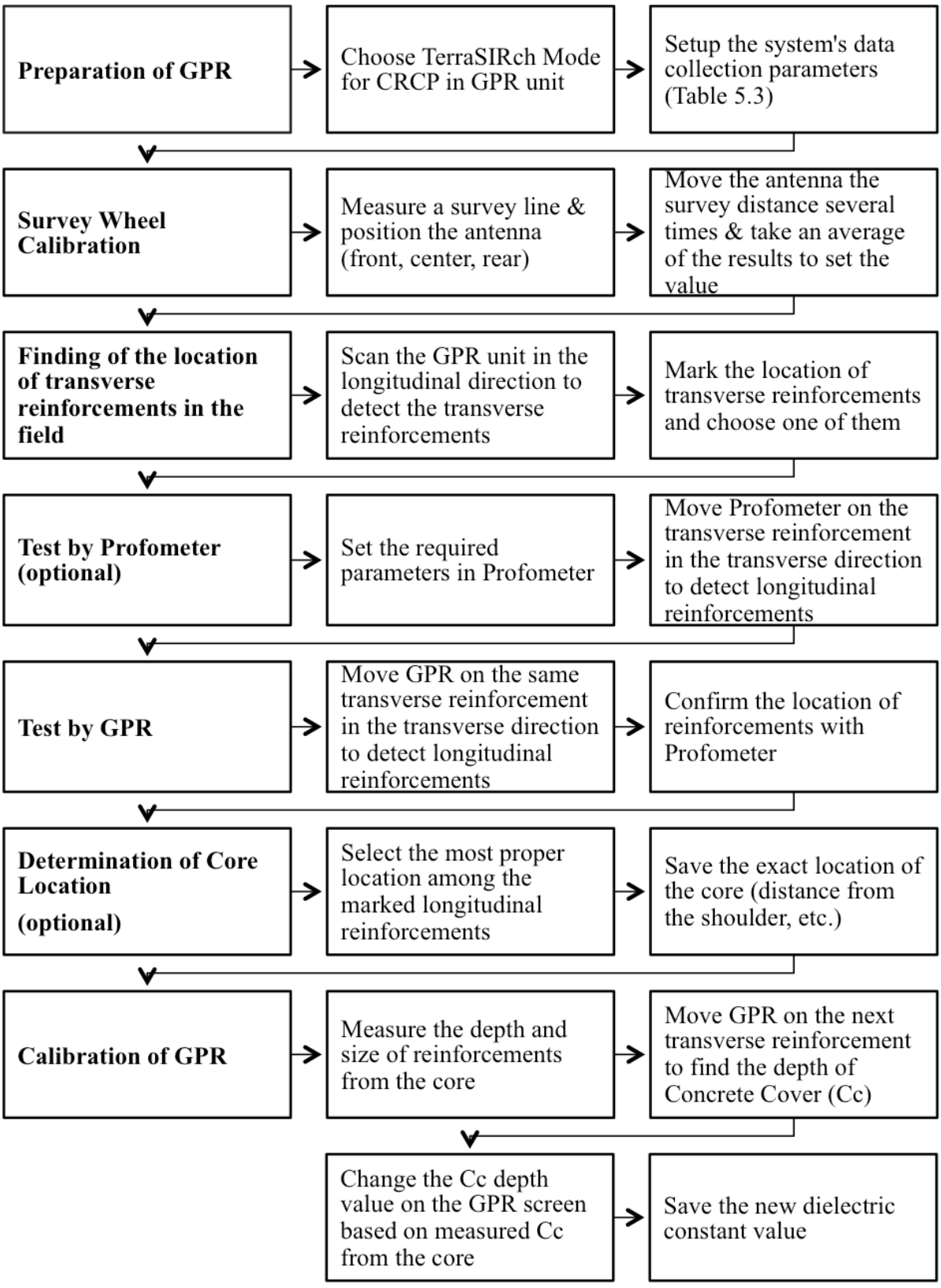

Figure 24 – The Flowchart of the Steps of the Calibration Process of GPR in the Field

The selected CRCP sections and their locations, together with their project name used in this study, are listed in Table 9.

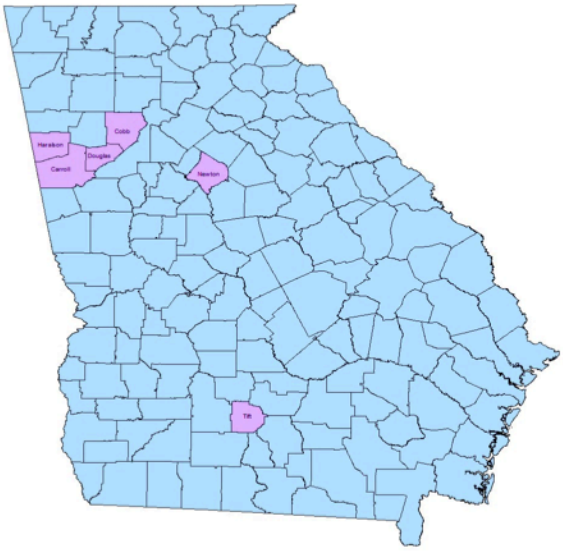

Figure 25 – Selected Sites in Georgia for RP 16-39

Table 9 – Information of Sites Selected in Georgia

Sorting of Site Surveys	Abbreviation of Site Names	Expansion of Site names
Site 1	SR6NBCMP0-1	**S**tate **R**oute **6** **N**orth **B**ound **C**obb County **M**ilepost **0-1**
Site 2	I20EBHMP4-5	**I**nterstate **20** **E**ast **B**ound **H**aralson County **M**ilepost **4-5**
Site 3	I20WBCMP24-25	**I**nterstate **20** **W**est **B**ound **C**arroll County **M**ilepost **24-25**
Site 4	I20EBNMP92-93	**I**nterstate **20** **E**ast **B**ound **N**ewton County **M**ilepost **92-93**
Site 5	I75NBCMP267-268	**I**nterstate **75** **N**orth **B**ound **C**obb County **M**ilepost **267-268**
Site 6	I75NBTMP57-58	**I**nterstate **75** **N**orth **B**ound **T**ift County **M**ilepost **57-58**

6. EXPERIMENTAL RESULTS

6.1 Analysis of GPR Images Using Post-Processing Software

This study aimed to analyze GPR data and images recorded during the field investigations by using a post-processing software program with the goal of presenting an overall summary report showing the details of the images such as the reinforcement position within the CRCP section, direction of traffic, etc.

Additionally, the data obtained from the survey investigations was transferred to a PC and analyzed by using a post-processing software program. The primary advantages of using post-processing software are that it allows the user to interpret data and visually review radargrams by (GSSI 2006):

- Using advanced processing and filtering capabilities
- Determining the correct velocity with migration
- Printing the output.

When using a GPR unit, radiowaves sent into the ground are reflected by buried objects below the ground. A receiver antenna detects and records the time taken for signals to be reflected back to the surface, which can then be used to determine the depth of the reflective object. The radargram is a measure of the reflection amplitudes and the travel time that the reflections take.

In this study, RadView software (compatible with the TerraSIRch SIR System-3000 GRP device) was used for the post-processing. The data collected from the site were uploaded to the program. Radargrams showing steel reinforcement locations, thicknesses of layers, and material properties such as frequency, dielectric values, etc., are presented in detail within this report section.

6.2 Definition of Terms

Project-specific terms utilized during the field investigation and post-processing of data are defined below.

- *Subsite* – The name given to each of the divided four segments of a site investigation.
- *Transverse direction* – The direction of site investigation performed from the shoulder to inner lane of the roadway.
- *Longitudinal direction* – The direction of site investigation performed in the direction of traffic.
- *Longitudinal Crack* – Crack that is predominantly parallel to the pavement centerline.
- *Single transverse crack* – Each transverse crack that is predominantly perpendicular to the pavement centerline.
- *Cluster of single transverse cracks* – A group of closely spaced transverse cracks.
    - Average of five or more consecutive transverse cracks with spacing less than 2 ft (61 cm) (Kohler and Roesler 2004).
- *Spacing between single transverse cracks* – The distance measured from one transverse crack to another in a cluster or separately.
- *Spacing between clusters of single transverse cracks* – The distance measured from the last single transverse crack in the cluster to the first single transverse crack in the next cluster.

6.3 Analysis and Synthesis of Outcomes

Based on information and knowledge collected from the field investigation, results were analyzed to answer the three questions identified in the 'Study Objectives' section (Section 1.2). In addition, the results were evaluated on whether they were within an acceptable range

according to the specifications. Furthermore, other factors that may affect the formation of distresses were recommended for future investigation, in conjunction with outcomes resulting from the field investigation and evaluation of the records.

The NDT methods, GPR and Profometer, were used at each site survey. The GPR unit was moved over the wheel path closest to the shoulder, on the outside lane of each site, to collect data in the longitudinal direction. A 6.00in (152mm) core was taken on the centerline of the slab at each site to measure the depth and size of longitudinal and transverse reinforcements and concrete layer thickness (Figure 26). The length of cores varied depending on the CRC thickness of the sites. The lengths of core specimens, including the asphalt layer, were 15.00in (381mm) for Sites 2, 4, and 6. The Site 1 core was 12.00in (305mm) in length and included a thin asphalt layer that was damaged during the process of coring. The core lengths for Site 3 and Site 5 were 9.00in (229mm) and 12.00in (305mm), respectively.

Figure 26 – Core Specimens taken from Site Investigations.

6.3.1 SR-6 Cobb County

6.3.1.1 Data Collection

Non-destructive testing methods were employed to conduct a forensic investigation of a CRCP site on State Route 6 in Cobb County using Ground Penetrating Radar (GPR) and a Profometer. State Route 6 (SR 6) is a state highway that runs northwest to southeast. Detailed information regarding the working procedures of these devices is provided in Section 5.1.

The outside lane on North Bound (NB) SR-6 located between MP 0 and MP 1 in Cobb County was investigated in this study. The CRC pavement was reported to be in relatively good condition, although it exhibited some visual signs of distress such as clusters of transverse cracks. The construction drawings obtained from GeoPI (see Appendix A) indicate that the section was built in 2005. The location of this site is shown in Figure 27.

Figure 27 – SR-6 MP 0-1 Cobb County Site Location (Google Maps, 2017)

The design and other parameters critical for assessing distress are presented in Table 10. The site exhibited clusters of transverse cracks. No punchouts were observed in the

1.0mi (1.6km) section. To confirm the size and location of longitudinal and transverse reinforcements and pavement thickness before collecting data, a 6.00in (152mm) core was taken from the site. The transverse crack pattern on the investigated lane is illustrated in Figure 28. The section was constructed as a 12.00in (305mm) CRC slab above a 0.75in (19mm) recycled asphaltic concrete layer over a 12.00in (305mm) thick graded aggregate base layer. The longitudinal and transverse reinforcements consisted of #6 and #4 grade 60 rebar, respectively. The concrete cover depth to the top of the longitudinal reinforcement was measured to be 3.50in (89mm) from the core specimen. The site was investigated in four stages in terms of density of crack types and existence of other distress types. The stages were denoted as S1-a, S1-b, S1-c, and S1-d. They refer to the first (a), second (b), third (c), and fourth (d) subsite (S) number (1) or 'S1' segments of the SR6 site examined in this study.

Table 10 – CRC Design Parameters and NDT Results for SR6NBCMP0-1

SR-6 COBB COUNTY	**Design Parameters**						
	Site Condition	Age (Years)	CRC Thickness (in)	Longitudinal Rebar Size/ Spacing (in)	Transverse Rebar Size/ Spacing (in)	Longitudinal Rebar Depth (in)	Transverse Rebar Depth (in)
	Good	12 (2005)	12.00	#6 / 5.00	#4 / 36.00	3.50	4.40
	Distress Parameters Examined						
	Spacing between single transverse cracks (ft)		Spacing between clusters of transverse cracks (ft)		Transverse crack width (in)	Longitudinal crack width (in)	Number of Punchouts / mile
	1.0~ 4.0 (typical 1.0)		46.0		0.04 ~ 0.14 (typical 0.08)	0.00	0

The site had transverse cracks in groups at close intervals, i.e. cluster cracking, as shown in Figure 29. The minimum and maximum distance between the clusters of transverse

cracks was measured as approximately 46.0ft (14.0m). The single transverse cracks were spaced at the range of approximately 1.0-4.0ft (0.3-1.2m) as shown in Figure 28 with a typical spacing of 1.0ft (0.3m). Transverse crack widths were measured with a crack gauge tool illustrated in Figure 30 and varied in the range of 0.04-0.14in (1-4mm) with a typical width of 0.08in (2mm). There were no visible longitudinal cracks.

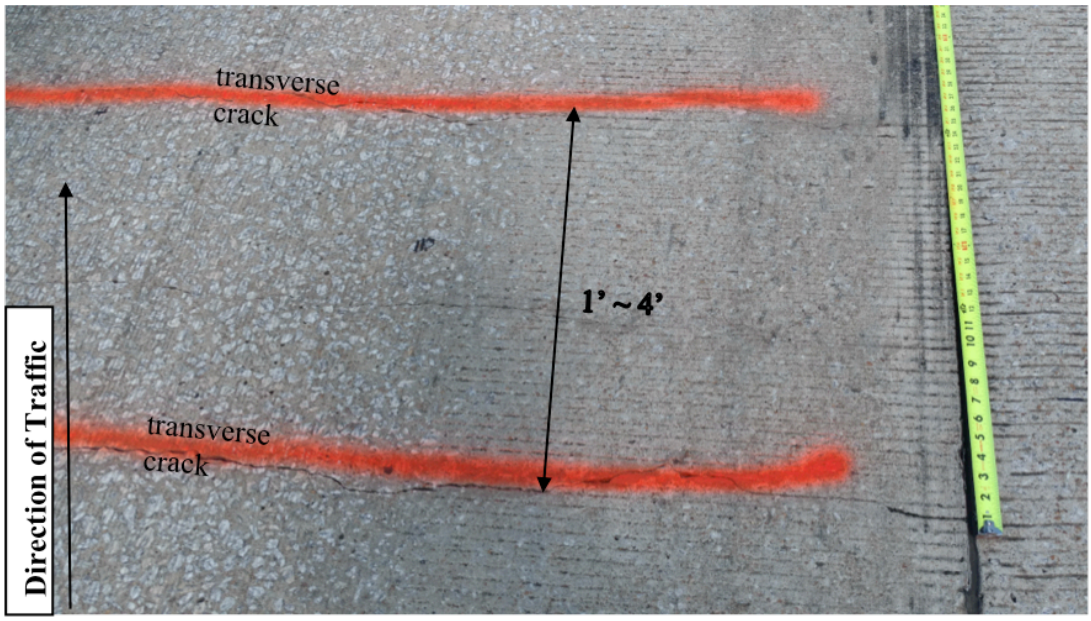

Figure 28 – Typical Single Transverse Crack Pattern (S1-b)

6.3.1.2 Data Post-Processing

The GPR unit scans were visualized in RadView software. Figure 31 shows the location of four transverse reinforcement bars and the concrete pavement layer thickness through the vertical profile. Based on findings, the sections for which cracks formed were over the steel transverse reinforcements. The site did not show significant depth change of transverse and longitudinal reinforcements across the section scanned. Figure 32 indicates the depth of longitudinal reinforcement and CRC thickness in the transverse direction. The longitudinal reinforcement bars are placed lower from the top surface toward the fast lane of the surveyed section.

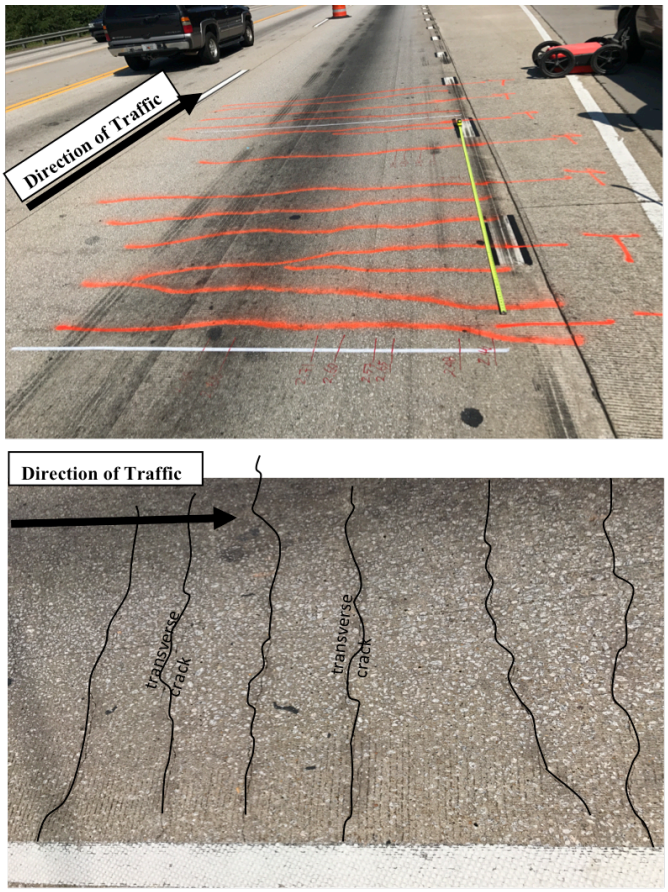

Figure 29 – Typical Cluster Crack Pattern at S1-a and S1-b

Figure 30 – Crack Width Measuring at S1-b, S1-c, and S1-d

Each subsite segment was scanned by GPR and Profometer. At least ten single transverse cracks existed within each cluster. It was also observed that most cracks were formed over the transverse reinforcement. The depth of longitudinal rebar varied throughout the 1.0mi (1.6km)

section. Figure 33 illustrates the crack pattern and the change in concrete cover depth along this section. The GPR values in the graph indicate the average depth of longitudinal reinforcements, which were located over one transverse reinforcement selected from the distressed area in each segment.

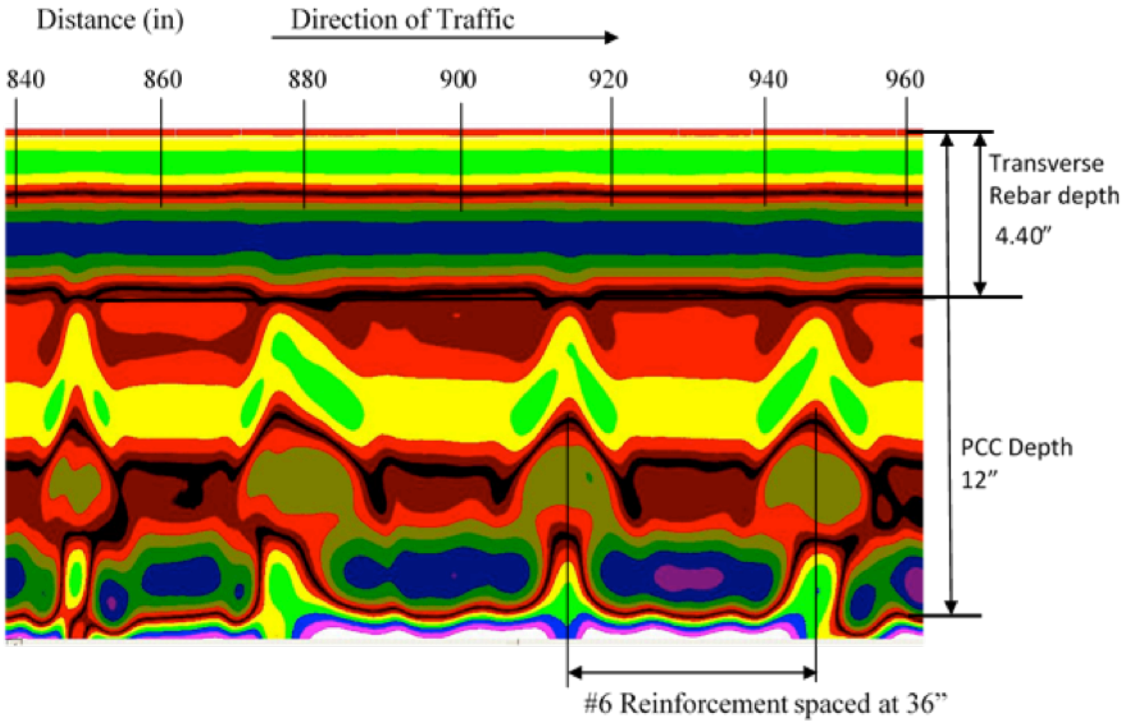

Figure 31 – GPR Scan in the Longitudinal Direction (S1-b)

6.3.1.3 Interpretation of Radargrams and Findings

As shown in Figure 33, the depth of longitudinal reinforcement at subsite 'S1-c' is deeper than the other three segments when examined from the top surface. In addition, as shown in the crack pattern, the S1-c had the largest number of cracks among the four segments. The investigators believe the density of cracks relates to the concrete cover depth.

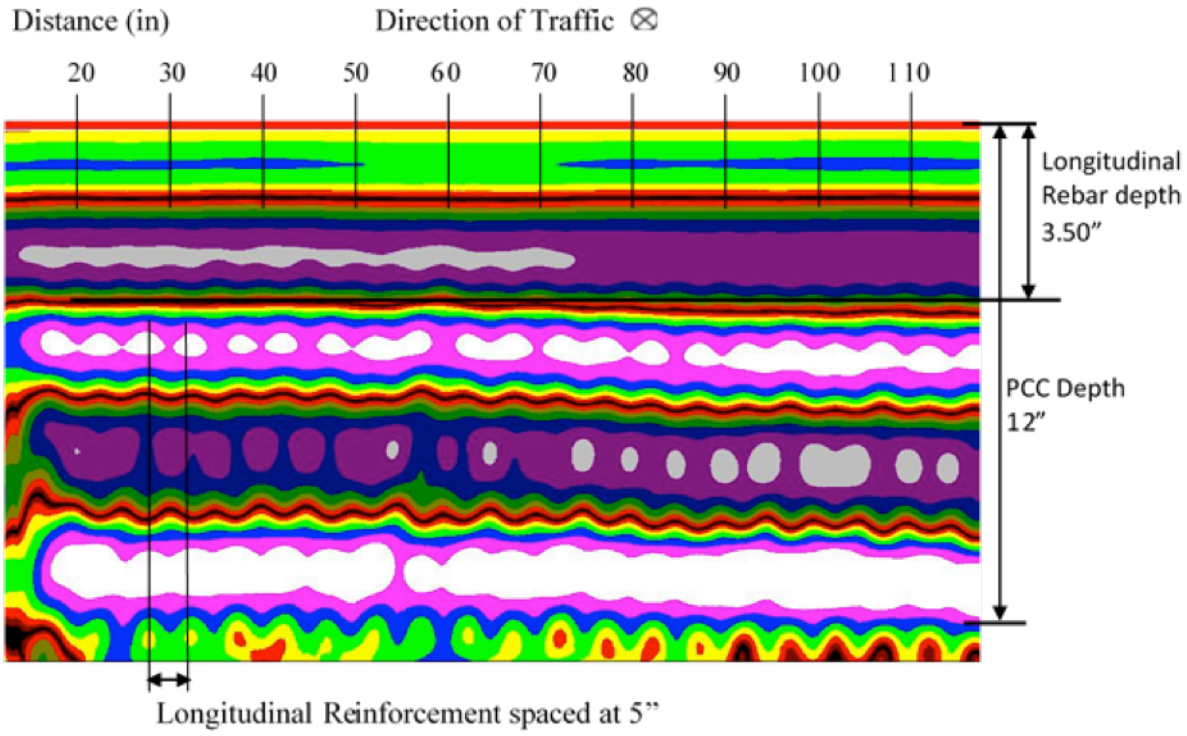

Figure 32 – GPR Scan in the Transverse Direction (S1-b)

Figure 34 and Figure 35 provide a direct comparison of the depths of longitudinal reinforcement detected by GPR and Profometer, between two single-transverse cracks in the transverse direction (S4-d). Before the GPR unit was calibrated, the depth collected from the site was deeper than the actual rebar depth from the surface (Figure 34). This illustrates that calibration of the concrete cover depth is critical. After sampling a core from the site, at the location shown in Figure 35, the cover depth measurement in GPR was calibrated to the measured actual depth, 3.50in (89mm), from the core. When calibration was completed successfully, the rebar cover depth measurements collected by GPR unit and Profometer agreed closely, as illustrated in Figure 35. This indicates that Profometer depth measurements may be used in the absence of a cored sample to calibrate a GPR device.

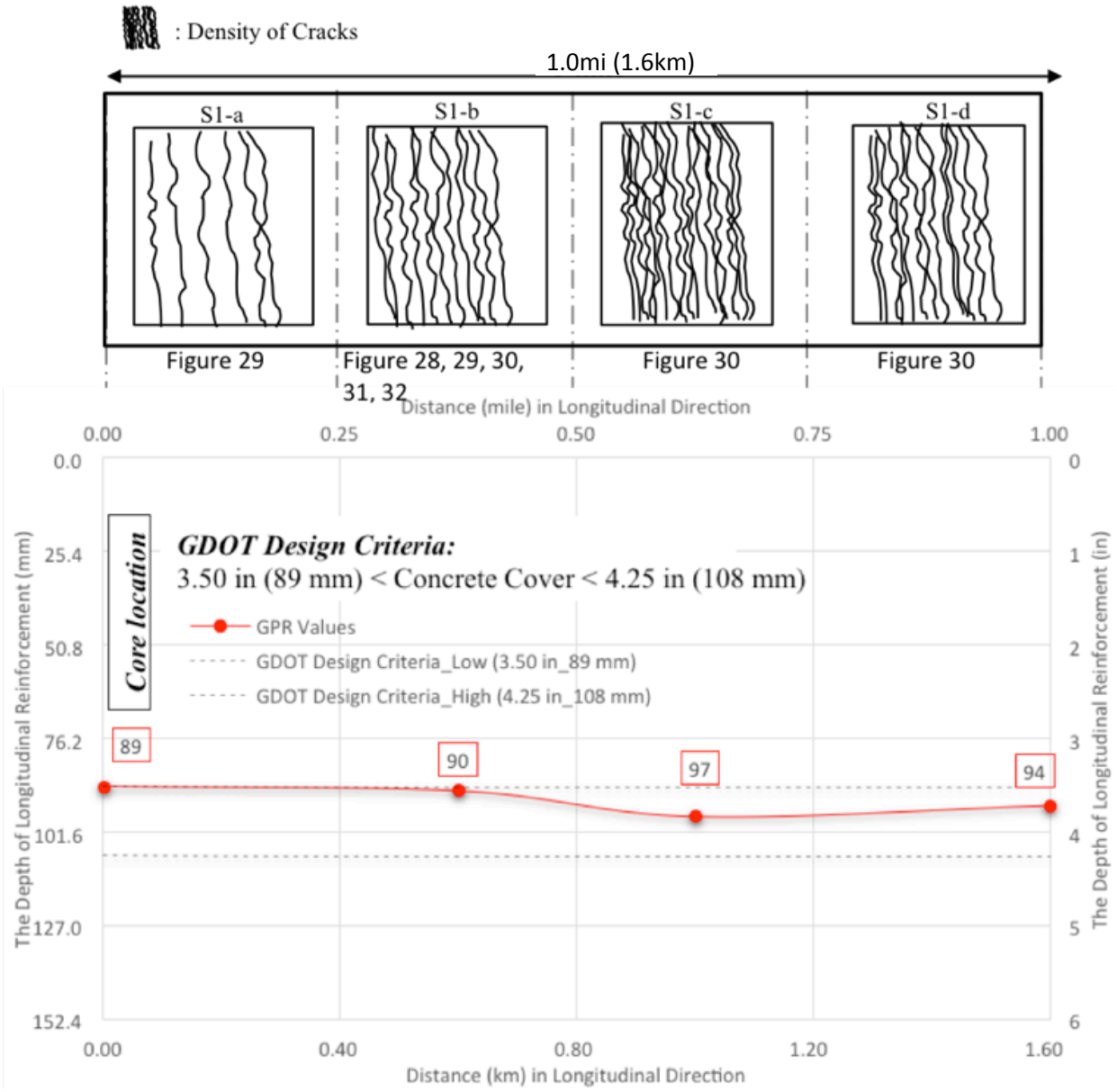

Figure 33 – Distress Pattern and Concrete Cover in Longitudinal Direction in Each Segment Along the 1.0mi (1.6km) Surveyed Site

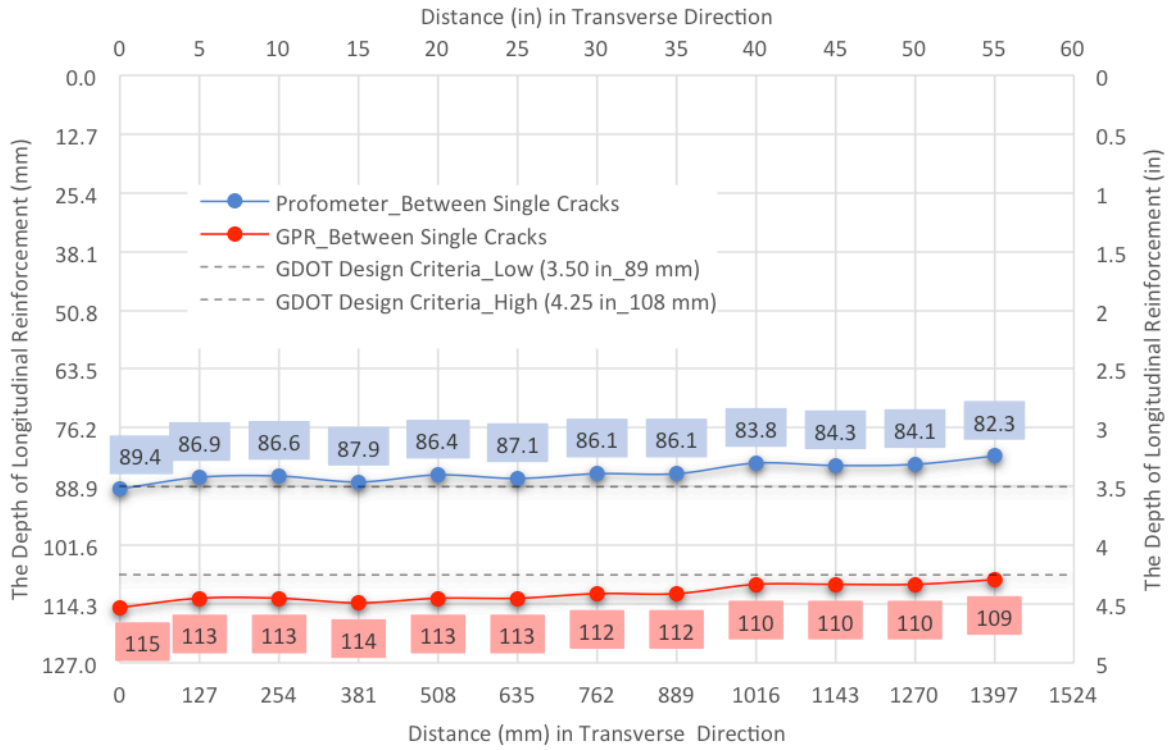

Figure 34 – Concrete Cover Depth Values Detected by Non-Calibrated GPR and Profometer in Transverse Direction at S1-d

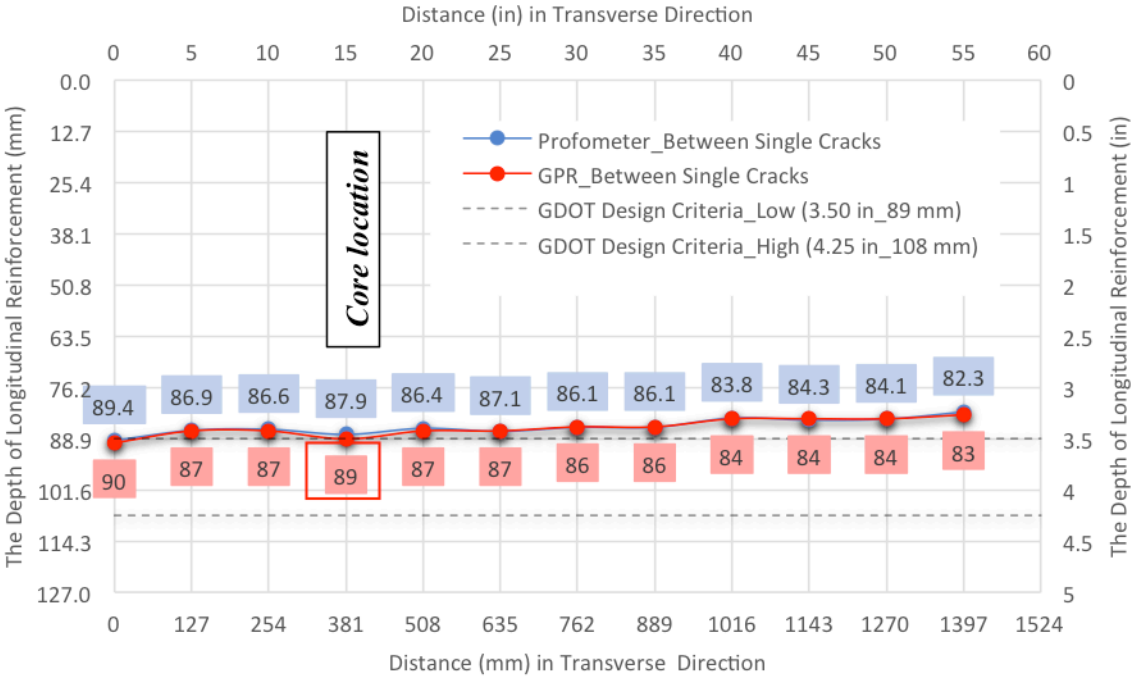

Figure 35 – Concrete Cover Depth Values Detected by Calibrated GPR and Profometer in Transverse Direction at S1-d

6.3.2 I-20 - Haralson County

6.3.2.1 Data Collection

Non-destructive tests were carried out on Interstate 20 in Haralson County using a Ground Penetrating Radar (GPR) device and Profometer. Detailed information regarding the working procedures of these units is presented in Section 5.1. The outside lane on East Bound (EB) I-20 located between MP 4 and MP 5 was selected for inclusion in this study. The CRC pavement was reported to be in good condition and exhibited clusters of transverse cracks. The construction drawings obtained from GeoPI (see Appendix B) indicate that the section was built in 1980. The location of this site is shown in Figure 36.

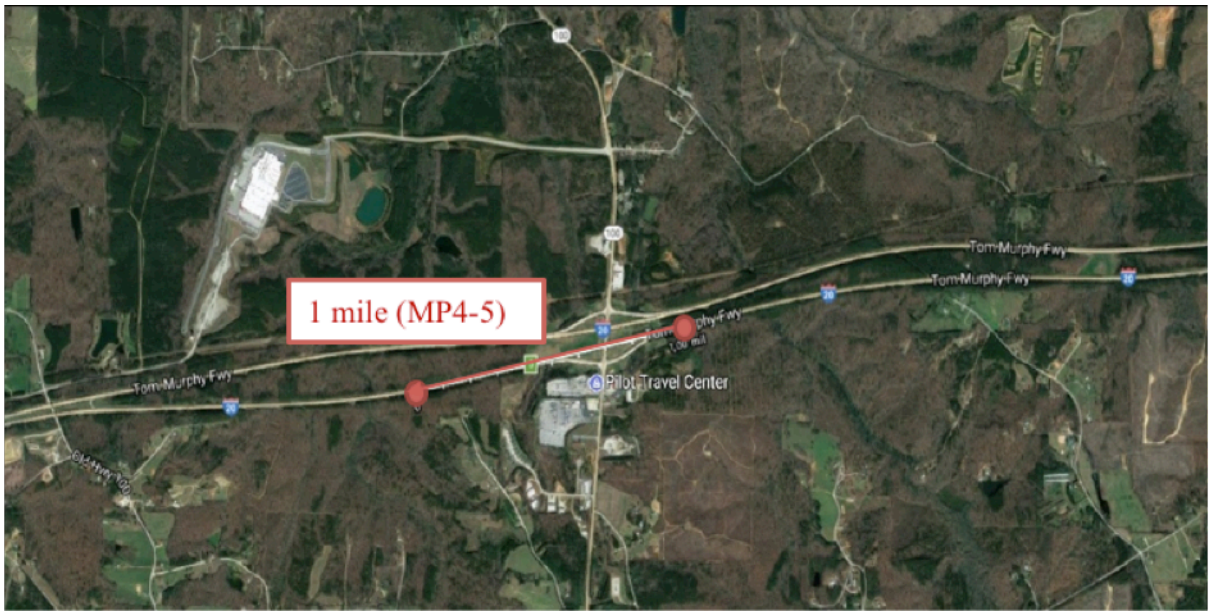

Figure 36 – I-20 MP 4 to MP 5 Haralson County Site Location (Google Maps, 2017)

The design parameters and distress parameters are presented in Table 11. The site exhibited clusters of transverse cracks and had no signs of concrete spalling or punchouts. To confirm the size and location of longitudinal and transverse reinforcement and pavement

thickness before collecting data, a 6.00in (152mm) diameter cored specimen was extracted from the site.

The transverse crack pattern on the investigated lane is shown in Figure 37. The section was constructed as an 11.00in (280mm) thick CRC slab above a 0.75in (19mm) asphalt concrete layer and 12.00in (305mm) thick graded aggregate (cement stabilized) subbase. However, the concrete layer thickness was measured 12.00in (305mm) from the cored specimen. The longitudinal and transverse reinforcement consisted of #6 rebar. The concrete cover depth to the top of the longitudinal reinforcement was measured to be 4.25in (108mm) from the cored specimen. The site was investigated in four stages in terms of density of crack types and existence of other distress types. The stages were referred to as S2-a, S2-b, S2-c, and S2-d. These refer to the first (a), second (b), third (c), and fourth (d) subsite (S) number (2) or 'S2' segments of the surveyed site.

Table 11 – CRC Design Parameters and NDT Results for I20EBHMP4-5

	Design Parameters						
HARALSON COUNTY	Site Condition	Age (Year)	CRC Thck. (in)	Longitudinal Rebar Size/ Spacing (in)	Transverse Rebar Size/ Spacing (in)	Longitudinal Rebar Depth (in)	Transverse Rebar Depth (in)
	Good	37 (1980)	12.00	#6 / 4.00 ~ 8.00	#6 / 23.00 ~ 46.00 (typical 39")	4.25	5.00
	Distress Parameters Examined						
	Spacing between single transverse cracks (ft)	Spacing between clusters of transverse cracks (ft)		Transverse crack width (in)		Longitudinal crack width (in)	Number of Punchouts / mile
	1.6 ~ 4.0 (typical 1.6)	24.0		0.03 ~ 0.10 (typical 0.08)		0.00	0

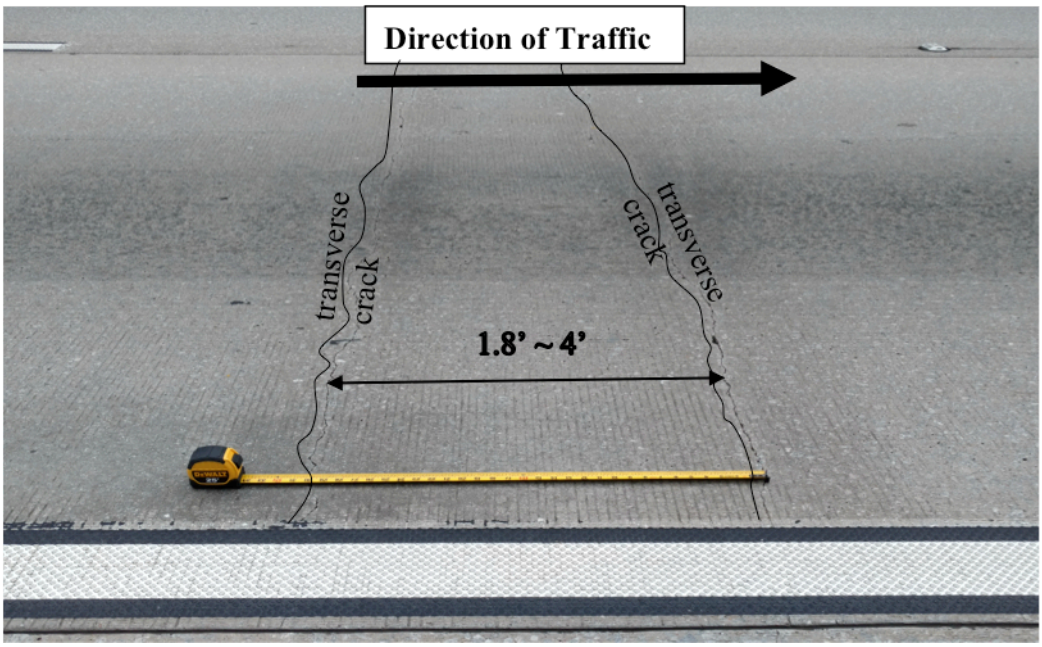

Figure 37 – Typical Single Transverse Crack Pattern (S2-a)

The single transverse cracks were spaced at the range of approximately 1.8-4.0ft (0.6-1.2m) with a typical crack space of 1.6ft (0.5m), as shown in Figure 37. The site had cluster cracks as shown in Figure 38. The measured distance between the clusters of transverse cracks was approximately 24.0ft (7.3m). Typical transverse crack width ranged from 0.03-0.10in (1-3mm). The site had many visible popouts caused by deleterious near-surface aggregate particles on the pavement surface, as shown in Figure 39. The popouts fit in the grid size of 1.5in x 3in (38mm x 76mm). No visibly longitudinal cracks were observed.

Figure 38 – Typical Cluster Transverse Cracks Pattern at (a) S2-a and (b) S2-c

Figure 39 – The Measurement of Crack Widths at S2-a and S2-c

6.3.2.2 Data Post-Processing

The GPR scans were visualized using RadView software. Figure 40 presents the location of four reinforcement bars and the concrete pavement layer thickness. Radargrams presented in this report were created using a consistent color scheme.

6.3.2.3 Interpretation of Radargrams and Findings

A parameter to be considered is the concrete cover depth as it varies among the top points of reflections in a radargram. This is due to the presence of transverse reinforcement bars with the dielectric constant approaching infinity. The tip of the hyperbola is formed when the GPR antenna is located directly at the top of reinforcement bars. Figure 40 shows the depth of the last transverse reinforcement when the pavement section was scanned in the longitudinal direction. The color change at the tip of the hyperbola indicates the existence of a crack at the reinforcement location. This means that more transverse cracks may develop when the transverse reinforcement is placed deeper below the top surface. Figure 41 indicates the depth of longitudinal reinforcement and CRC thickness when the pavement section was scanned in the transverse direction.

In the selected site, the depth of longitudinal rebar varied throughout the 1.0mi (1.6km) section, possibly due to construction practices. Typically the transverse bars are placed on chairs, with the longitudinal bars arranged on top. The S2-a and S2-c sections were scanned by both GPR and Profometer. There were over ten single transverse cracks in each cluster. In addition, most of these cracks were formed above the transverse bars. The S2-b and S2-d sections indicated the same repetitive crack distress pattern.

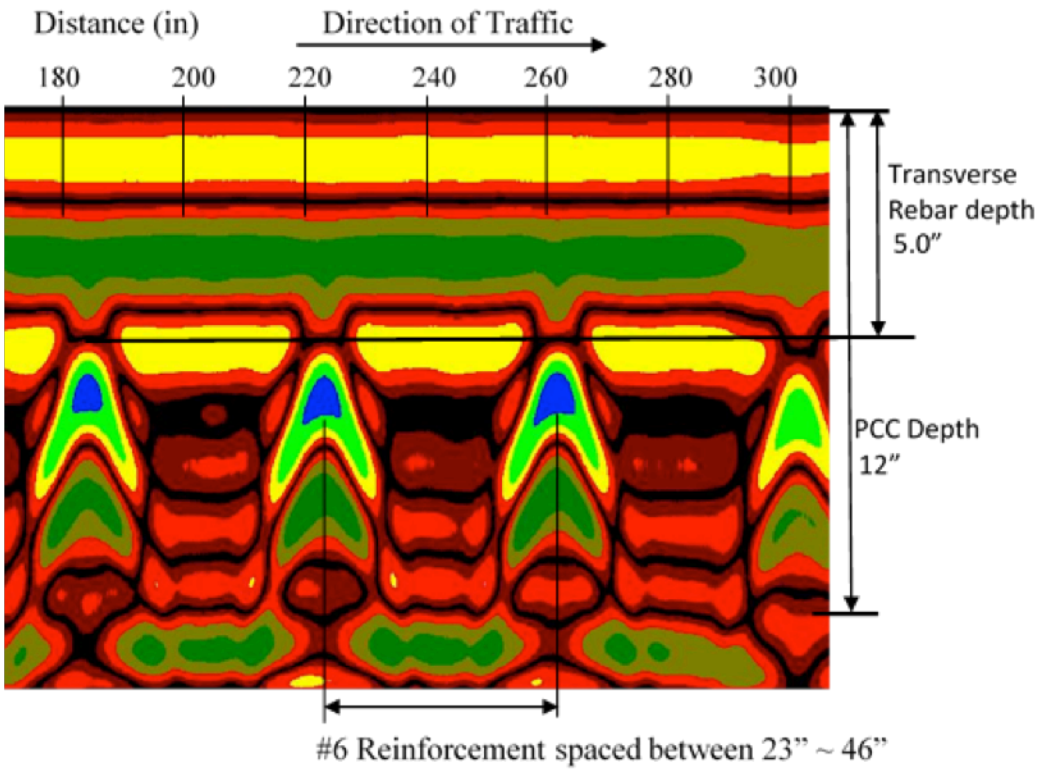

Figure 40 – GPR Scan in the Longitudinal Direction (S2-b)

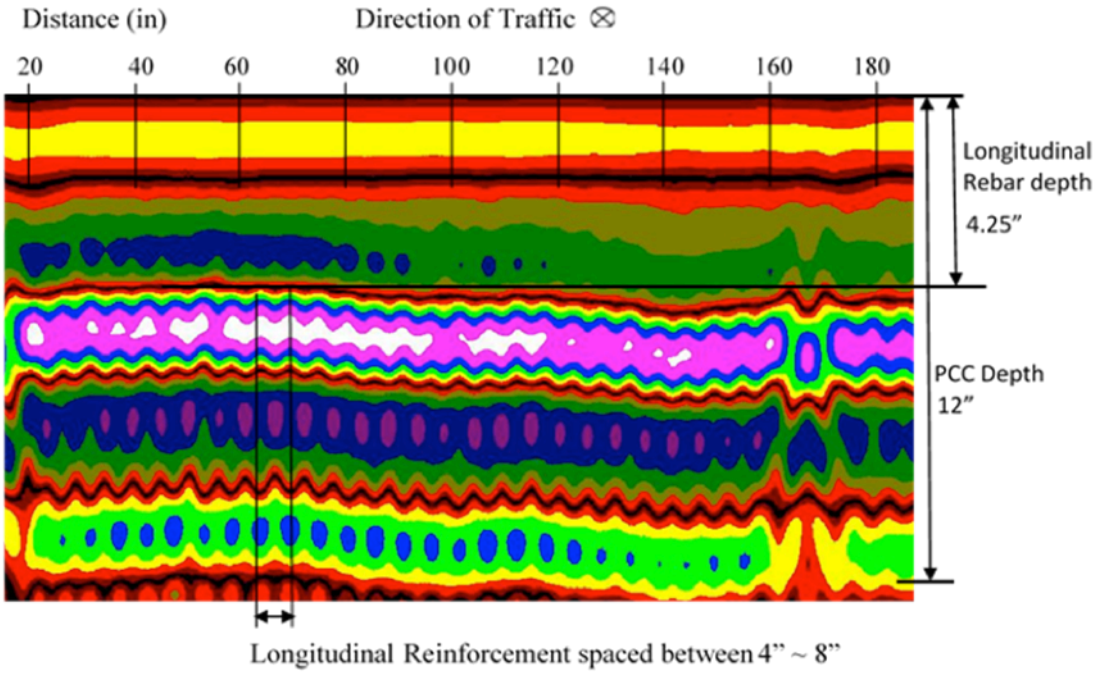

Figure 41 – GPR Scan in the Transverse Direction (S2-c)

It was observed that the reinforcement at S2-a and S2-c were placed at 4.25in (108mm) and 4.45in (113mm) below the top surface, which are outside the recommended range by GDOT. It was also observed that these two sites exhibit more severe symptoms of distress, as illustrated in Figure 42. The S2-c segment exhibits the most cracks on the pavement surface, followed by the S2-a segment.

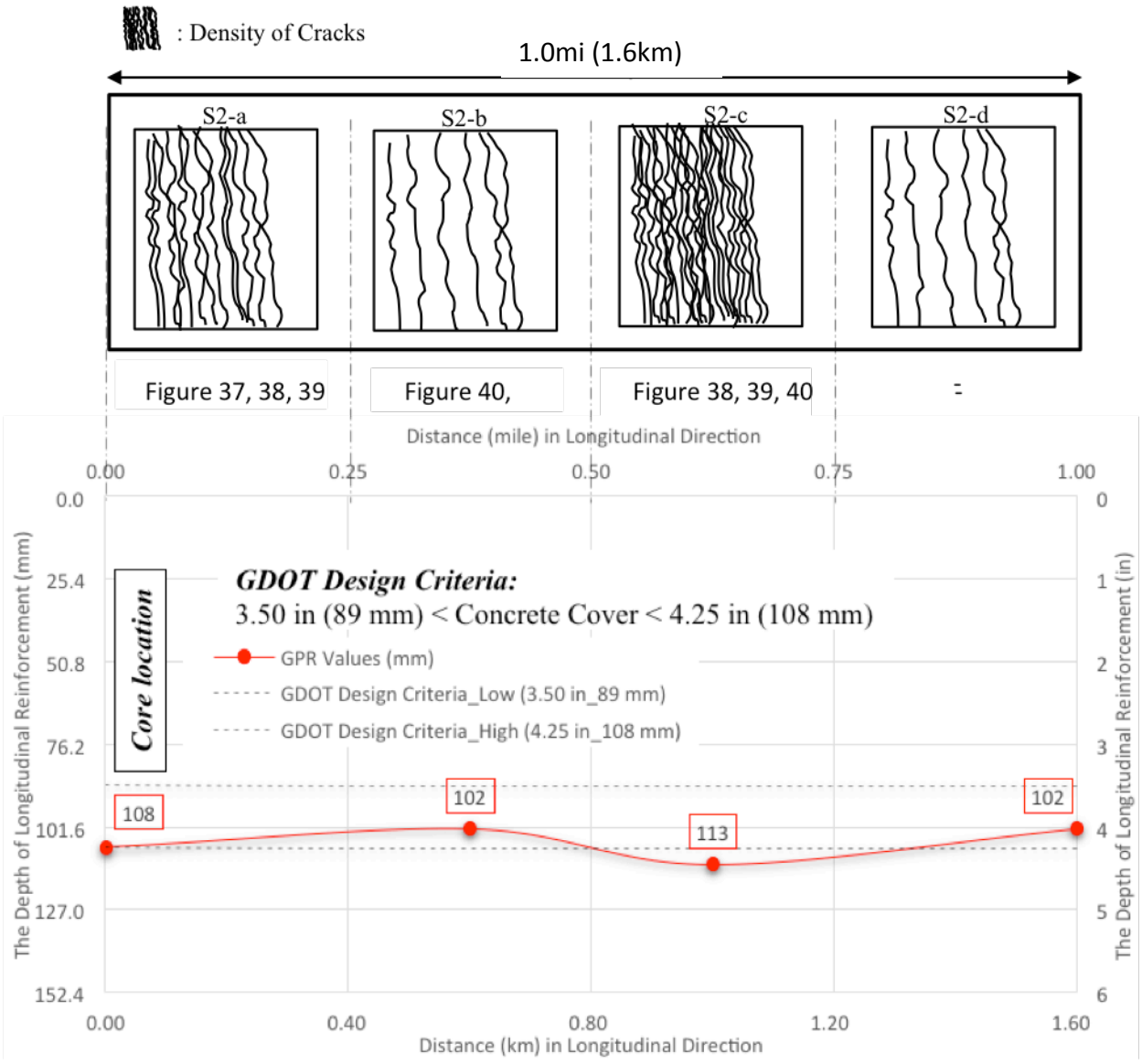

Figure 42 – Distress Pattern and Concrete Cover to Transverse Bars in Each Segment Along the 1.0mi (1.6km) Surveyed Site

The following graph (Figure 43) indicates the depths of the longitudinal bars, which were detected from the core location (S2-a) in the transverse direction. The GPR scan was collected from the shoulder to the adjoining inner lane by GPR and Profometer. Although the depth measurements taken by both devices produce a similar pattern in the graph, these measurements do not agree well (Figure 43). The reason for this is believed to be the result of varied materials, such as metal or other pieces of steel, which can be detected easily by Profometer units and thus form a basis for error. In addition, the cracks were observed to continue into the shoulder. As shown in the graph, the depth of longitudinal bars was lower near the shoulder. Regardless of the disagreement between the two devices, it is concluded that the concrete cover affects the density and/or severity of cracks as it did with the first site (or S1).

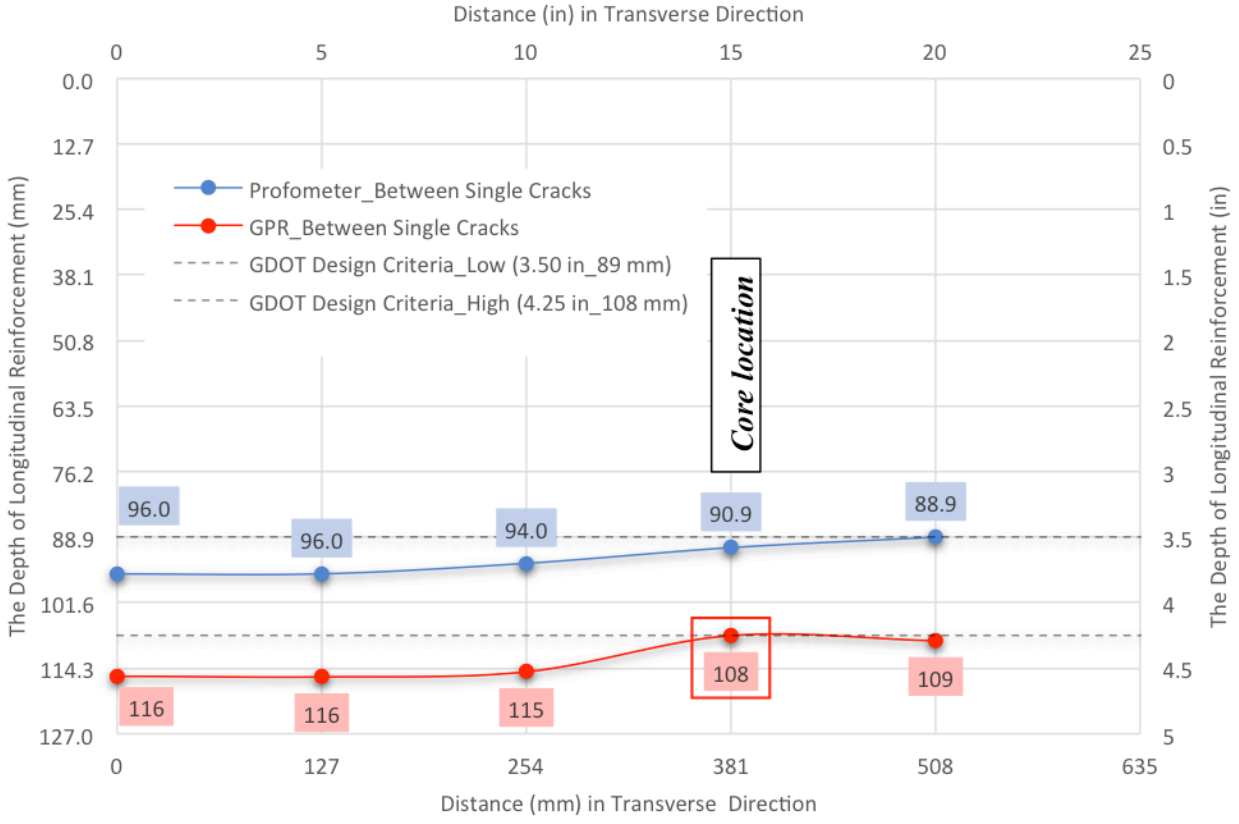

Figure 43 – Concrete Cover Depth Values Detected by calibrated GPR and Profometer in Transverse Direction at S2-a

6.3.3 I-20 - Carroll County

6.3.3.1 Data Collection

Non-destructive tests were conducted on Interstate 20 in Carroll County by means of the Ground Penetrating Radar (GPR) and Profometer. Detailed information regarding the working procedures of these units is presented in Section 5.1.

The outside lane on West Bound (WB) I-20 located between MP 24 and MP 25 in Carroll County was investigated. The CRC pavement was reported to be in poor condition and thus exhibited many visible distresses such as transverse cracks, punchouts, and patched areas. The original construction drawings obtained from GeoPI (see Appendix C) indicate that the section was built in 1972, although the drawings were last revised in 1976. The location of this site is shown in Figure 44.

Figure 44 – I-20 MP 24 to MP 25 Carroll County Site Location (Google Maps, 2017)

The design and distress parameters are presented in Table 12. The site exhibited several punchouts, patched areas, and a few severe cracks. It was determined that the selected section

had approximately 10 punchouts per mile. Based on the investigation, the number of patched areas appears to be a good indicator for the occurrence of punchouts.

Table 12 – CRC Design Parameters and NDT Results for I20WBCMP24-25

	Design Parameters						
CARROLL COUNTY	Site Condition	Age (Years)	CRC Thickness (in)	Longitudinal Rebar Size/ Spacing (in)	Transverse Rebar Size/ Spacing (in)	Longitudinal Rebar Depth (in)	Transverse Rebar Depth (in)
	Poor	45 (1972)	8.70	#6 / 8.00	-	4.00	-
	Distress Assessment						
	Spacing between single transverse cracks (ft)		Spacing between clusters of transverse cracks (ft)		Transverse crack width (in)	Number of Punchouts / mile	
	5.0-6.5		10.0 ~ 20.0		0.06 ~ 0.12 (typical 0.10)	10	

The transverse crack pattern on the investigated lane is shown in Figure 45. The section was constructed as a 9.00in (229mm) thick CRC slab above a 1.00in (25mm) thick asphalt concrete layer over a 5.00in (127mm) thick graded aggregate (cement stabilized) subbase layer. However, the concrete layer thickness was measured as 8.70in (221mm) from the cored specimen, which is 3.70in (94mm) thicker than what the drawing indicates. The longitudinal and transverse bars consisted of #6 bars. It was observed that there was no transverse reinforcement throughout the investigated section, although two transverse bars were found at irregular locations. The concrete cover depth to the top of the longitudinal bar was measured to be 4.00in (102mm) from the core specimen. The site was investigated in four stages in terms of density of cracks, crack types, and the existence of other distress. The stages were denoted as S3-a, S3-b,

S3-c, and S3-d. These refer to the first (a), second (b), third (c), and fourth (d) subsite (S) number (3) of 'S3' segments of the Carroll County site.

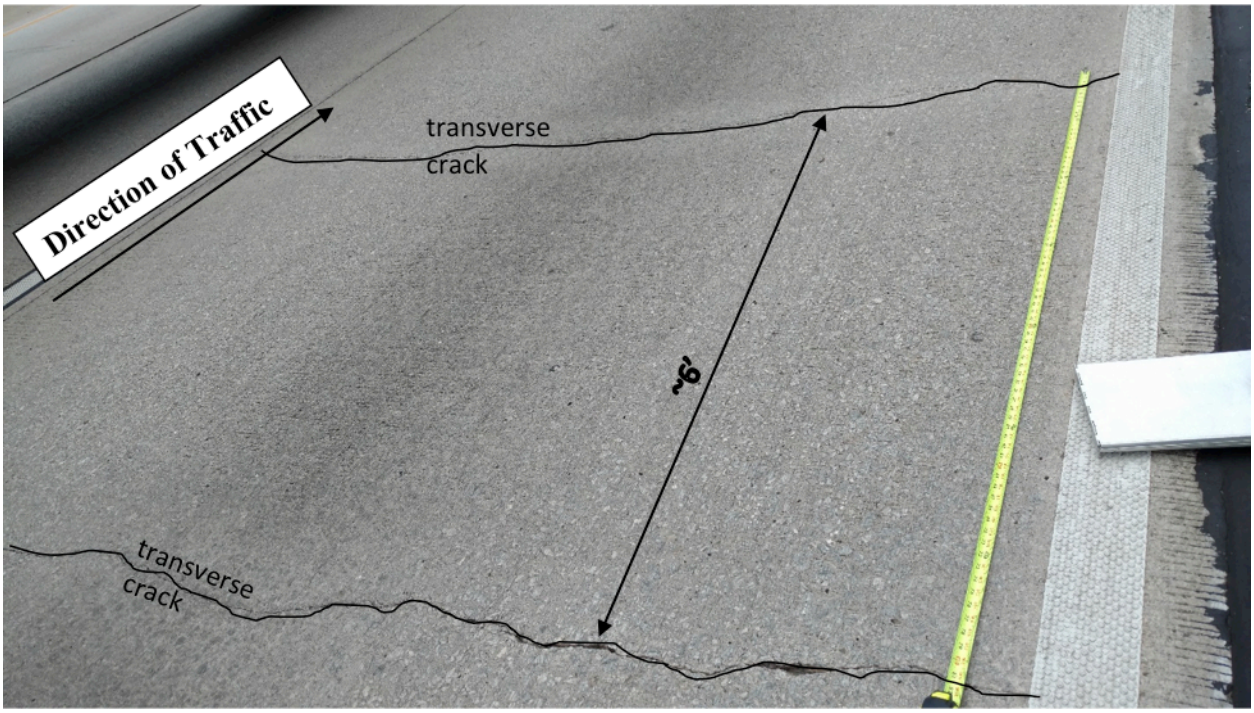

Figure 45 – Typical Single Transverse Crack Pattern (S3-a)

The site had a considerable number of cluster transverse cracks, as shown in Figure 46. The minimum and maximum distance between the clusters of transverse cracks were measured to range from 10.0-20.0ft (3.1-6.1m). The single transverse cracks were spaced at the range of approximately 5.0-6.5ft (1.5-2.0m), as shown in Figure 45. It was detected that the site had punchouts at the location of the cluster transverse cracks (Figure 46). As illustrated in Figure 47, the crack widths were measured using a crack width gauge and varied from 0.06-0.12in (2-3mm).

Figure 46 – Typical Cluster Transverse Cracks Pattern at S3-a and S3-c

A few patched areas observed in this project were examined using GPR and Profometer. Although the punchout areas had been previously patched, the repairs had become severely distressed again, with significant punchouts observed during the field investigation. Figure 48 and Figure 49 show the patched area with a punchout at S3-b during investigation. Another problem area was located near MP 24 WB. This area had a few punchouts on the wheel-path located on the patched area near the inside lane (S3-d), as shown in Figure 50 and Figure 51.

Figure 47 –Crack Width Measuring at S3-a

Figure 48 – A Patched Area of the Outside Lane at S3-b

Figure 49 – A Patched Area of the Outside Lane at S3-b (Google Maps, 2017)

Figure 50 – A Patched Area of the Outside Lane at S3-d

Figure 51 – A Patched Area of the Outside Lane at S3-d (Google Maps, 2017)

6.3.3.2 Data Post-Processing

While the GPR unit scans the varied materials with different dielectric constant values, the results show the different reflections and color in the GPR images. The following images were obtained using RadView software. Figure 52 clearly shows the layer thickness, since this location does not have transverse reinforcement. Figure 53 indicates the depths of longitudinal reinforcements and layer thicknesses in the transverse direction.

6.3.3.3 Interpretation of Radargrams and Findings

There was no transverse reinforcement throughout the 1.0mi (1.6km) section of the selected site. The S3-a was scanned by GPR and Profometer. The S3-b had an increased number of punchouts and patched areas, as well as cracks. Along the site, section S3-c had the largest amount of irregular cracking. Section S3-d exhibited significant punchouts and patched areas.

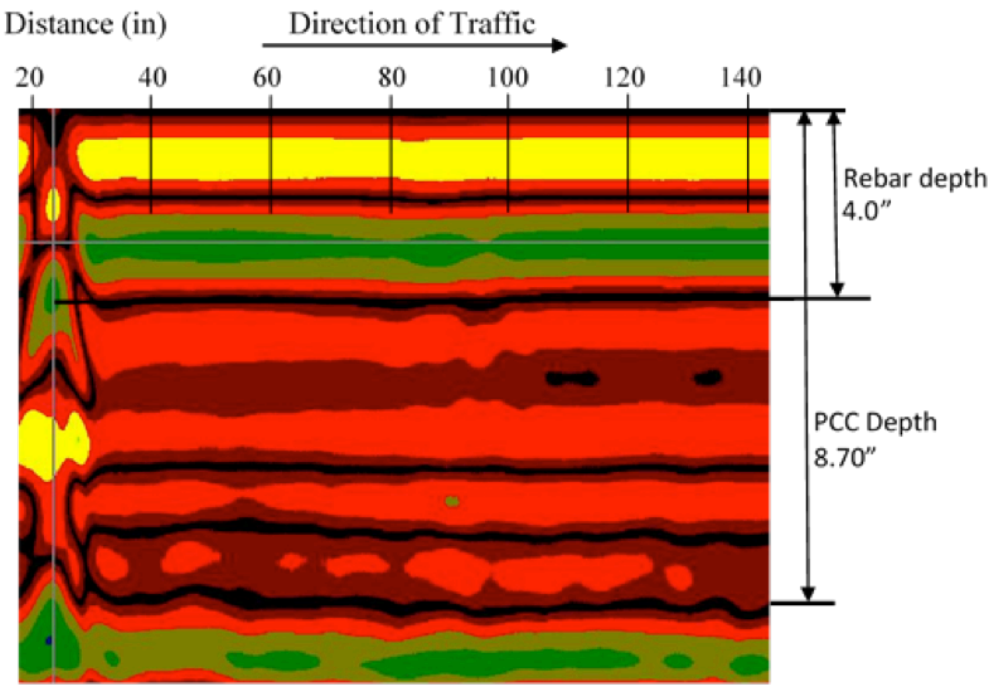

Figure 52 – GPR Scan in the Longitudinal Direction (S3-a)

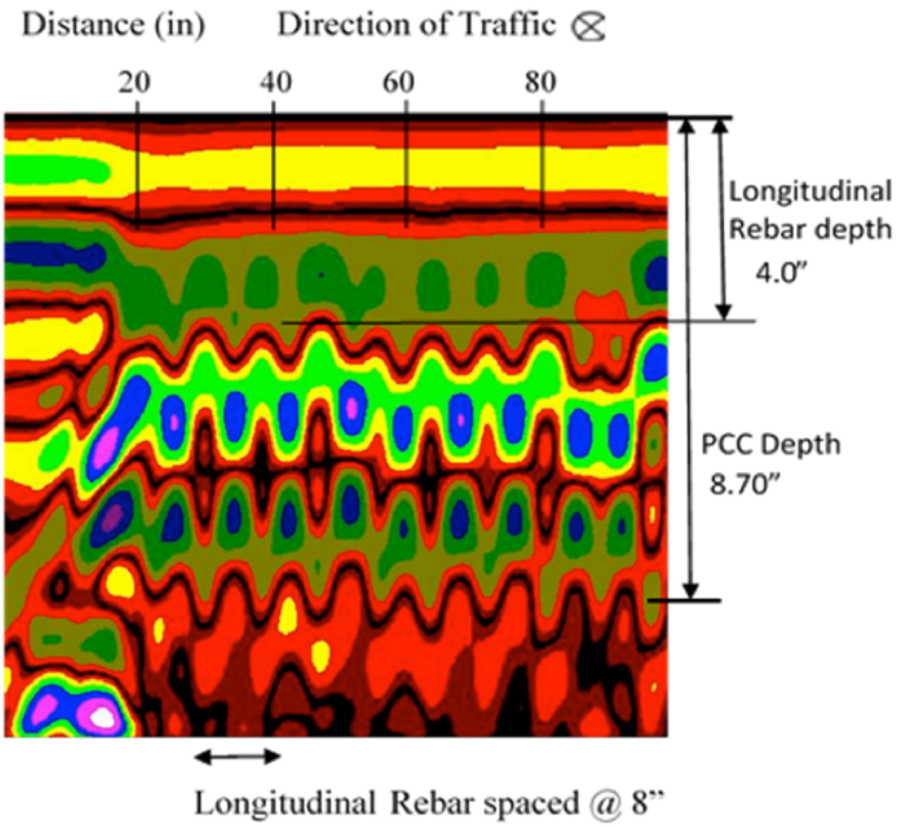

Figure 53 – GPR Scan in the Transverse Direction (S3-a)

The graph in Figure 54 indicates the location of core, patched area, and transverse cracks. The GPR data at S3-b and S3-d were collected from left, over, and right of the patched area that had high severity punchouts at the edges. It showed that the longitudinal bars were deeper at the location of the patched area than to the left and right. The S3-c segment, surveyed over the cluster cracking area, had the deepest longitudinal rebar location and relatively more cracks. In addition, the concrete cover depth measurements were outside the range recommended by GDOT.

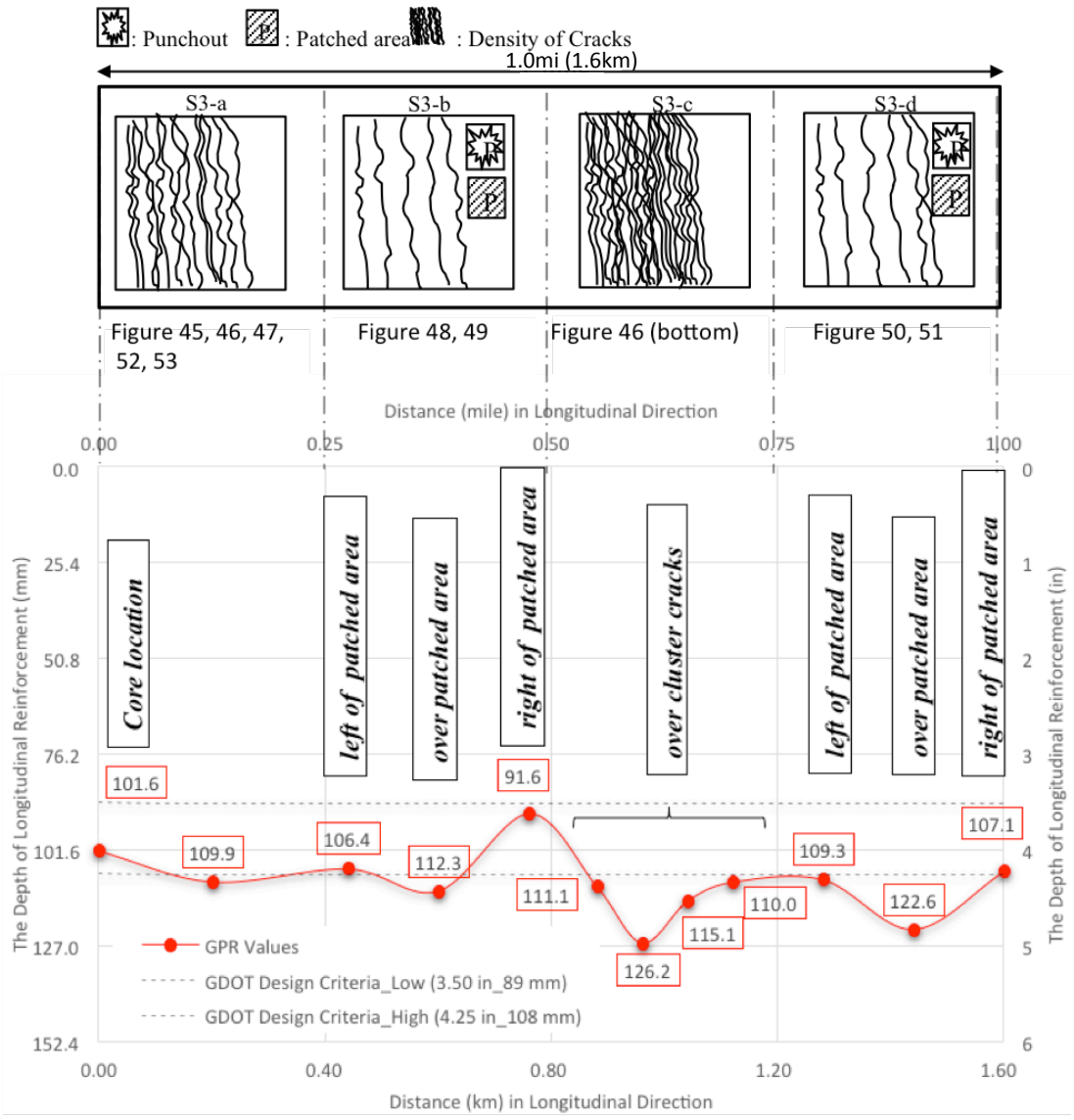

Figure 54 – Stress Pattern and Concrete Cover in Longitudinal Direction in Each Segment Along 1.0mi (1.6km)

Figure 55 indicates the depths of longitudinal rebars which were obtained from between the single transverse cracks using GPR and Profometer (S3-a). The depth measurements taken by both techniques almost overlapped and are in considerable agreement. Likewise, S3-b indicates a similar pattern as shown in Figure 56 and Figure 57 despite the fact that the data was not calibrated. Section S3-b included data taken to the left of the patched area (see in Figure 57).

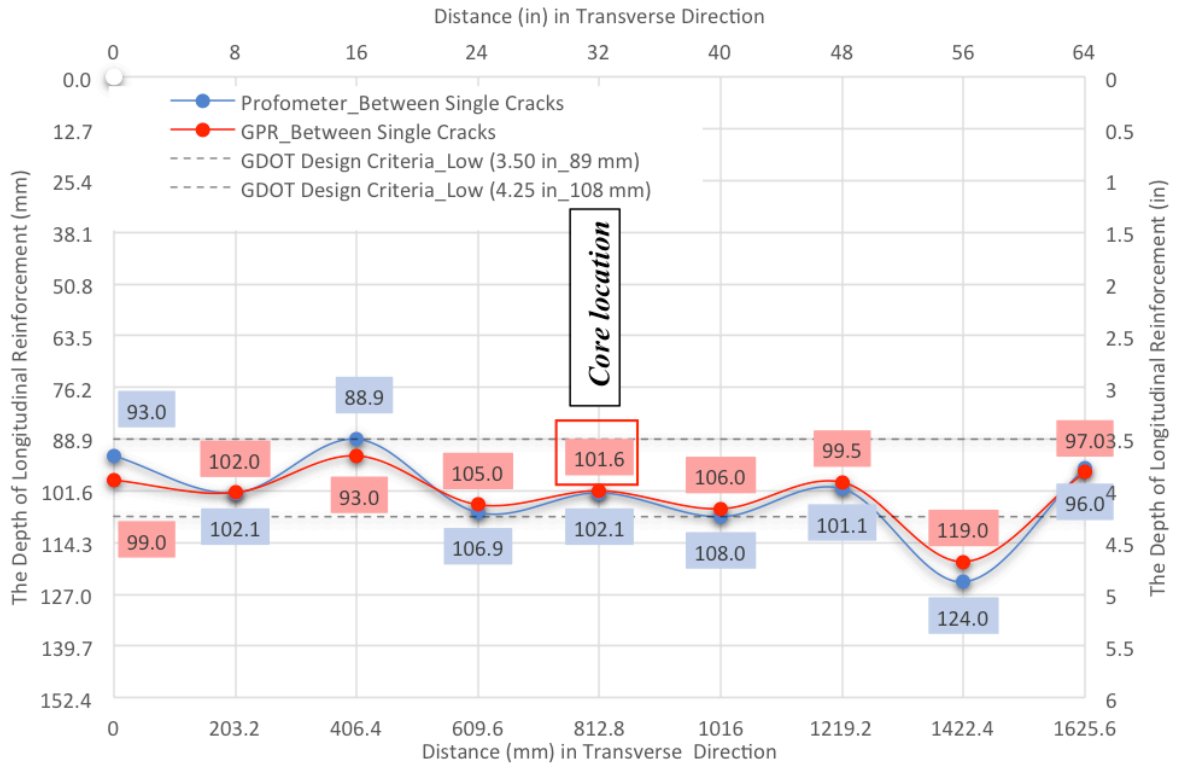

Figure 55 – Concrete Cover Depth Values Detected by Calibrated GPR and Profometer in Transverse Direction at S3-a

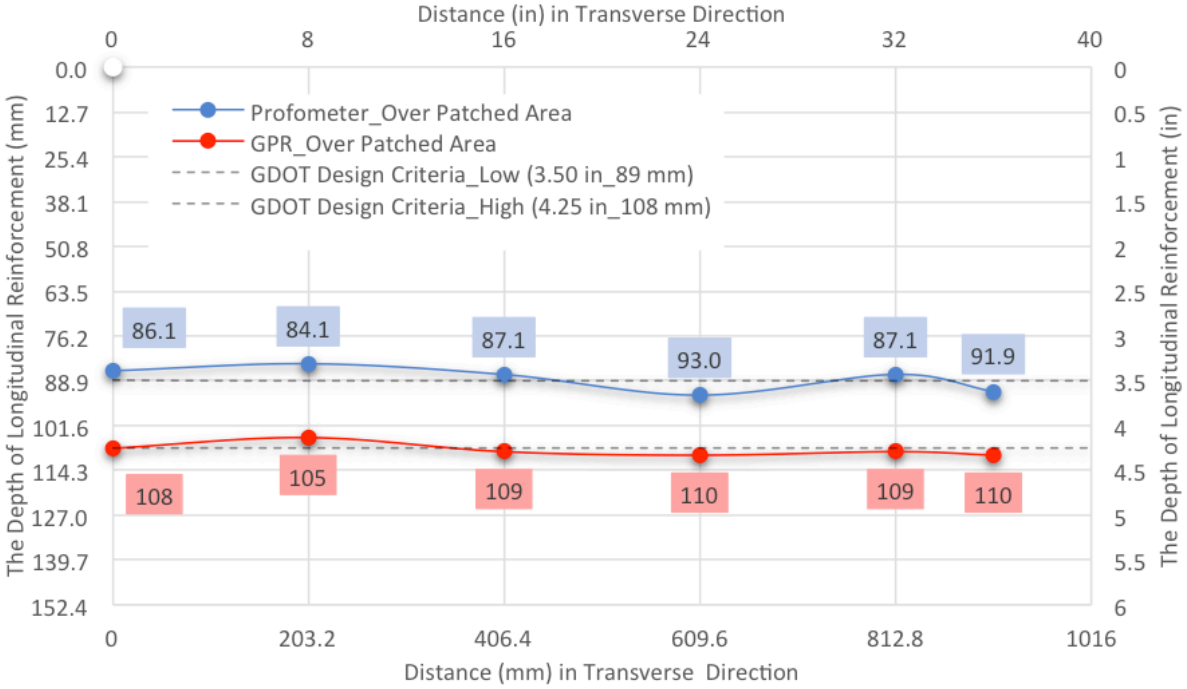

Figure 56 – Concrete Cover Depth Measurements over Patched Area, Detected by Non-Calibrated GPR and Profometer in Transverse Direction at S3-b

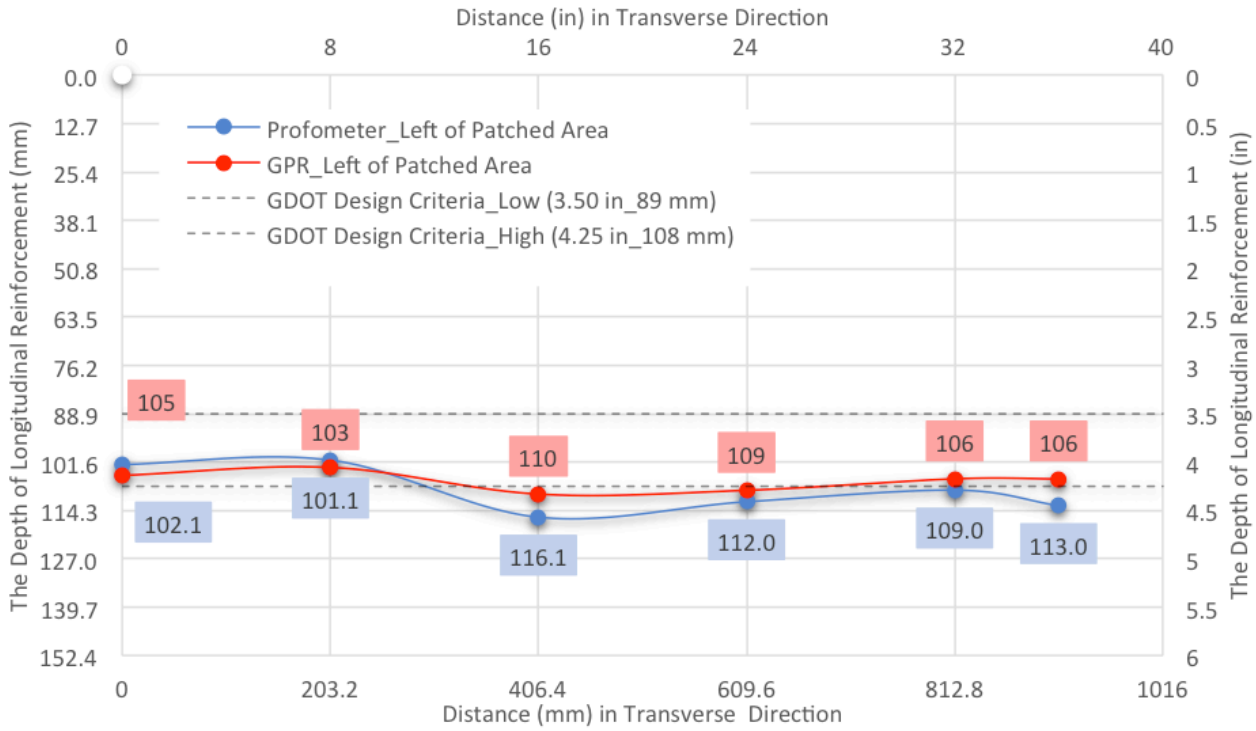

Figure 57 – Concrete Cover Depth Measurements over left of Patched Area, Detected by Non-Calibrated GPR and Profometer in Transverse Direction at S3-b

6.3.4 I-20 - Newton County

6.3.4.1 Data Collection

Non-destructive testing methods were used on Interstate 20 in Newton County using a Ground Penetrating Radar (GPR) device and Profometer. Detailed information regarding the working procedures of these units is described in Section 5.1.

The outside (slow) lane on East Bound (EB) I-20 located between MP 92 and MP 93 in Newton County was investigated. The CRC pavement was reported to be in fair condition, indicating many visible distresses such as clusters of transverse cracks, longitudinal cracks, and possibly material issues. The construction drawings obtained from GeoPI (see I20EBNMP92-93 in Appendix D) indicate that the section was built in 2005. The location of this site is shown in Figure 58.

Figure 58 – I-20 MP 92 to MP 93 Newton County Site Location (Google Maps, 2017)

The design and distress parameters are presented in Table 13. The site exhibited clusters of transverse cracks and a few longitudinal cracks on the wheel-paths. It was determined that the selected section did not have punchouts. To confirm the size and location of longitudinal and transverse bars and pavement thickness before collecting data, a 6.00n (152mm) diameter core was extracted from the site.

The transverse crack pattern on the investigated lane is shown in Figure 59. The section was constructed as a 12.00in (305mm) CRC slab. The longitudinal and transverse reinforcement consisted of #6 and #4 reinforcement, respectively. The concrete cover depth to the top of the longitudinal reinforcement was measured to be 4.00in (102mm) from the core specimen. The site was investigated in four stages in terms of density of crack types and existence of other distress types. The stages were named as S4-a, S4-b, S4-c, and S4-d. They refer to the first (a), second (b), third (c), and fourth (d) subsite (S) segments of Newton County.

Table 13 – CRC Design Parameters and NDT Results for I20EBNMP92-93

	Design Parameters						
NEWTON COUNTY	Site Condition	Age (Year)	CRC Thickness (in)	Longitudinal Rebar Size/ Spacing (in)	Transverse Rebar Size/ Spacing (in)	Longitudinal Rebar Depth (in)	Transverse Rebar Depth (in)
	Fair	12 (2005)	12.00	#6 / 5.00	#4 / 36.00	4.00	4.75
	Distress Parameters Examined						
	Spacing between single transverse cracks (ft.)		Spacing between clusters of transverse cracks (ft.)	Transverse crack width (in)	Longitudinal crack width (in)	Number of Punchouts / mile	
	1.0 ~ 10.0 (typical 1.0)		12.0 ~ 60.0 (typical 12.0)	0.03 ~ 0.12 (typical 0.04)	0.01~0.08	0	

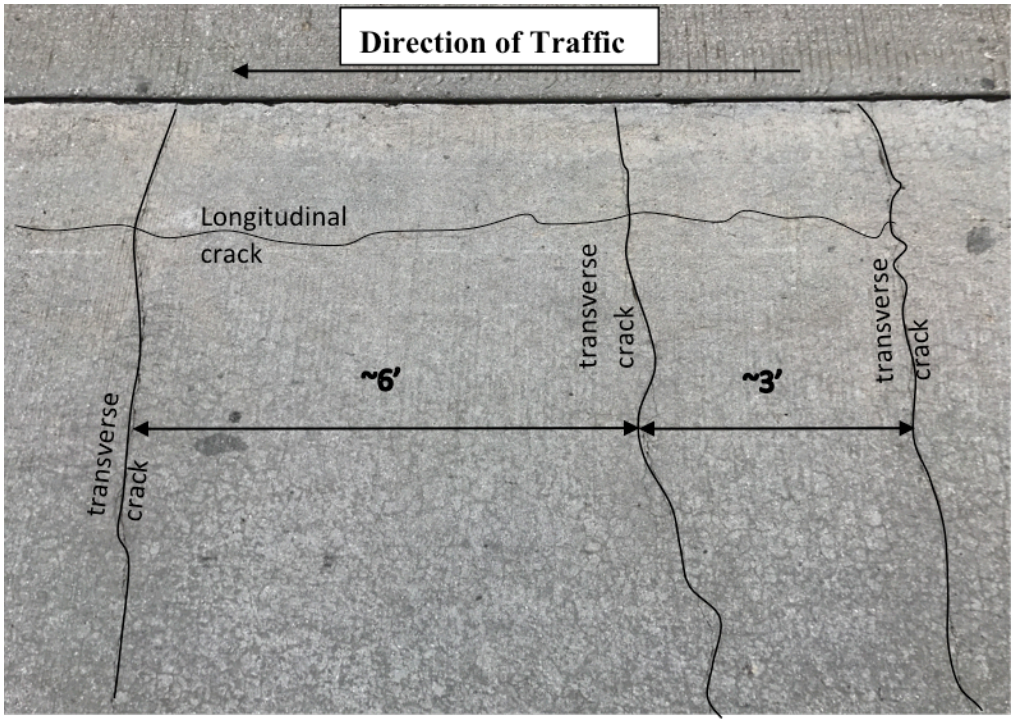

Figure 59 – Typical Single Transverse Crack Pattern (S4-a)

The site had cluster transverse cracks as shown in Figure 60. Cracks over transvers reinforcement were marked as 'TC' in Figure 60. The minimum and maximum distance

between the clusters of transverse cracks were measured to range between 12.0-60.0ft (3.7-18.3m). The single transverse cracks were spaced at the range of approximately 1.0-12.0ft (0.3 -3.7m) with most cracks spaced 1.0ft (0.3m). Figure 59 illustrates the crack spacing. Figure 61 illustrates the use of a tape measure and crack width guage for using in measuring the pavement crack widths. The typical transverse crack width varied between 0.03-0.12in (1-3mm), and the maximum transverse crack width was 0.50in (13mm). S4-a, S4-b, and S4-d had longitudinal cracks that ranged between 0.03-0.10in (1-3mm) in width. Longitudinal cracks were not present at S4-c, though the site had the signs of potential longitudinal cracks at the location of the cluster cracks.

6.3.4.2 Data Post-Processing

The GPR unit scans were visualized in RadView software. Figure 62 shows the location of six reinforcement bars and the layer thickness. Based on findings, there was no crack on the 1st, 2nd, or 6th steel transverse reinforcements, while some transverse cracks appeared over the 3rd, 4th, and 5th transverse reinforcements. As it is shown in the GPR scan (Figure 62), the deeper the transverse reinforcements, the more transverse cracks appeared.

6.3.4.3 Interpretation of Radargrams and Findings

Figure 63 indicates the depth of longitudinal reinforcement and CRC thickness in the transverse direction. An increase in the depth of transverse reinforcements results in deeper longitudinal reinforcement depth. The result of this vertical movement appears to create transverse cracks on the pavement surface. Figure 64 shows the comparison of images (or radargrams) obtained by scanning over transverse reinforcement bars in the pavement section

with and without visible cracks observed on the pavement surface. It is concluded from Figure 64 that the cracks are formed when the reinforcement is placed deeper.

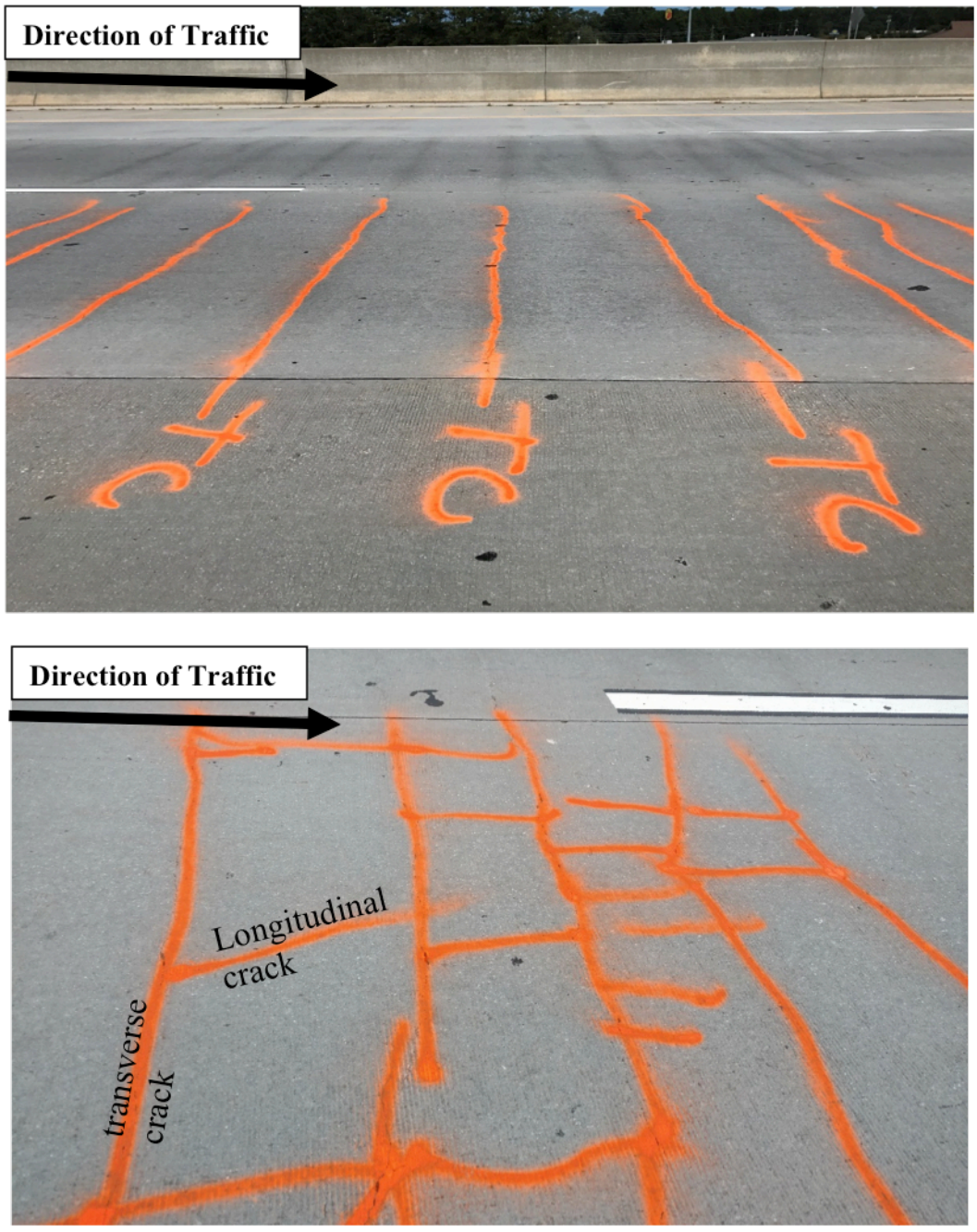

Figure 60 – Typical Cluster Transverse Crack Pattern at (Top) S4-b and (Bottom Figure) S4-d

Figure 61 –Sample Crack Widths at S4-a and S4-c

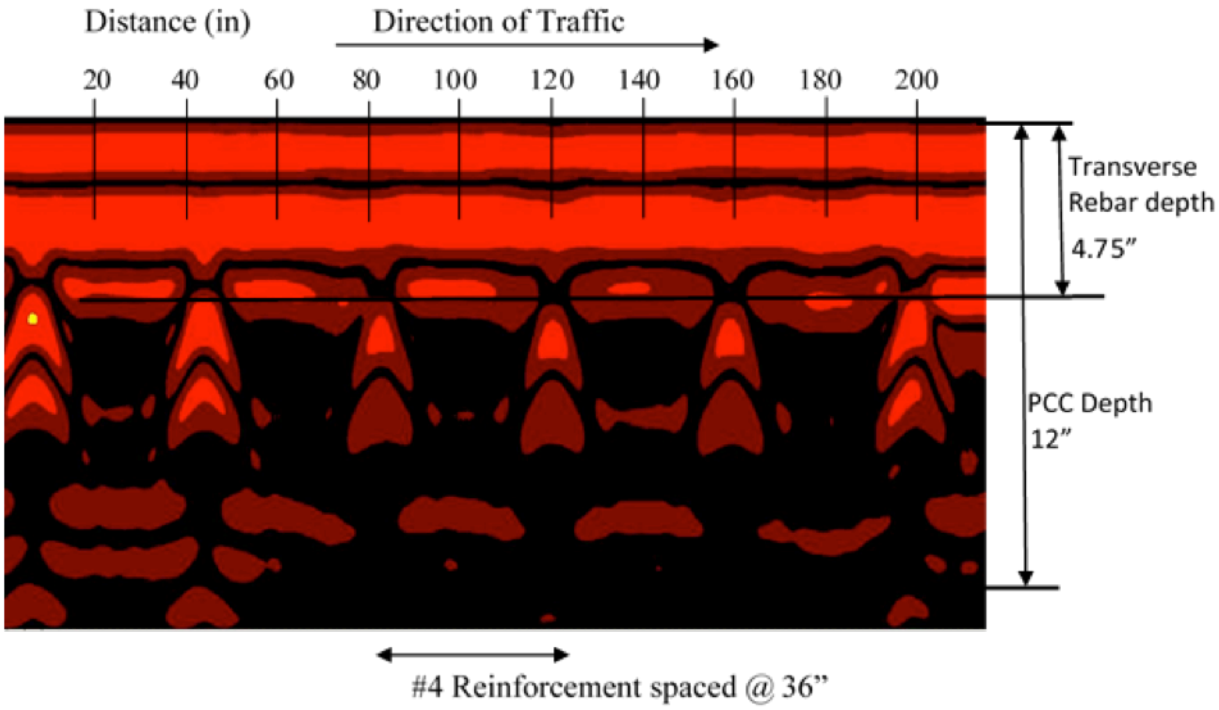

Figure 62 – GPR Scan in the Longitudinal Direction (S4-a)

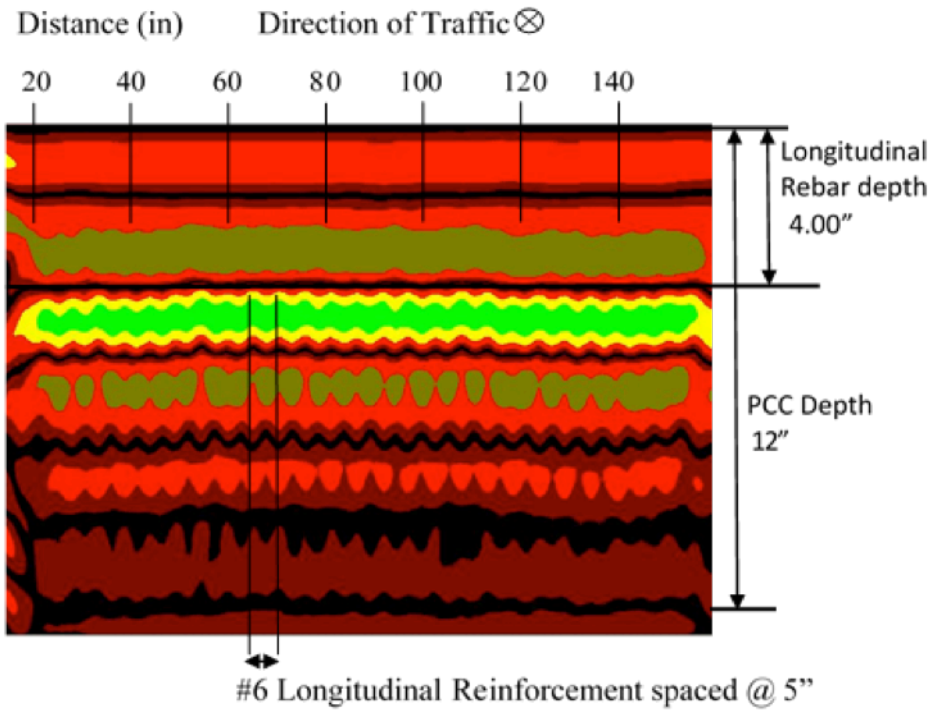

Figure 63 – GPR Scan in the Transverse Direction (S4-b)

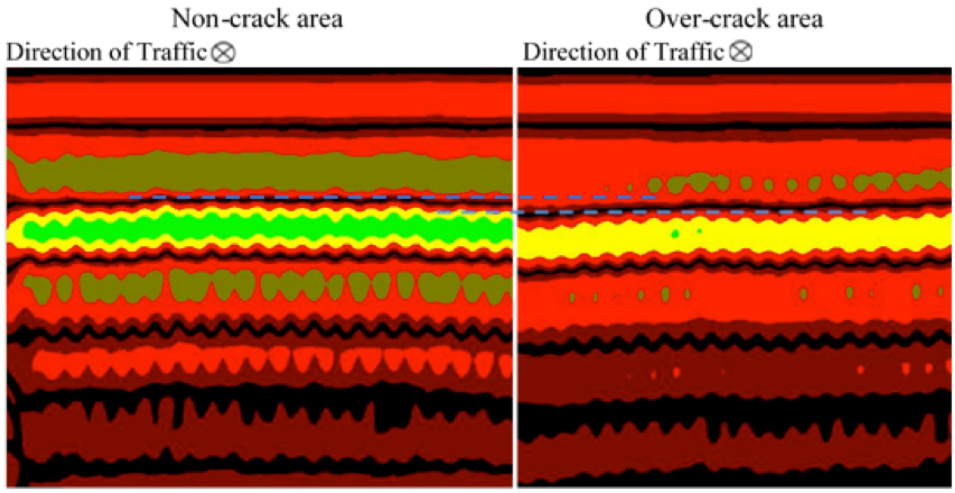

Figure 64 – Comparison of GPR Scans Obtained from Non-Crack Area and Over-Crack Area in the Transverse Direction (S4-a)

At the selected site, the depth of longitudinal rebar is varied throughout the 1.0mi (1.6km) section (see Figure 65). The S4-a was scanned by GPR and Profometer because of the existence of over ten single transverse cracks in a cluster. In addition, most cracks formed over the transverse reinforcement locations. The S4-b has a large distance, 10ft (3.1m), between two single transverse cracks in a cluster cracking. The S4-c was selected because of the existence of multiple transverse cracks. The cluster had more than twenty cracks which were formed over transverse reinforcement, but no longitudinal cracks. In contrast, the S4-d segment exhibited five transverse cracks and many longitudinal cracks.

The concrete cover depth significantly decreased from S4-b to S4-d segments. It is believed that the sudden change in depth between S4-b and S4-c caused numerous transverse cracks at S4-c. In addition, as the reinforcements moved higher in the pavement cross-section, the number of longitudinal cracks appear to increase, although the number of transverse cracks did not increase.

Figure 66 indicates the depths of longitudinal bars which were detected using GPR and Profometer within the section located between the single transverse cracks (S4-a). Although the depth measurements taken by both techniques show a similar pattern in the graph, these values do not agree well. The reason for this is believed to be the result of varied materials, such as metal or other pieces of steel which can be detected easily by GPR and Profometer units and form the basis for error.

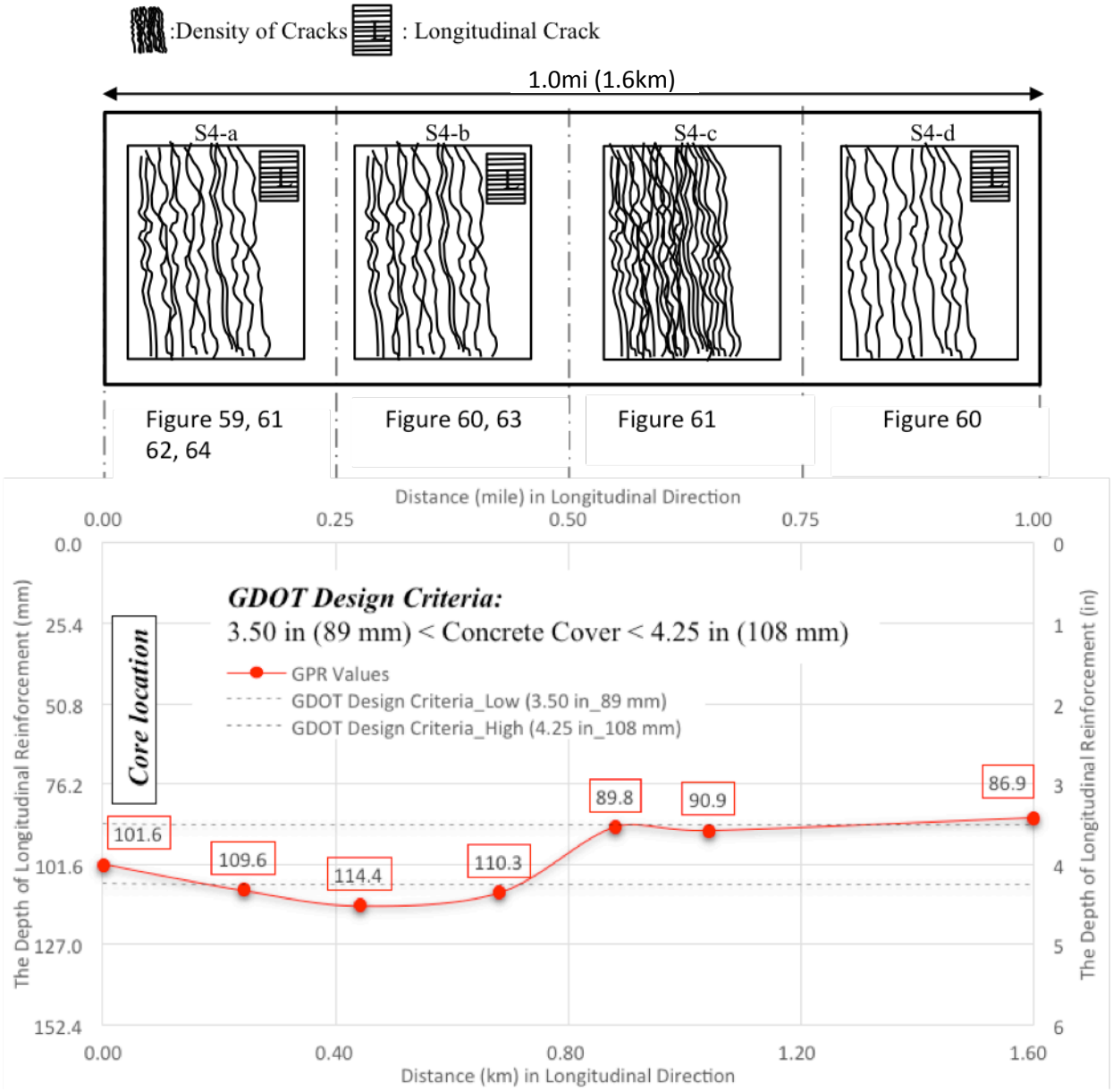

Figure 65 – Stress Pattern and Concrete Cover in Longitudinal Direction in Each Segment Along 1.0mi (1.6km)

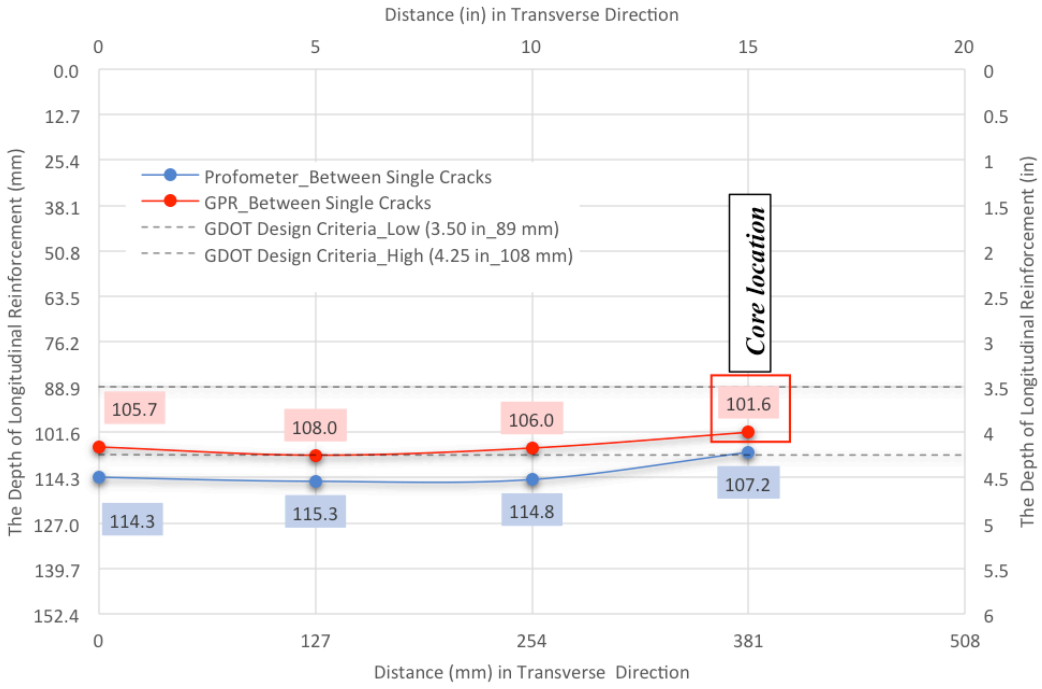

Figure 66 – Concrete Cover Depth Values Detected by Calibrated GPR and Profometer in Transverse Direction at S4-a

6.3.5 I-75 Cobb County

6.3.5.1 Data Collection

Non-destructive tests were carried out on Interstate 75 in Cobb County using GPR and Profometer devices. Detailed information regarding the working procedures of these units is presented in Section 5.1. The outside lane on North Bound (NB) I-75 located between MP 267 and MP 268 in Cobb County was studied. The CRC pavement was reported to be in poor condition, indicating many visible distresses such as transverse and longitudinal cracks, potential punchouts, and map cracking. The construction drawings obtained from GeoPI (see I75NBCMP267-268 in Appendix E) indicate that the plans of the section were completed in 1979 and later revised in 1985. The location of this site is shown in Figure 67. The design and

distress parameters are presented in Table 14. This 1.0mi (1.6km) pavement section had no punchouts.

Figure 67 – I-75 MP 267 to MP 268 Cobb County Site Location (Google Maps, 2017)

Table 14 – CRC Design Parameters and NDT Results for I75NBCMP267-268

	Design Parameters						
COBB COUNTY	Site Condition	Age (Years)	CRC Thickness (in)	Longitudinal Rebar Size/ Spacing (in)	Transverse Rebar Size/ Spacing (in)	Longitudinal Rebar Depth (in)	Transverse Rebar Depth (in)
	Poor	32 (1985)	10.25	#6 / 5.00 ~ 9.50	#4 / 25.00 ~40.00 (typical 39.00)	4.50	5.25
	Distress Assessment						
	Spacing between single transverse cracks (ft.)		Spacing between clusters of transverse cracks (ft.)		Transverse crack width (in)	Longitudinal crack width (in)	Number of Punchouts / mile
	1.5~ 4.3 (typical 3.3)		No Grouping (typical 1.0)		0.10 ~ 0.15 (typical 0.15)	0.05	0

The transverse crack pattern on the investigated lane is shown in Figure 68. The section was planned as a 9.00in (229mm) CRC slab above a 1.00in (25mm) asphaltic concrete layer, 5.00in (127mm) of graded aggregate (cement stabilized) subbase, and 6.00in (152mm) of crushed aggregate subgrade. Based on the revised constructional drawings, the pavement was redesigned as a 9.00in (229mm) CRC slab above a 5.00in (127mm) asphaltic concrete base (or alternatively portland cement concrete base), and 7.00in (178mm) of graded aggregate (cement stabilized) sub-base. However, the concrete layer thickness was measured as 10.25in (260mm) from the cored specimen. The longitudinal and transverse reinforcements consisted of #6 and #4 rebar, respectively. The concrete cover depth to the top of the longitudinal reinforcement was measured to be 4.50in (114mm) from the core specimen. The site was investigated in four stages to determine density of crack types and existence of other distress types. The stages were named S5-a, S5-b, S5-c, and S5-d. They refer the first (a), second (b), third (c), and fourth (d) subsite (S) number (5) or 'S5' segments of I-75 in Cobb County. The site contained cluster transverse cracks as shown in Figure 69.

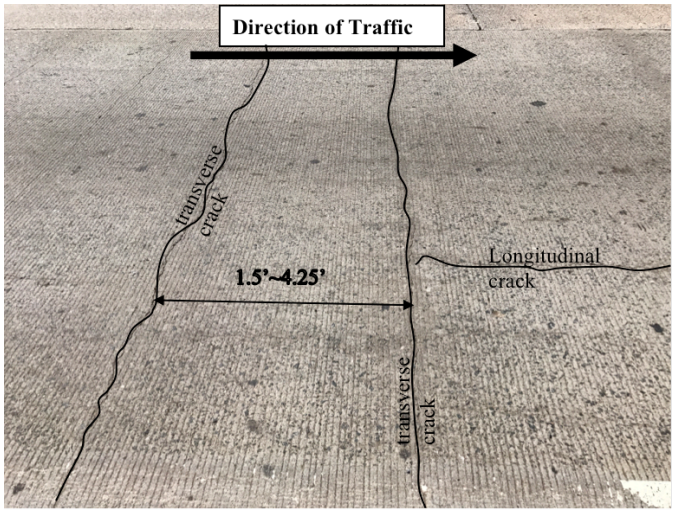

Figure 68 – Typical Single Transverse Crack Pattern (S5-a)

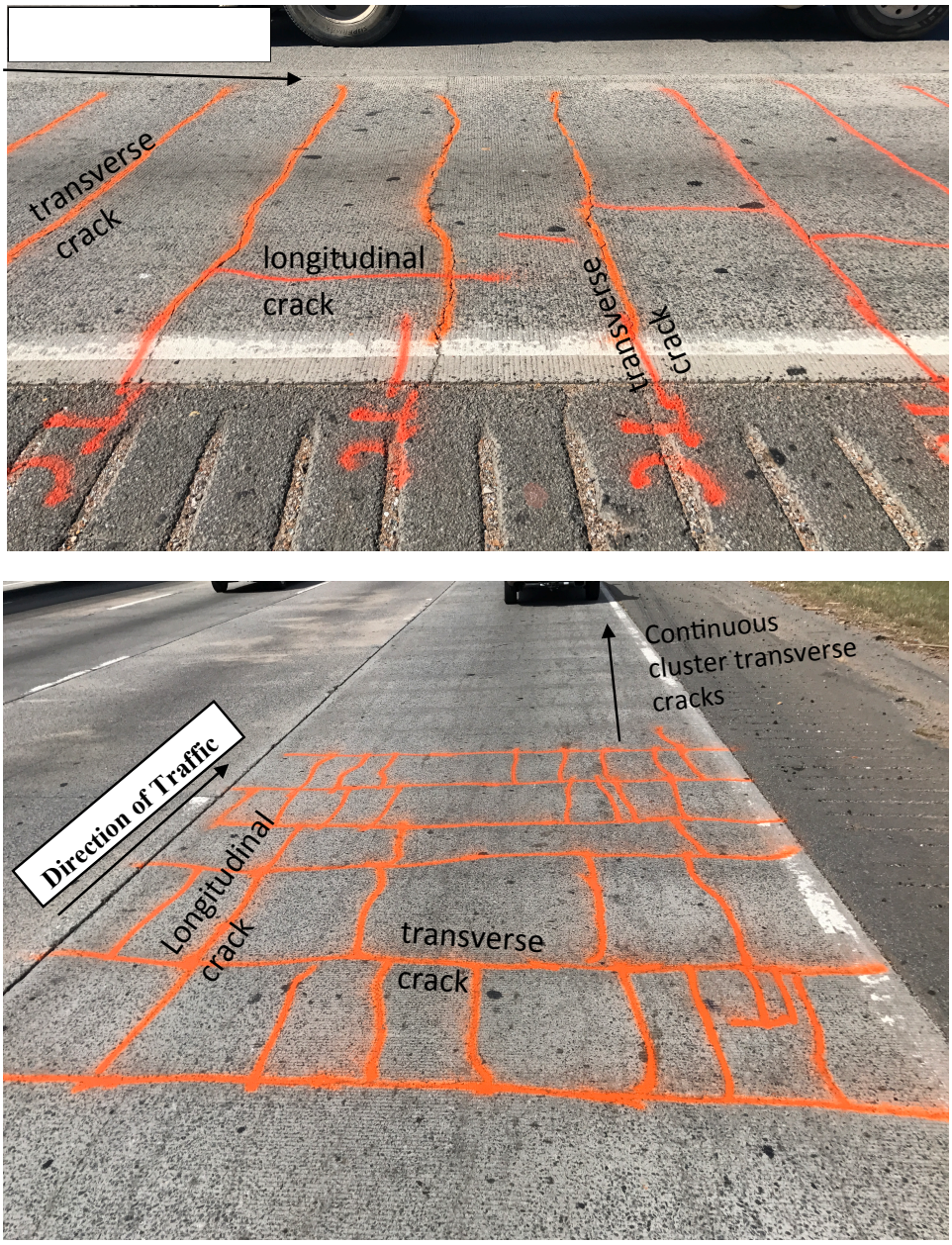

Figure 69 – Typical Cluster Transverse Crack Pattern at (Top) S5-a and (Bottom Image) S5-d

There is no clear distance between the clusters of transverse cracks because the site indicated a continuous pattern of cluster transverse cracks. The single transverse cracks were spaced at a range of approximately 1.5-4.3ft (0.5-1.3m) with typical crack spacing of 3.3ft (1.0m). The typical transverse crack width varied in the range of 0.10-0.15in (3-4mm), and the maximum transverse crack width was 1.00in (25mm). Although the longitudinal crack typically

ranged between 0.03-0.10in (1-3mm) in width, it was observed that the maximum longitudinal crack width was 0.50in (13mm) shown in Figure 70. It was detected that the site had signs of potential punchouts at the location of the cluster transverse cracks in S5-c. It is predicted that there is a potential risk of S5-c forming a number of punchouts in the near future because of the existence of high-severity longitudinal cracks between transverse cracks (Figure 71).

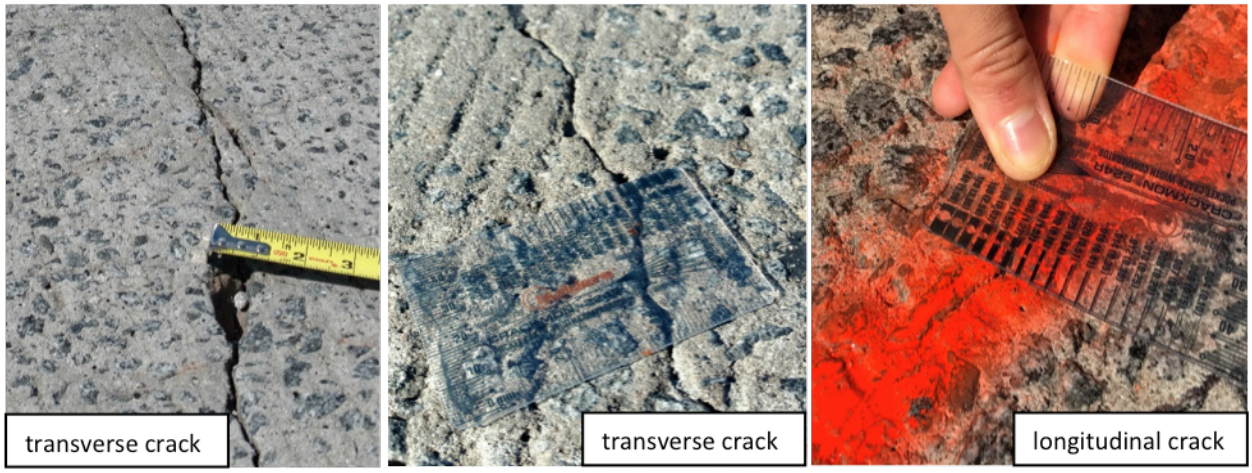

Figure 70 – The Measurement of Non-Typical Crack Widths at S5-a and S5-d

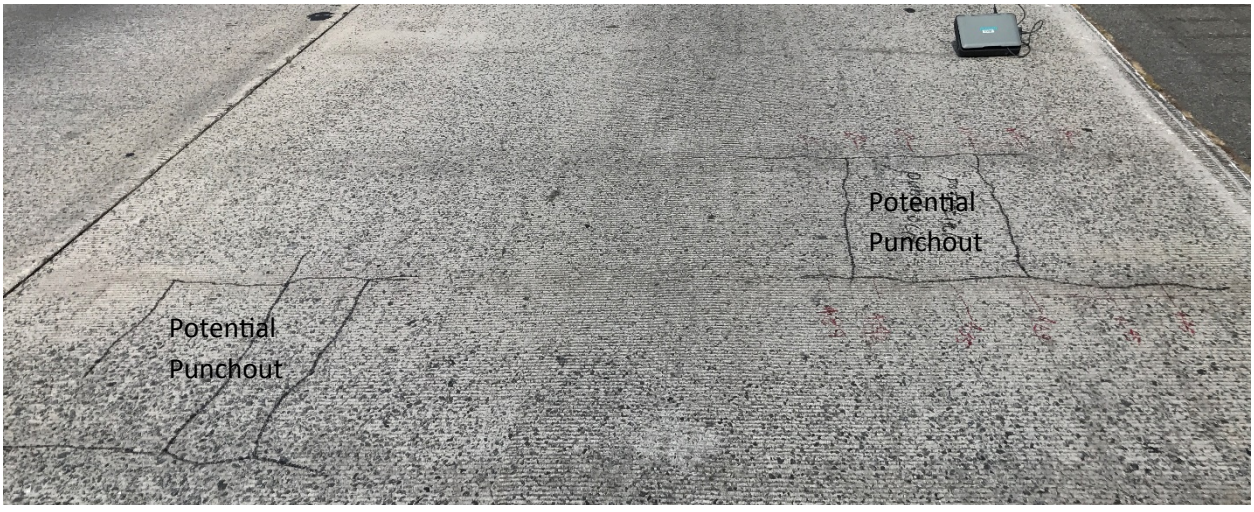

Figure 71 –Potential Punchout Sections at S5-c

6.3.5.2 Data Post-Processing

The GPR unit scans were visualized in RadView software. Figure 72 shows the location of six reinforcements and the concrete layer thickness. The depth difference among the top points of the reflections of transverse reinforcement indicates a sign of distress on the pavement. Based on findings from this site and investigation and post-processing via the software (Figure 72), there was no crack over the 4th transverse reinforcement, while transverse cracks were found over the rest of transverse reinforcement.

Ultimately, the results indicate an increased number of transverse cracks when the transverse reinforcement is placed deeper in the pavement cross-section. Figure 73 indicates the depths of longitudinal reinforcement and CRC thickness in the transverse direction. The deeper the transverse reinforcement, the deeper the accompanying longitudinal reinforcements. Thus, the result of this vertical movement causes the transverse cracks on the pavement surface.

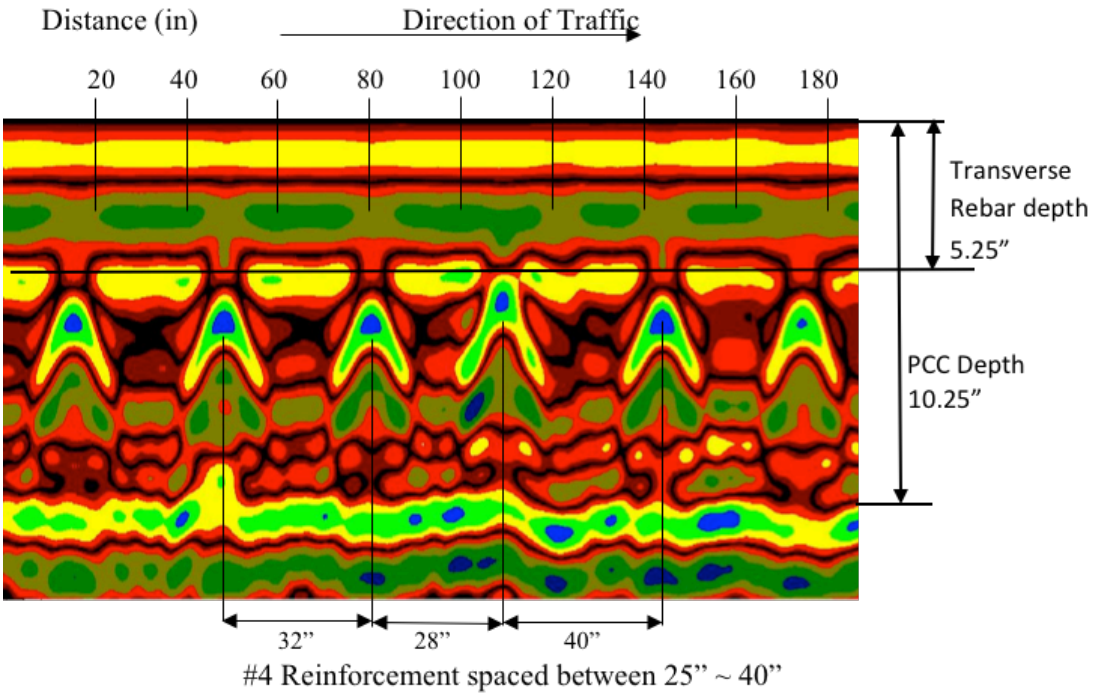

Figure 72 – GPR Scan in the Longitudinal Direction (S5-a)

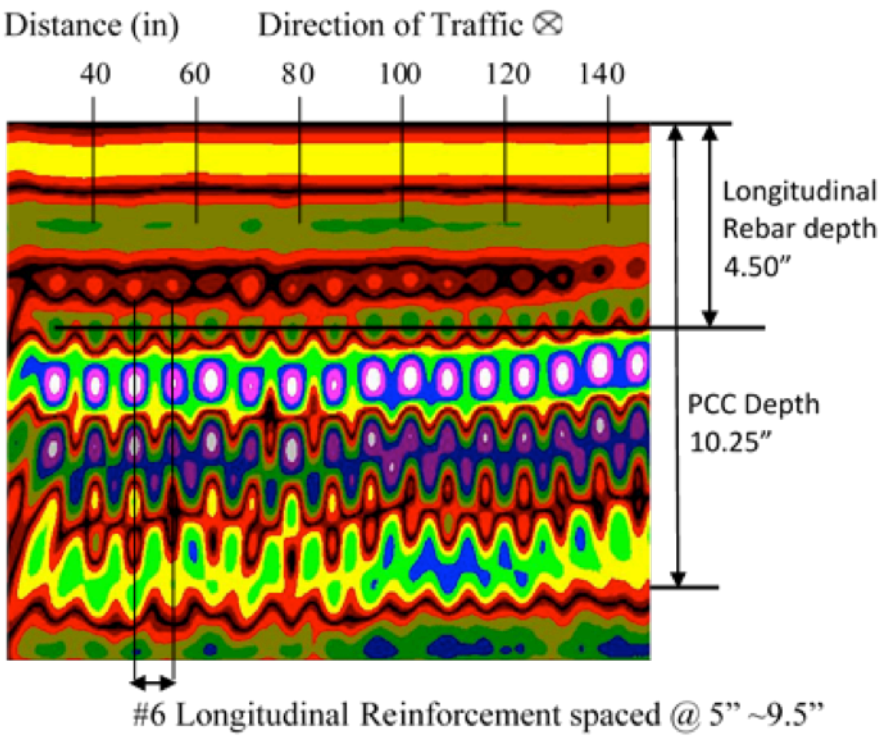

Figure 73 – GPR Scan in the Transverse Direction (S5-d)

6.3.5.3 Interpretation of Radargrams and Findings

At the selected site, the depth of longitudinal reinforcement is varied throughout the 1.0mi (1.6km) section due to the construction processes. The S5-a segment was scanned by GPR and Profometer because of the existence of approximately 20 single transverse cracks in the cluster. In addition, most of these cracks formed above the transverse reinforcement. The S5-b section showed map cracking distress along with transverse and longitudinal cracks over the rightmost wheel path. The S5-c segment was chosen because of the potential occurrence of punchout. The S5-d segments had many longitudinal cracks and transverse cracks. It was found that this segment had deeper transverse reinforcement than other segments at around 6.50in (165mm) in depth from the top surface. Similarly, when comparing the longitudinal reinforcement in S5-b and S5-d, a clear change in the cover depth between these segments (Figure 74) was observed.

Therefore, large crack openings of 1.00in (25mm) in width appeared in the S5-d segment. As shown in Figure 74, the concrete cover depth measurements obtained from scanning over cracked areas were greater than cover depth measurements from the non-cracked areas (S5-a and S5-d).

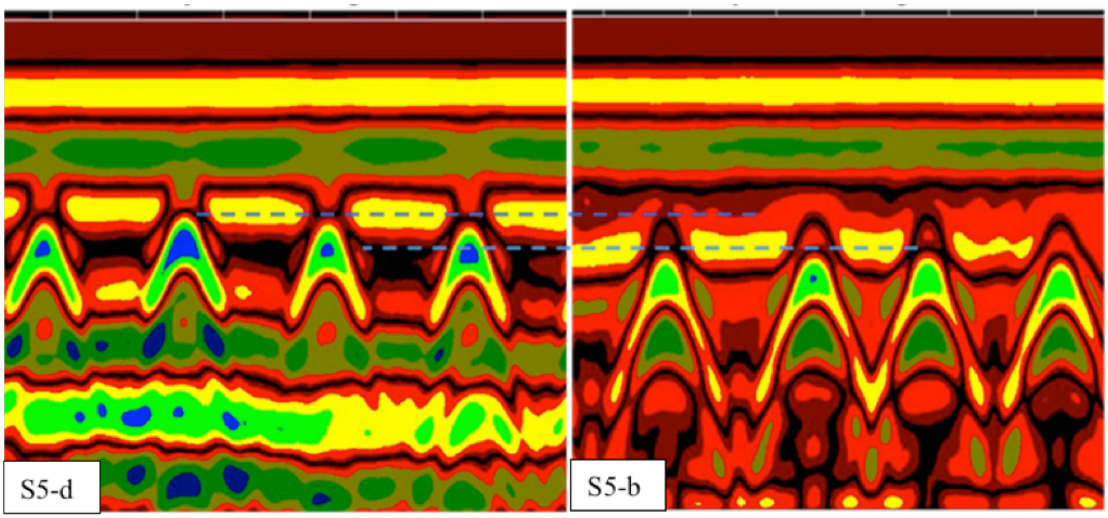

Figure 74 – The Comparison of Transverse Reinforcements in Depth for S5-b and S5-d

Figure 75 indicates the depths of longitudinal reinforcements, which were detected from the pavement site. Although the rebar depth measured by both techniques shows a similar pattern in the graph, these values do not agree well (Figure 76). As with other sections, the reason for this is believed to be the result of varied materials such as pieces of metal or steel that can be detected easily by GPR, and particularly Profometer units, thus forming the basis for error.

6.3.6 I-75 Tift County

6.3.6.1 Data Collection

Non-destructive tests were carried out on Interstate 75 in Tift County using GPR and Profometer. Detailed information regarding the working procedures of these units is included in Section 5.1.

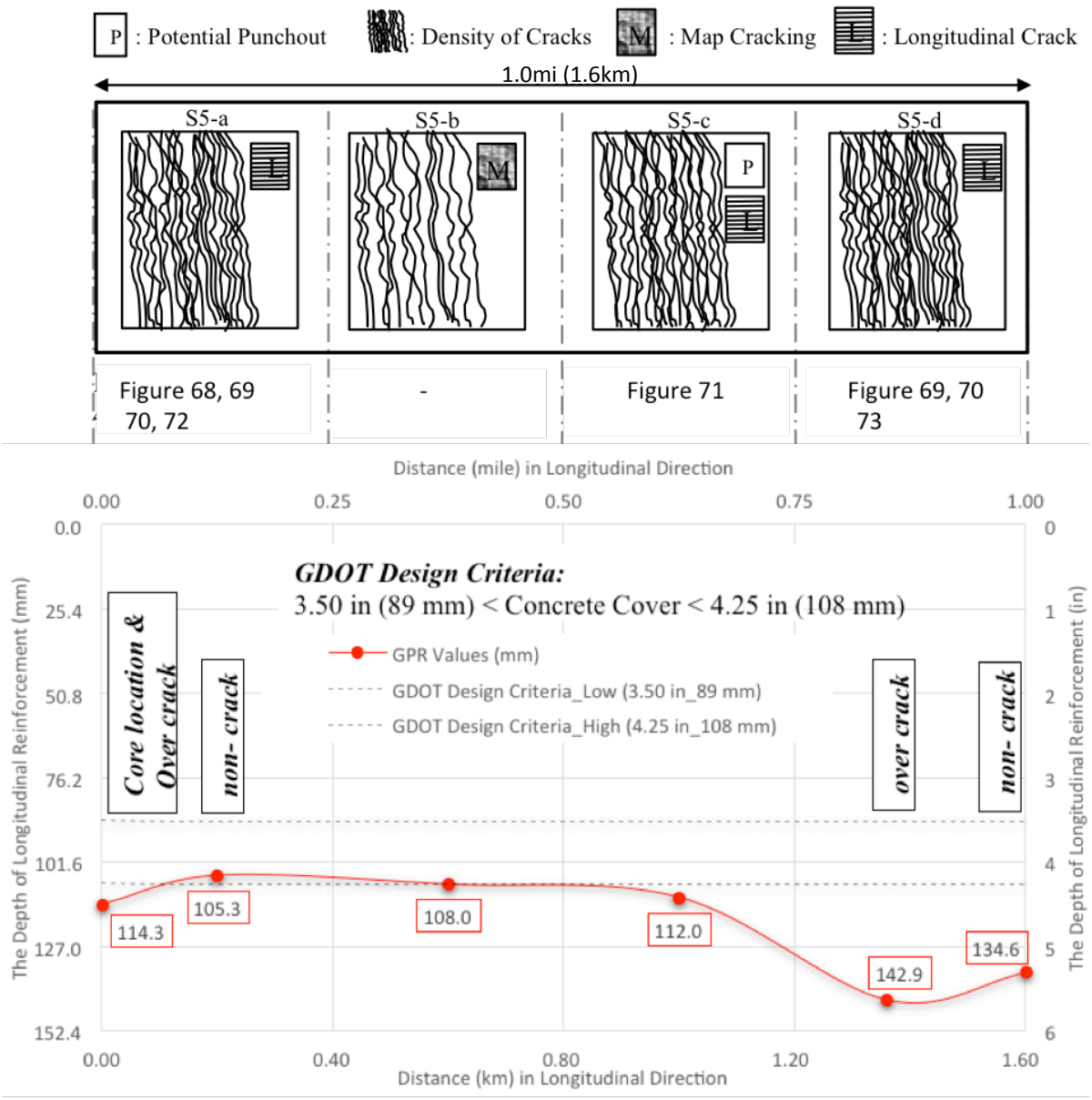

Figure 75 – Stress Pattern and Concrete Cover in Longitudinal Direction in Each Segment Along 1.0mi (1.6km)

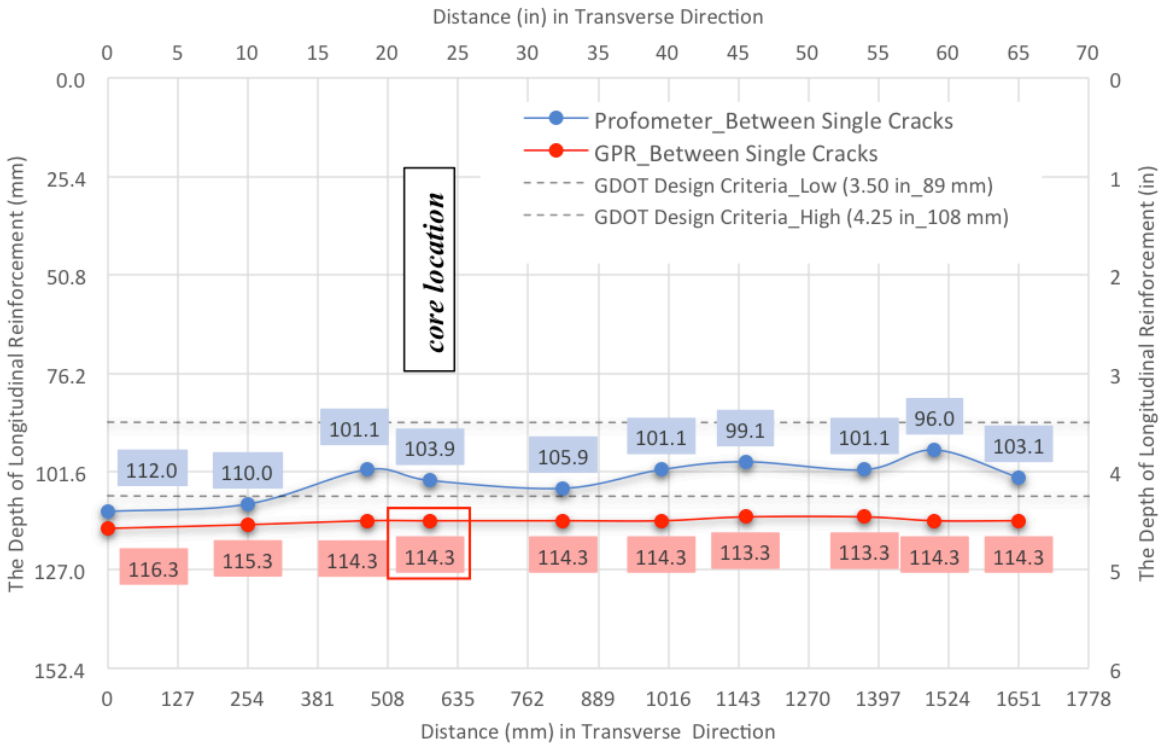

Figure 76 – Concrete Cover Depth Values Detected by calibrated GPR and Profometer in Transverse Direction at S5-a

The outside lane on North Bound (NB) I-75 located between MP 57 and MP 58 in Tift County was investigated. The CRC pavement was reported to be in fair condition, which exhibited continuous clusters of transverse cracks. The construction drawings obtained from GeoPI (see I75NBTMP57-58 in Appendix F) indicate that the plans of the section were completed in 2006, and, the constructional drawings were later revised in 2008. The location of this site is shown in Figure 77. The design and distress parameters are presented in Table 15. It was detected that the selected section had no punchouts over the 1.0mi (1.6km) surveyed segment shown in Figure 77.

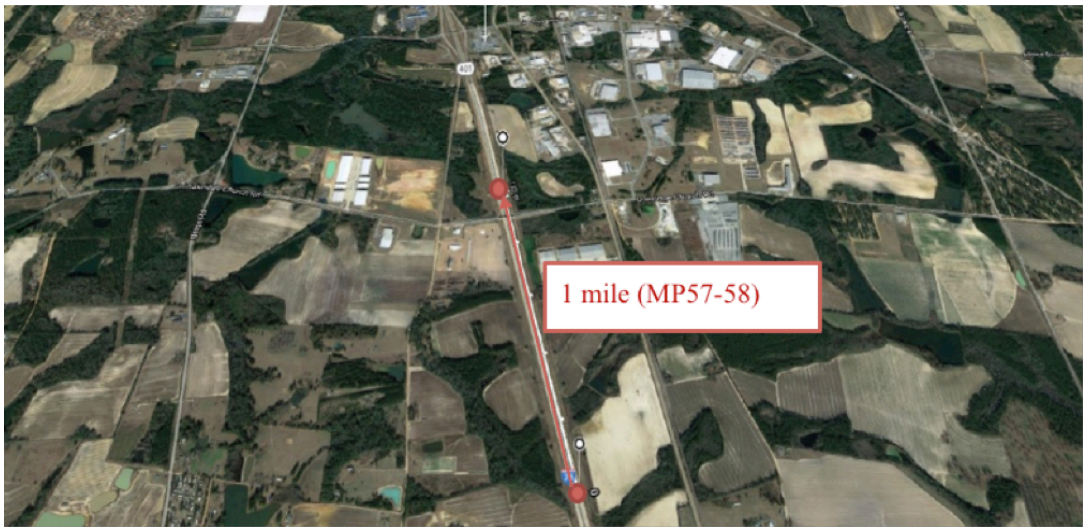

Figure 77 – I-75 MP 57 to MP 58 Tift County Site Location (Google Maps, 2017)

Table 15 – CRC Design Parameters and NDT Results for I75NBTMP57-58

	Design Parameters						
	Site Condition	Age (Years)	CRC Thickness (in)	Longitudinal Rebar Size/ Spacing (in)	Transverse Rebar Size/ Spacing (in)	Longitudinal Rebar Depth (in)	Transverse Rebar Depth (in)
TIFT COUNTY	Fair	9 (2008)	12.00	#6 / 5.00	#4 / 36.00 ~ 40.00 (typical 36.00)	3.75	4.50
	Distress Assessment						
	Spacing between single transverse cracks (ft)		Spacing between clusters of transverse cracks (ft)		Transverse crack width (in)	Longitudinal crack width (in)	Number of Punchouts / mile
	1.0~ 3.0 (typical 1.0)		6.0 ~ 12.0 (typical 6.0)		0.01 ~ 0.08 (typical 0.06)	0.06	0

The transverse crack pattern on the investigated lane is shown in Figure 78. The section was constructed as a 12.00in (305mm) thick CRC slab above a 0.75in (19mm) thick asphalt concrete superpave layer, over a 12.00in (305mm) graded aggregate base layer. The longitudinal and transverse bars consisted of #6 and #4 rebars, respectively. The concrete cover depth to the

top of the longitudinal reinforcement was measured to be 3.75in (95mm) from the cored specimen. The site was investigated in four segments selected based on density of crack and distress types. The segments S6-a, S6-b, S6-c, and S6-d refer to the first (a), second (b), third (c), and fourth (d) subsite (S) number (6) or 'S6' segments of Tift County.

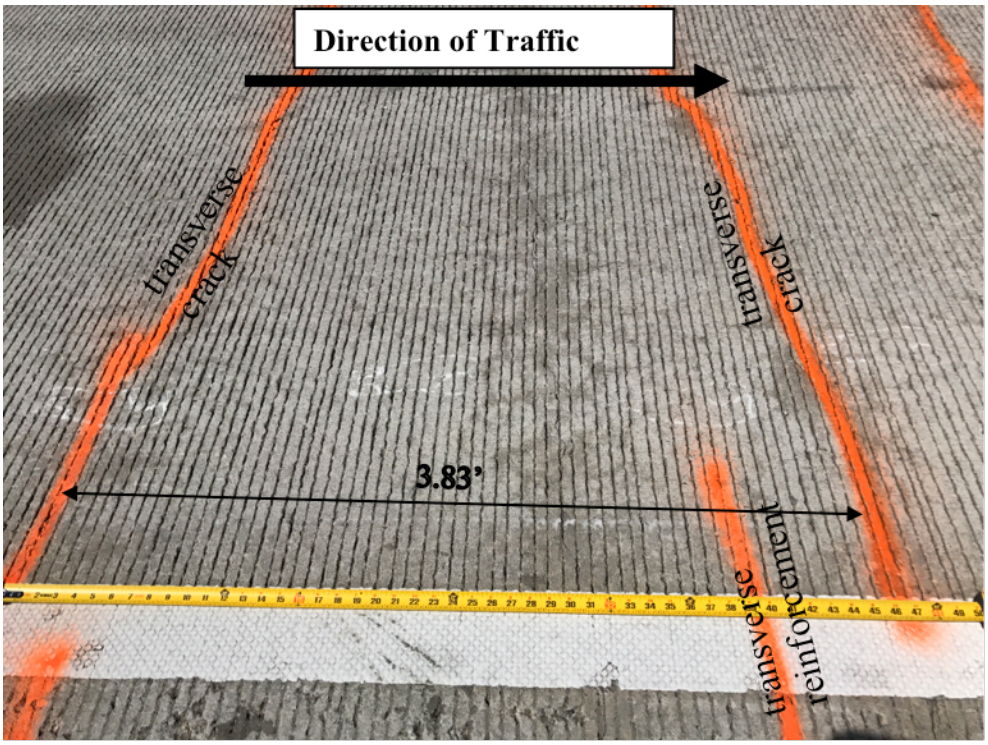

Figure 78 – Typical Single Transverse Crack Pattern (S6-a)

The site indicated the same pattern along the 1.0mi (1.6km) stretch shown in Figure 77, and included continuous clusters of transverse cracks at regular intervals (Figure 79). Transverse reinforcement location and cracks over transverse reinforcement were marked along the pavement shoulder of the section being investigated. The distance between the clusters of transverse cracks changed from 6.0-12.0ft (1.8-3.7m), but typicaly about 6.0ft (1.8m). Single transverse cracks were typically spaced at about 1.0ft (0.3m) with a range of approximately 1.0-3.0ft (0.3-0.9m) (Figure 78). The typical transverse crack width ranged from 0.01-0.08in (0.3-

2mm) while typical longitudinal crack width was approximately less than 0.01in (0.3mm) (Figure 80). Finally, the site had signs of potential punchouts at the location of the cluster of transverse cracks in the 'S6-c' segment.

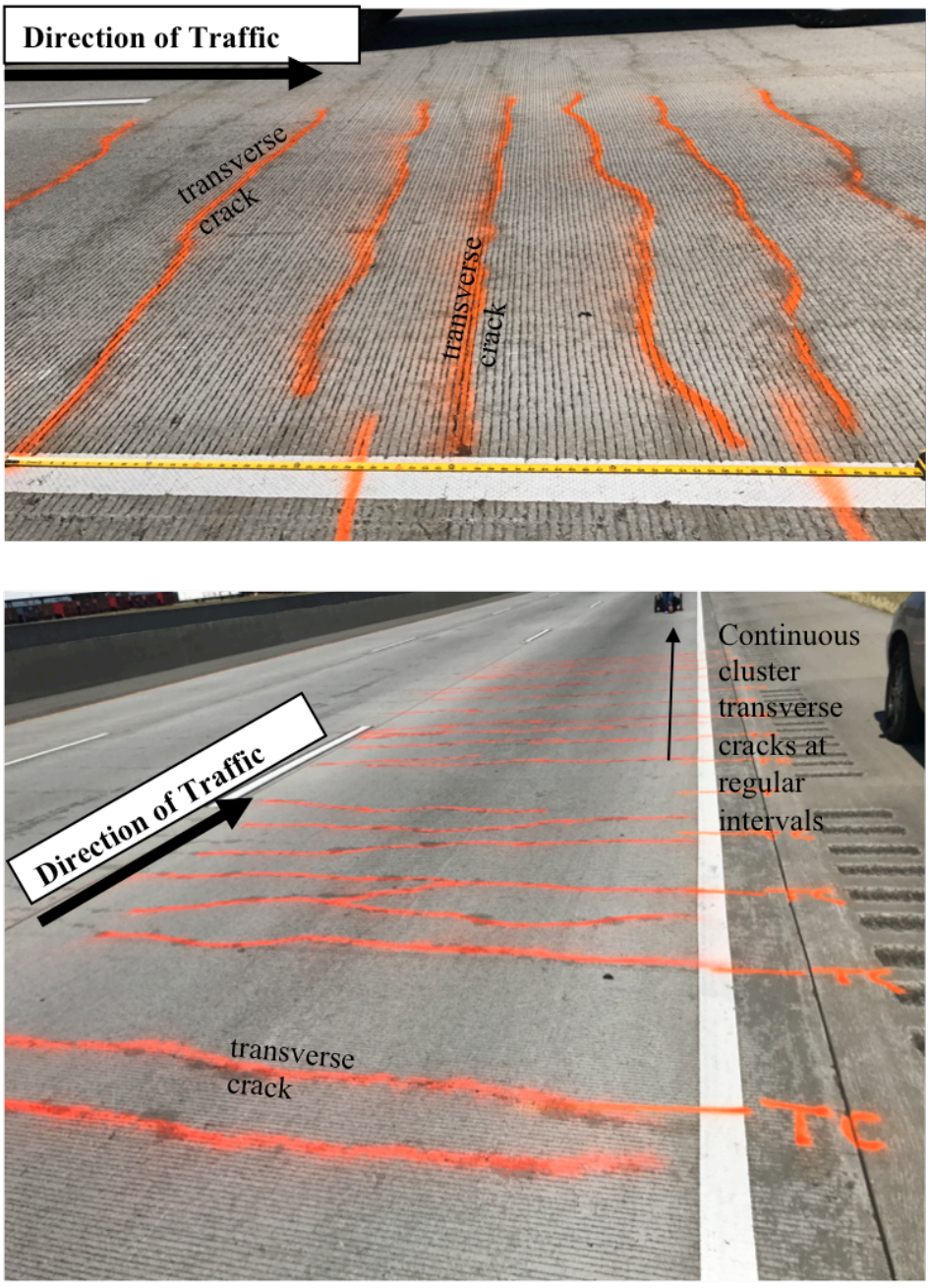

Figure 79 – Typical Cluster Transverse Crack Pattern at S6-a and S6-c

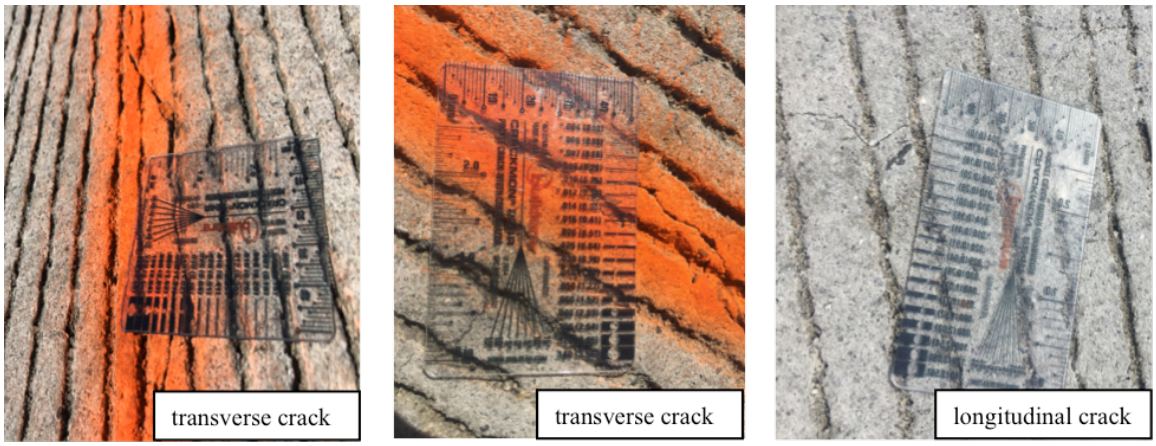

Figure 80 – The Measurement of Typical Crack Widths at S6-a and S6-b

It is predicted that the S6-c segment shown in Figure 81 will develop into a punchout in the near future because of the existence of high-severity longitudinal cracks between transverse cracks.

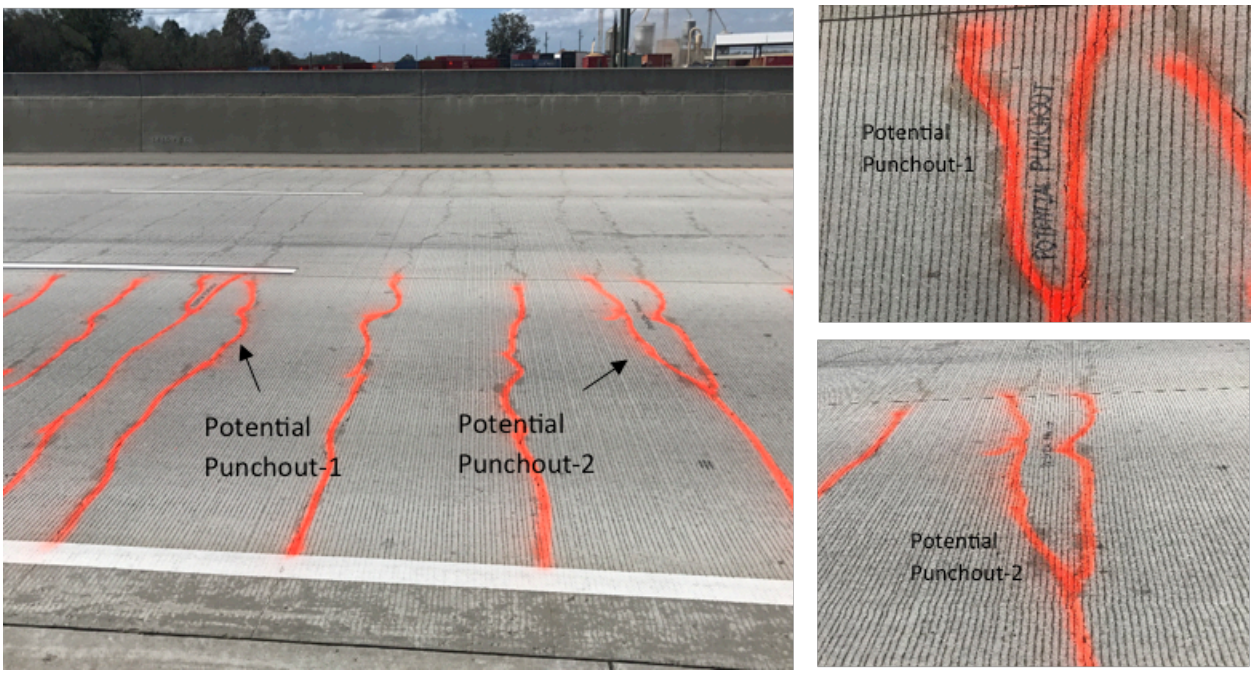

Figure 81 – Potential Punchout Sections at S6-c

6.3.6.2 Data Post-Processing

The GPR unit scans were visualized in RadView software. Figure 82 clearly shows the location of six reinforcements and concrete layer thickness. The depth difference among the top points of the reflections of transverse reinforcements indicated a sign of distress forming at the pavement surface. Based on findings obtained from the site investigation and the GPR scan image, there were no cracks on the 4th, 5th, and 6th transverse reinforcements, while some transverse cracks appeared on the rest of the transverse reinforcements. As shown in the GPR scan (Figure 82), the lower the transverse reinforcements within the pavement section, the lower the accompanying longitudinal reinforcements. Therefore, more transverse cracks appear on the surface. Figure 83 indicates the depths of longitudinal reinforcements and CRC thickness in the transverse direction.

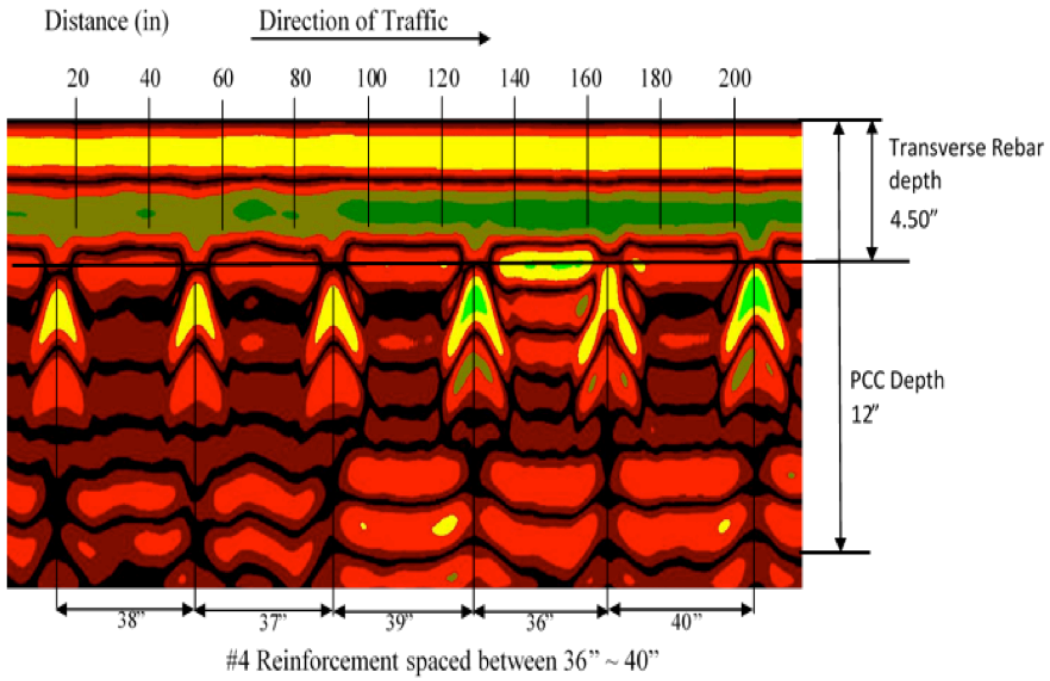

Figure 82 – GPR Scan in the Longitudinal Direction (S6-a)

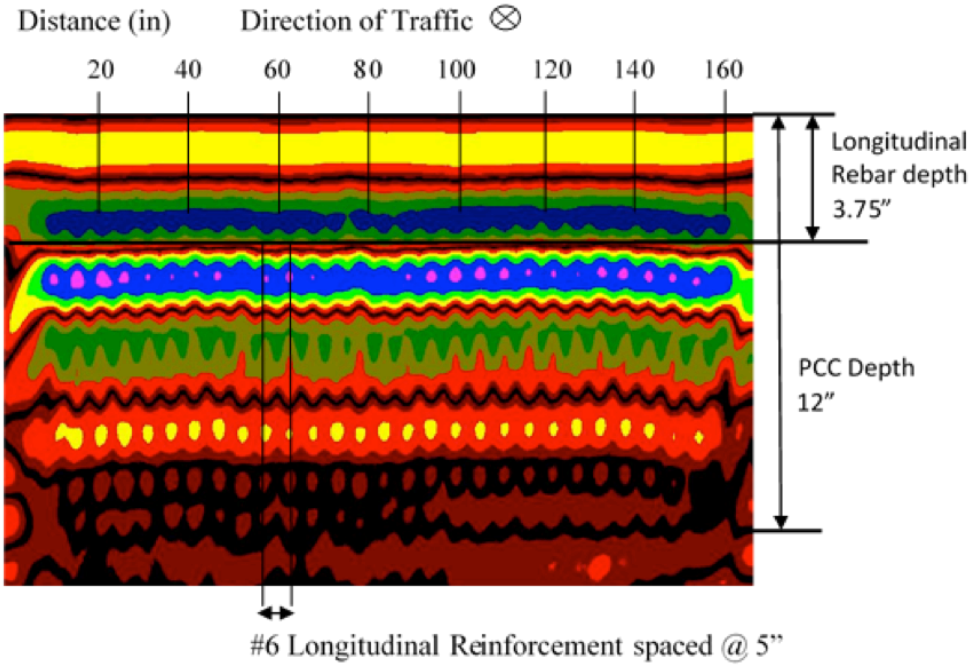

Figure 83 – GPR Scan in the Transverse Direction (S6-a)

6.3.6.3 Interpretation of Radargrams and Findings

At the selected site, the depth of longitudinal reinforcement varied throughout the 1.0mi (1.6km) section. The S6-a segment was scanned by GPR and Profometer because of the existence of approximately twenty single transverse cracks within a cluster of cracks, with the additional presence of longitudinal cracks. Most of these cracks formed over the transverse reinforcement. The S6-b segment had cluster transverse cracks and fewer longitudinal cracks over the wheel path, which was close to the shoulder. The S6-c segment was chosen because of the occurrence of potential punchout areas. It was determined that the longitudinal reinforcement in the S6-a and S6-c segments was placed deeper than other segments, at approximately 3.75in (95mm) in depth (Figure 84).

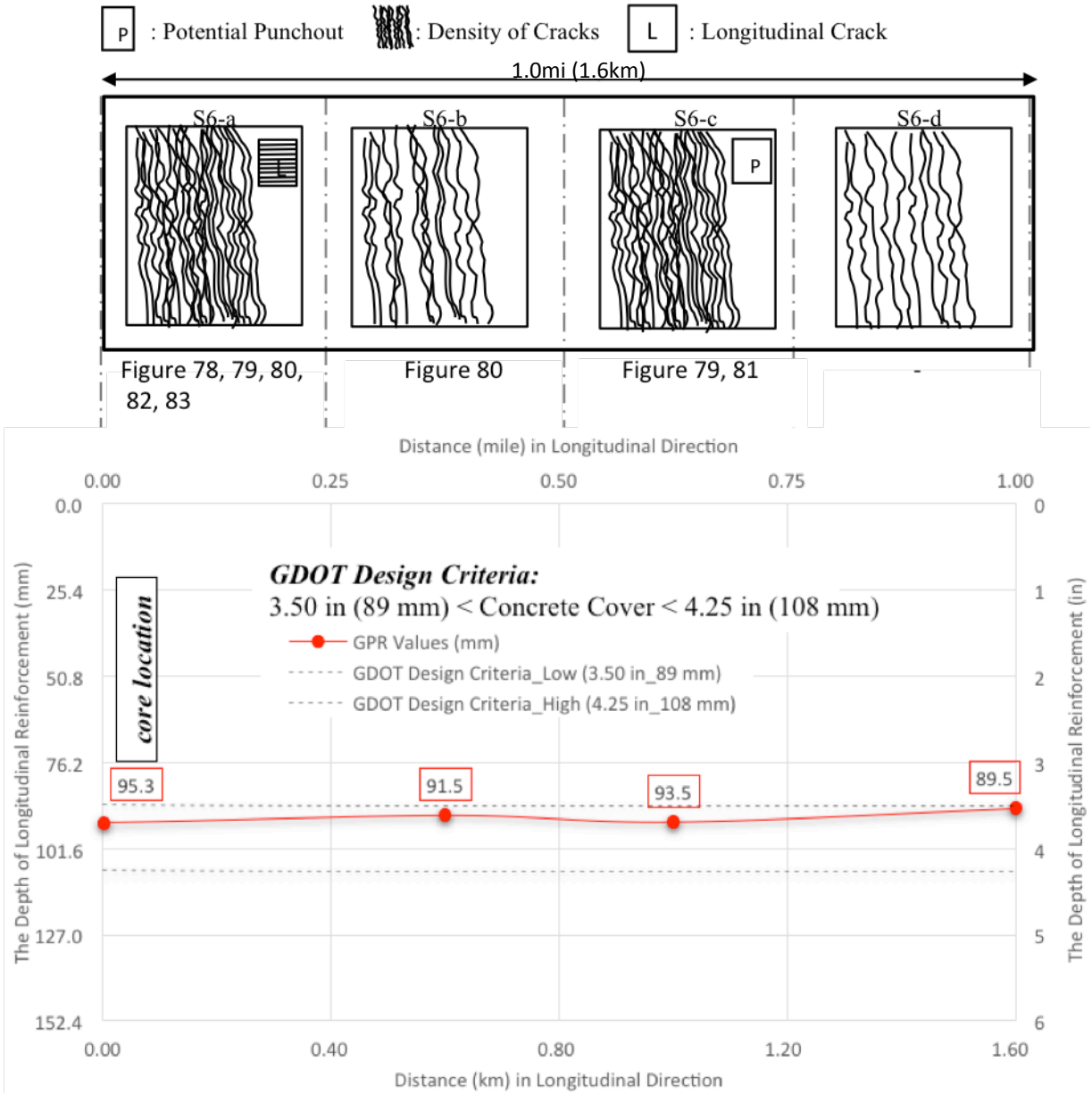

Figure 84 – Stress Pattern and Concrete Cover in Longitudinal Direction in Each Segment Along 1.0mi (1.6km)

Figure 85 indicates the depths of longitudinal reinforcement over a single transverse crack in S6-a. Although the depth measured by both techniques shows similar patterns in the graph, these values do not agree (Figure 85). As with other sections, the reason for this is

believed to be the result of varied materials such as pieces of metal which can be detected easily by GPR and Profometer units, forming the basis for this error.

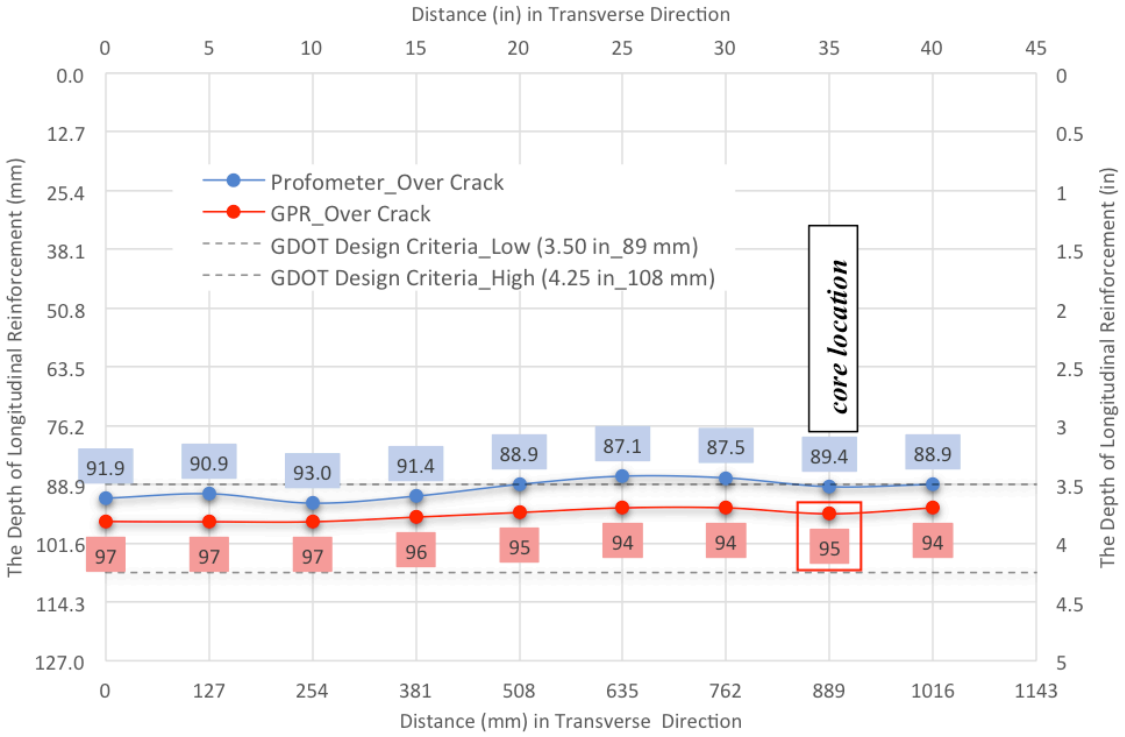

Figure 85 – Concrete Cover Depth Values Detected by Calibrated GPR and Profometer in Transverse Direction at S6-a

6.4 Comparison of Results Obtained from All Site Investigations

6.4.1 Evaluation of the Accuracy of Profometer

To confirm the accuracy of the eddy current technique, Profometer, for detecting the rebar cover depth, the results found by this instrument were compared with the cover depths measured directly from cores extracted from the six test sections. Table 16 presents the actual concrete cover and the depth estimated by the Profometer, together with the percentage of error in detection.

In addition, Table 16 includes the difference in depth values between the actual cover depths measured on the core specimens and the estimated cover depth from the Profometer. Although the Profometer mostly indicated cover depths less than the measured cover depths from the cored specimens, it occasionally estimated the higher concrete cover depth. Based on the difference of the measured and estimated concrete cover size, the percentage error in detection was calculated.

Table 16 – Accuracy of Profometer

	Site Names	Core Cover Depth, in (mm)	Profometer Cover Depth, in (mm)	Difference Depth Values between both technique, in (mm)	Error in detection (%)
Site 1	SR6NBCMP0-1	3.50 (89)	3.46 (88)	0.04 (1)	1.1
Site 2	I20EBHMP4-5	4.25 (108)	3.58 (91)	0.67 (17)	15.8
Site 3	I20WBCMP24-25	4.00 (102)	4.02 (102)	-0.02 (-0.5)	-0.5
Site 4	I20EBNMP92-93	4.00 (102)	4.22 (108)	-0.22 (-6)	-5.5
Site 5	I75NBCMP267-268	4.50 (114)	4.09 (104)	0.41 (10)	9.1
Site 6	I75NBTMP57-58	3.70 (94)	3.52 (89)	0.18 (5)	4.9

The manufacturer indicates that the cover measuring accuracy might vary from ±0.04-0.16in (1-4mm). Based on the results of this study, the 15.8% and 9.1% errors in detection of the concrete cover for Site 2 and 5, respectively, were determined. This error may be a result of Site 2 and 5 having the deepest concrete covers, with 4.25in (108mm) and 4.50in (114mm) of depth, respectively. Site 3 indicated a detection error of 0.02in (0.5mm) which is within the manufacturer's accuracy range mentioned previoulsy. Site 4 with the same concrete cover as Site 3 resulted in an error slightly outside the same manufacturer's accuracy range. Based on these results, it is clear that even though there was not a linear relationship between an increase in depth and the percentage of error, the accuracy of the Profometer decreases as the depth of concrete cover increases -- although rebar size could also affect the results. The manufacturer's manual and other available studies supported this interpretation.

6.4.2 Correlation Between Distresses and Normalized Cover Depth and CRC Thickness

The relationship between the concrete cover depth (C_c) and pavement thickness (D) might affect the formation of distresses on the pavement. Therefore, this relationship was evaluated by comparing the six sites having different concrete layer thicknesses and cover depths (Table 17). The severity of pavement distress (e.g., cluster cracking and punchouts) appears to increase as the thickness decreases and cover depth increases.

Table 17 – The Normalized Concrete Cover Depth / Concrete Thickness

	Site Names	Core Cover Depth, in (mm)	Concrete Pavement Thickness, in (mm)	Normalized 1 - C_c /D
Site 1	SR6NBCMP0-1	3.50 (89)	12.00 (305)	0.71
Site 2	I20EBHMP4-5	4.25 (108)	12.00 (305)	0.65
Site 3	I20WBCMP24-25	4.00 (102)	8.70 (221)	0.54
Site 4	I20EBNMP92-93	4.00 (102)	12.00 (305)	0.67
Site 5	I75NBCMP267-268	4.50 (114)	10.25 (260)	0.56
Site 6	I75NBTMP57-58	3.70 (94)	12.00 (305)	0.69

The concrete cover depths recommended by GDOT are in the range of 3.50in (89mm) and 4.25in (108mm) for a concrete slab thickness of 11.00in (279mm) or 12.00in (305mm). Cover depths were found to be a contributing factor to the density and severity of distresses in this study (Figure 86).

Figure 86 – The Density of Transverse Cracks in Sites 1, 3, and 5

Based on the literature review, the Mechanistic-Empirical Pavement Design Guide (MEPDG) recommends an ideal range of the mean crack spacing between 3.0-6.0ft (0.9-1.8m). A range of 3.5-8.0ft (1.1-2.4m) is recommended by the 1993 AASHTO CRCP design guide. Sites 1, 3, 4, and 6 had similar transverse crack spacing, typically 1.0ft (0.3m). The transverse crack spacing of Site 2 and Site 5 was typically 1.6ft (0.5m) and 3.3ft (1m), respectively. Therefore, according to MEPDG, the transverse crack spacing of the investigated sites was outside of the recommended range, except for Site 5. The potential for punchouts was observed in Sites 5 and 6.

Figure 87 indicates the relation of normalized ratios (1-Cc/D) for six investigated sites, where Cc is the concrete cover depth and D is the thickness of concrete pavement. As presented in this graph, the sites with the low value of the normalized ratio showed poor performance compared to the others. This study demonstrates the importance of placing the longitudinal steel reinforcement at the top third of the concrete thickness. This should ensure better performance than concrete with steel placed at the mid-depth of concrete thickness.

Figure 88 indicates the relationship between crack width of transverse cracks (CW) and the normalized ratios (1-Cc/D). As the steel is placed at or around the mid-depth of concrete thickness, the concrete pavement produces wider transverse cracks. The sites in poor conditions indicated wider transverse cracks between 0.10-0.15in (3-4mm), as shown in Figure 88.

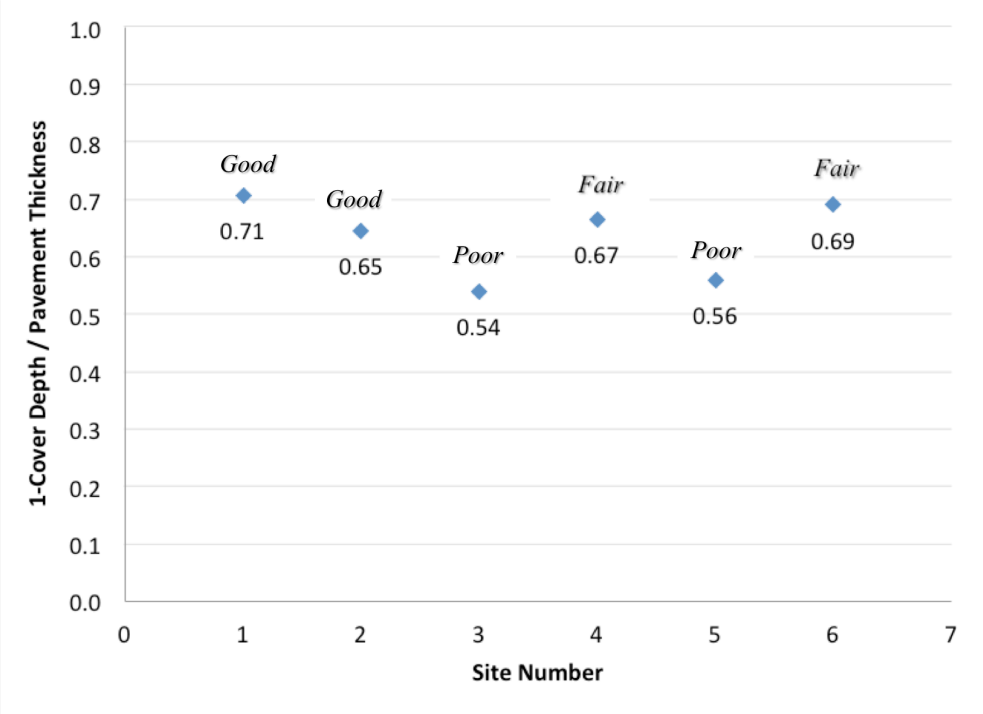

Figure 87 – The Relation between the Normalized Ratio (1 - Cc /D) and Sites

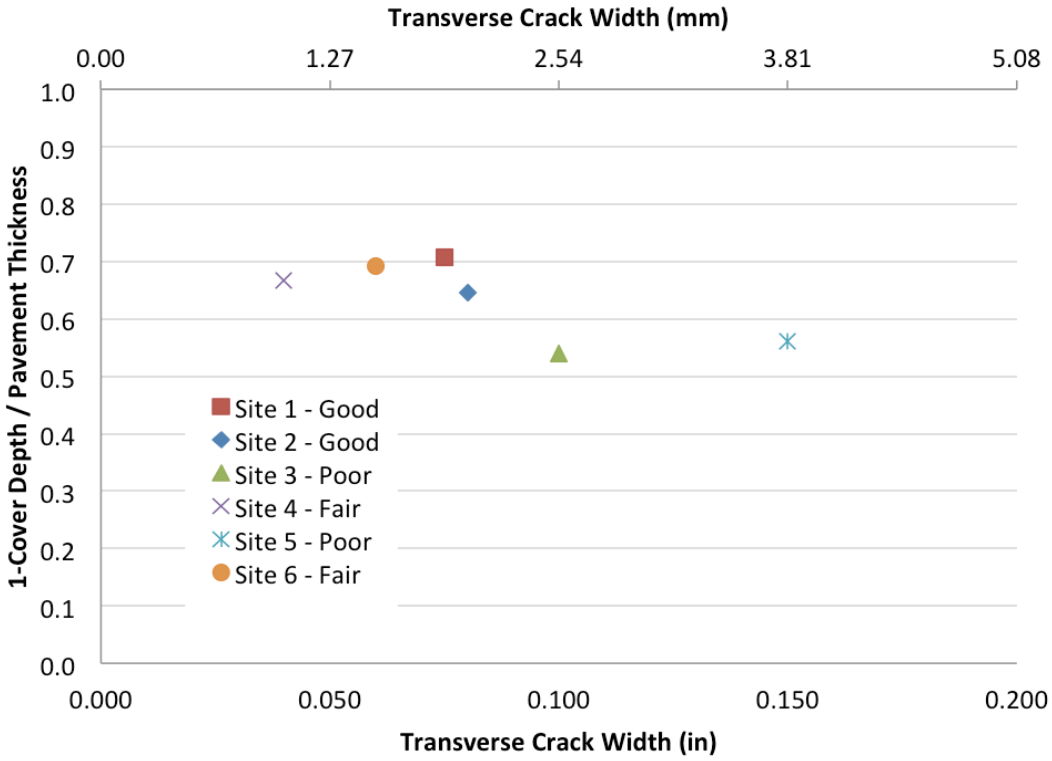

Figure 88 – The Relation between the Normalized Ratio (1 - Cc /D) and Transverse Crack Width

It is concluded that the transverse crack width is wider when the concrete cover depth and concrete thickness were not in the recommended range. As shown in Figure 89, Site 5 had the highest value of concrete cover of 4.50in (114mm) with a concrete pavement thickness of 10.25in (260mm). At this site, the average width of transverse cracks was typically 0.15in (4mm) even though locally it had a few cracks with a maximum width of 0.50in (13mm). The reason for this is that as the steel is placed lower within the pavement depth, the cracks will not be held tight by steel reinforcement. Thus, the data recorded in this study verified the hypothesis that wider cracks result from deeper reinforcement.

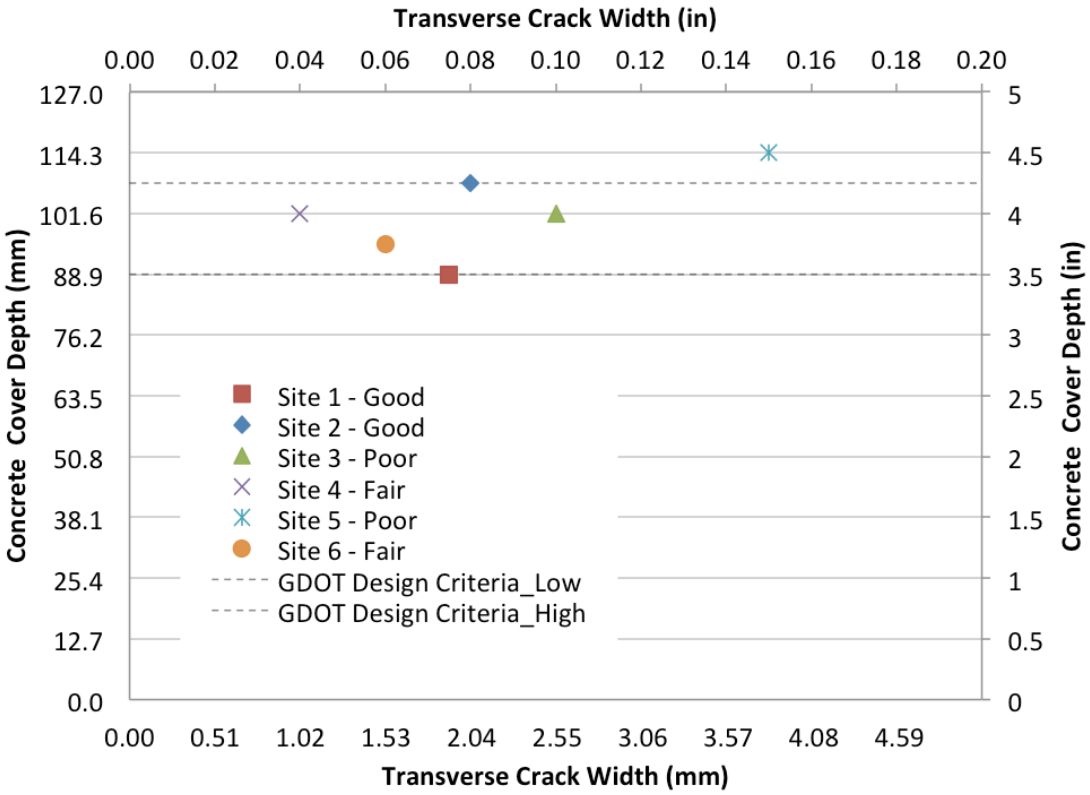

Figure 89 – The Relation Between the Concrete Cover Depth and Transverse Crack Width

6.5 Analysis of Findings and Summary

In this research, each site was evaluated within four divided segments. Most segments had clusters of transverse cracks. Based on the clusters of transverse cracks and crack spacing measurements, the number of transverse cracks formed within a 100.0ft (30.5m) section was estimated. According to the results, the sites in fair condition had a significant number of transverse cracks within a 100.0ft (30.5m) section (Figure 90). However, it was expected that the sites in poor condition would have more cracks and distresses. Therefore, it was understood that both the transverse cracks and the longitudinal cracks must be evaluated together in order to be able to assess the condition of field performance relative to each site.

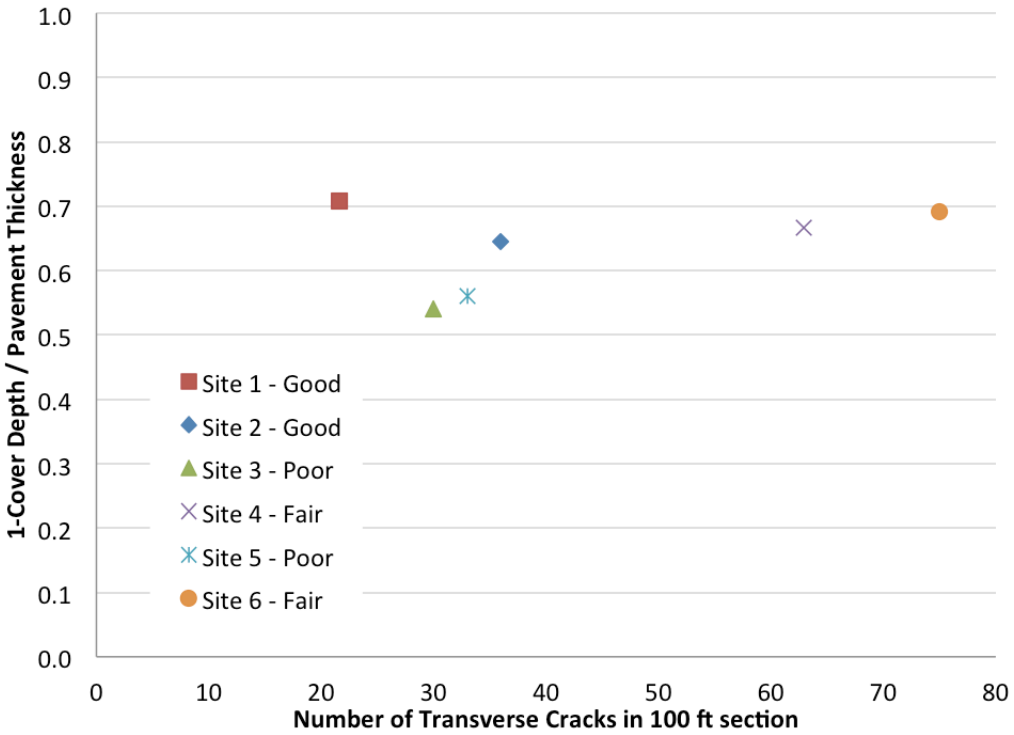

Figure 90 – The Relation Between the Normalized Ratio and Number of Transverse Cracks in a 100 ft Section

Although there were no visible longitudinal cracks in Sites 1, 2, and 3 (except for the cracks causing punchouts in Site 3), Sites 4, 5, and 6 had visible longitudinal cracks with typical

widths of 0.05 in (1mm), 0.05in (1mm), and 0.06in (2mm), respectively. Based on observations in the field, some of these cracks will lead to potential punchouts. To evaluate both transverse and longitudinal cracks together, a distress factor was created by considering the number of transverse cracks in 100.0ft (30.5m) section, as well as the total length of longitudinal cracks in a 100.0ft (30.5m) section. The total length of longitudinal cracks was estimated based on the crack patterns recorded during the site investigation. This total length included the continued and discontinued longitudinal cracks in a cluster. The total length was determined to be more than 100.0ft. (30.5m) if a cluster has a significantly large number of longitudinal cracks. Ultimately, a distress factor was computed by determining the proportion of the number of transverse cracks to the total length of longitudinal cracks in a 100.0ft (30.5m) section. Figure 91 presents a comparison of the normalized ratio of the six sites in terms of their distress factors. Based on the results, the distress factor appears to be a good indicator of pavement performance. For instance, Sites 3 and 5, in poor condition, had high distress factors with 3.33 and 3.23, respectively. Alternatively, Sites 1 and 2 are in good condition, and thus had much lower distress factors (0.05 and 0.03, respectively).

When considering the results obtained from the six sites, a question arises: why are the sites classified as being in "good," "fair," and "poor" condition in the first place? In response to this question, many factors can be considered, such as the number of transverse cracks, total length of longitudinal cracks, transverse crack widths, and traffic loads. In this project, the pavement evaluation began by considering the normalized ratio of the sites. As shown in Table 18, the sites with similar normalized ratios were compared. It was shown that even if the design parameters are the same/similar, the pavement performance was different depending on the distress factor. Moreover, a relationship was found between the distress factor and the Average

Annual Daily Traffic (AADT). In other words, the most important factors in labeling the site conditions as good, fair, and poor were the density of distress, including punchouts and AADT, as listed in Table 18. Overall, the conditions and pavement performance levels of the six sites were evaluated relative to each other by considering the criteria previously described. Based on the analysis of this table, Sites 1 and 2 were described as being in good condition, whereas Sites 3 and 5 were in poor condition. Sites 4 and 6 were in fair condition. Finally, a summary table including all pavement information and data collected in this study is presented in Appendix G.

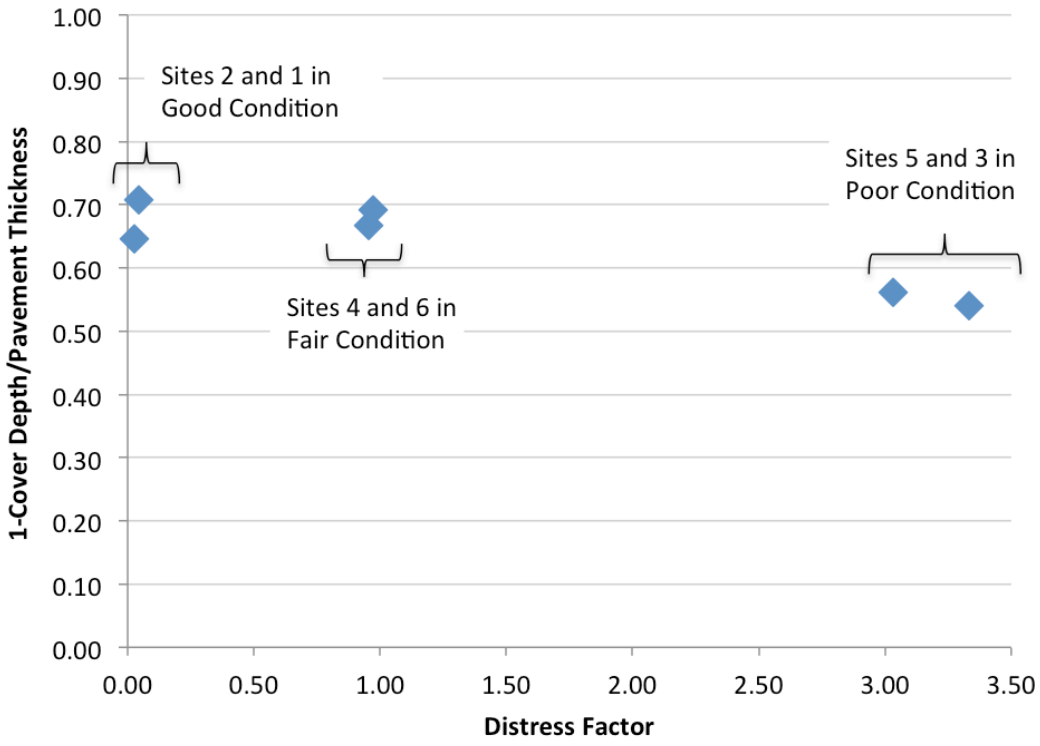

Figure 91 – The Comparison of the Normalized Ratio and Distress Factors

Table 18 –Comparison of the Site Conditions

	Site 1 vs Site 6	Site 2 vs Site 4	Site 3 vs Site 5
Normalized Ratio	0.71 > 0.69	0.65 < 0.67	0.54 < 0.56
Transverse Crack Width (in)	0.08 > 0.06	0.08 > 0.04	0.10 < 0.15
Transverse Rebar Spacing (ft)	3.0 = 3.0	3.3 > 3.0	No > 3.3
Cluster of Transverse Crack Spacing (ft.)	46.0 > 6.0	24.0 > 12.0	15.0 > 1.0 (no grouping)
Number of Transverse Cracks in 100 ft. Section	22 < 75	35 < 61	30 < 31
Total Length of Longitudinal Cracks in 100 ft. Section	1 < 73	1 < 60	100 = 100
Distress Factor	0.05 < 0.97	0.03 < 0.98	3.33 > 3.23
AADT (2016)	37000 < 44600	36400 < 66300	67900 < 215000
Comparison of the Site Conditions	**Site 1 ➔ Good** **Site 6 ➔ Fair**	**Site 2 ➔ Good** **Site 4 ➔ Fair**	**Site 3 ➔ Poor** **Site 5 ➔ Poor**

7. DEVELOPMENT OF GDT

As discussed in the objectives in Section 1, this work is split into two distinct sections: one considering the pavement performance of CRCP in Georgia using GPR technology together with eddy current technology and Profometer, and another evaluating the utility of Profometer in the absence of a cored sample for the calibration process of GPR in the field. In addition, the forensic investigation procedure employed in this study is summarized in Appendix H. The developed method describes the process applied during site investigations and post-processing. Finally, a recommended GDT non-destructive test method for GPR has been created for future use when evaluating the pavement performance.

Appendix H has been defined under eight subtitles, including scope, apparatus, CRCP test section limits, equipment installation, site investigation procedure, and post-processing procedures, calculations, and report. This test method is used to evaluate the performance of CRCP using GPR technique. Appendix I includes a draft GDT-GPR standard for evaluating rebar depth/spacing/location and pavement layer thickness using a ground penetrating radar (GPR) device.

7.1 Scope and Apparatus

The first section of the CRCP investigation procedure (Appendix H) and GDT-GPR standard (Appendix I), presents the scope explaining the content of the standard and the purpose. The second section, ‘apparatus’, provides detailed information regarding the necessary equipment to conduct a survey when gathering data taken from a GPR pavement evaluation. The investigation requires the use of major components of a GPR unit, including antenna, survey wheel, and power supplies, a core equipment providing the accurate measurements for calibration of GPR, and Manufacturer’s Instruction Manuals.

7.2 CRCP Test Section Selection

In Appendix H, the 'limitations and recommendations for selecting CRCP test sections' subsection presents recommended practices during and before a site investigation. Based on this research, the CRCP sections shall be tested in 1.0mi (1.6km) lengths and divided into 3-4 sub-segments by considering the density of the transverse and longitudinal cracks, punchouts, and the existence of any distress types. Each sub-segment shall be surveyed by using a GPR unit over damaged and non-damaged areas in the transverse directions. In addition, the distance between sub-segments shall be surveyed using GPR in the longitudinal direction (traffic direction). The reason for this is to detect the location of longitudinal and transverse reinforcement bars and the concrete cover and to establish relationships between the locations of cracks and reinforcement patterns.

Appendices H and I provide the notes and limitations that allow for a survey to be conducted properly. One of these limitations is whether the site is wet, in which case, the survey shall not be conducted because the dielectric constant of pavement materials are affected and thus the results will be affected by this condition. Additionally, the other requirement is to investigate the site in the longitudinal direction as the GPR travels on the wheel-paths. The basis for this is the fact that wheel-path locations experience greater stresses, resulting in increased distress and surface wear.

7.3 Equipment Calibration Procedure

Equipment installation/calibration procedure in the GDT-GPR standard details the experimental work for a site investigation. This section discusses the preliminary preparations, including the required equipment, adjustments made on settings of the equipment, and the survey wheel calibration of GPR. These preparations shall be fulfilled to collect more accurate results

throughout field investigation before surveying site. For the 'TerraSIRch SIR-System' 3000 device, the following settings are recommended if concrete material is surveyed:

- Frequency: 1.5 GHz (Model 5100)
- Transmit Rate (T_RATE): 100 KHz
- Samples per Scan: 512
- Format (Resolution, bits): 16 bits
- Range (nS): 12 nS
- Scan per Unit: 5/inch
- Number of Gain Points: 2
- Vertical IIR High Pass (HP_IIR): 10 MHz
- Vertical Low Pass Filter (LP_FIR): 3000 MHz
- Vertical High Pass Filter (HP_FIR): 250 MHz

In addition, this section of the standard provides a detailed procedure for the calibration process of GPR in the field by taking a core sample. Calibration of a GPR device in the field is the part of the survey most important to obtaining accurate data from the investigation, as discussed in Section 5.1. The procedure used for calibration presented in Appendix H was derived from the manufacturer's manual (GSSI 2003) and the author's experiences at the sites.

7.4 GPR Operation Procedure

Appendix H includes a recommended site investigation procedure which includes the general steps on how to survey a site and operate a GPR device. This section pays particular attention to a few subjects to be considered in evaluating the performance of pavement in the field. Namely, each sub-segment should be surveyed to collect GPR data in longitudinal and transverse directions. In this study, the locations of the longitudinal and transverse bars are determined with

respect to the locations of transverse cracks detected. Finally, all collected data is recorded, taken by a compatible storage system, and uploaded to the software program for post-processing.

7.5 Post-Processing Procedure and Interpretation of Data

Post-processing covers the period after a site investigation and the procedure for post-processing. A software program compatible with a GPR device shall be used to accurately interpret the data collected from the site. For the 'TerraSIRch SIR System-3000' GPR model, the 'RadView' software program is recommended because they are compatible with one another. If there is a need, the images (or radargrams) might be calibrated or scaled in this software by considering the accurate measurements taken from the core specimens or Profometer technology. After reviewing the adjusted (e.g., applying a filter) and calibrated radargrams, the depth and location of reinforcement are to be interpreted. Furthermore, continuous thickness readings (or variations) over a surveyed segment should be obtained.

7.6 Calculations and Report

There is no need for calculations in this test. This report has been prepared to present all data and results obtained from post-processing and a review of radargrams.

7.7 Summary

Appendix H provides a detailed procedure for investigating CRCPs using the TerraSIRch SIR System-3000 device. In addition, there is a need to develop a GDT for the use of any GPR model/device when determining rebar depth, location, and/or spacing in concrete pavements, as well as thickness of concrete/asphalt concrete pavement and sub-base layers. Therefore, Appendix I presents a draft GDT standard for evaluating pavement layers with a GPR device and thus reflects a more generalized procedure.

8. CONCLUSIONS AND RECOMMENDATIONS

8.1 Conclusions

In this project, the performance of CRCP sections was investigated using non-destructive testing methods that included the GPR and the eddy current technology Profometer. The influence of reinforcement placement and concrete cover on pavement distress was evaluated. In addition, eddy current technology was utilized as a non-destructive cover meter technique for calibrating the GPR unit in the absence of a cored sample. Based on the results of the field tests, the following conclusions were made:

1. GPR is an effective technology for measuring concrete cover depth in the field. Field calibration is necessary with known concrete cover depth. For the calibration process, core specimens are generally taken, because the assumed dielectric value of concrete must be corrected during the investigation. Concrete coring can be avoided/minimized when GPR and the Profometer are used simultaneously.
2. Profometer is a practicable technique for easily calibrating the GPR unit in the field. The technology gives the estimated cover depth values which are close to cored specimens. As the concrete cover depth increases, the accuracy of Profometer decreases, particularly when the rebar size remains constant (e.g., No. 6 bar). Due to having more sensitivity to external influence, Profometer gives results that might be affected by other factors such as bar diameter settings, existence of neighboring bars, or probe settings for shallow or deep areas. Based on the field test results and the manufacturer's manual, the Profometer is preferred when the concrete cover depth is not deep (or within a detectable range of the Profometer based on the rebar size and depth), and where the spacing between reinforcements is not small.

3. The existence of single transverse cracks or cluster cracking in CRCP is a common phenomenon in practice. However, the narrowly-spaced cluster cracking should be continuously monitored as it has a potential to form punchout, particularly when combined with longitudinal cracking.
4. As the transverse and longitudinal reinforcements are placed lower within the pavement cross-section, more transverse cracks occur. This results in wider crack widths and poses a fundamental problem, such as corrosion of steel within the pavement.
5. Based on the results, if the reinforcement is placed close to mid-depth of pavement thickness or deeper, the pavement distress increases. Therefore, it is recommended that the rebar shall be placed at the top-third of the total concrete thickness, rather than within a specified cover range of 3.50-4.25in (89-108mm). This places the cover depth at a ratio of the slab thickness rather than at a predetermined measurement.
6. Transverse cracks were frequently observed on top of transverse rebar locations, especially when the transverse rebar spacing was 3.5ft (1.1m). On the other hand, transverse cracks were observed between the transverse rebar locations when the spacing was 3.0ft (0.9m). It appears that decreasing the transverse rebar spacing less than 3.5ft (1.1m) does not help to reduce the number of transverse cracks.

8.2 Recommendations and Future Studies

The following are recommendations for future studies:

1. Continuous monitoring of the pavement performance is recommended to better understand the causes of distresses and crack development on the CRCP.

2. To increase the accuracy of the Profometer, a recent version of the instrument having more options in probe settings could be used for CRCP sections which have increased depths of concrete cover.
3. The utility of Profometer should be further investigated for the calibration of GPR in the absence of cored samples by taking more than one core specimen and using the latest version instrument in order to improve the reliability and accuracy.
4. The use of updated GPR model instead of the TerraSIRch SIR 3000 model containing a single antenna, is recommended for the future research. A GPR unit containing multiple antennas is strongly recommended to collect more detailed and reliable data. In addition, depending on the GPR model, the latest software should be used to reliably post-process the results.
5. In this study, a GPR system was primarily used to determine depth and alignment of reinforcement in pavements. GPR scans are also used to identify defects (e.g. weak bonds and/or voids between pavement layers) beneath the pavement layer and within the pavement layers, and determine the density of concrete/asphalt layers and material properties. Conducting GPR scans in conjunction with a rebar cover meter (e.g., Profometer) has the advantage of being rapid, efficient, and cost effective compared to conducting borings to assess existing pavement conditions. Furthermore, GPR systems deployed on roads and bridges can provide continuous measurements along a pavement alignment.

REFERENCES

1. AASHTO (1986, 1993). AASHTO Guide for the Design of Pavement Structures, American Association of State Highway and Transportation Officials, Washington, DC.

2. AASHTO, T 336 (2011). Coefficient of Thermal Expansion of Hydraulic Cement Concrete. Standard Specifications for Transportation Materials and Methods of Sampling and Testing.

3. ACPA (2016). Continuously Reinforced Concrete Pavement (CRCP). http://wikipave.org/index.php?title=Continuously_Reinforced_Concrete_Pavement_(CRCP). Accessed December 2016.

4. American Iron and Steel Institute (2014). Steel Works. https://www.steel.org/~/media/Files/SMDI/Construction/CRCP%20-%20Marketing%20-%20CRCP%20Brochure.pdf?la=en. Accessed December 2016.

5. Annan, A. P. (2004). Ground Penetrating Radar Principles, Procedures, and Applications. Mississauga, Canada: Sensors & Software

6. ARA, Inc. (2003). Guide for Mechanistic-Empirical Design of New and Rehabilitated Pavement Structures, Appendix LL: Punchouts in Continuously Reinforced Concrete Pavements. Champaign, Illinois.

7. ARA, Inc. (2004). Guide for Mechanistic-Empirical Design of New and Rehabilitated Pavement Structures Part 3. Design Analysis Chapter 4. Design of New and Reconstructed Rigid Pavements: National Cooperative Highway Research Program, Transportation Research Board, National Research Council.

8. ASTM-D6432 (2011). Standard Guide for Using the Surface Ground Penetrating Radar Method for Subsurface Investigation, ASTM International, West Conshohocken, PA. www.astm.org.

9. ASTM, C1202-12 (2012). "Standard Test Method for Electrical Indication of Concrete's Ability to Resist Chloride Ion Penetration." ASTM International, PA, USA.

10. ASTM C469 / C469M (2014). Standard Test Method for Static Modulus of Elasticity and Poisson's Ratio of Concrete in Compression, ASTM International, West Conshohocken, PA.

11. Caltrans (2015). Concrete Pavement Guide. State of California Department of Transportation.

12. Chen, D. H., & Scullion, T. (2008). Forensic investigations of roadway pavement failures. Journal of Performance of Constructed Facilities, 22(1), 35-44.

13. CMC (2007). Georgia-A Testament of CRCP Progress. Rebar Case Study, No. 02.

14. Conyers, L. B. (1995). The use of ground-penetrating radar to map the buried structures and landscape of the Ceren Site, El Salvador. Geoarchaeology, 10(4), 275-299.

15. Conyers, L.B. (1998). Ground-Penetrating Radar. http://mysite.du.edu/~lconyer/Johnson_book_gpr.pdf. Accessed December 2016.

16. CRSI (Concrete Reinforcing Steel Institute) (2003). CRCP in Georgia- Durable Pavement on Their Mind. Case History Report, No: 61.

17. Darter, M.I., S.A. LaCourseiere, and S.A. Smiley, (1979). Performance of Continuously Reinforced Concrete Pavement in Illinois. Transportation Research Record No. 715, Transportation Research Board, Washington, DC.

18. Delatte N. (2008). Concrete Pavement Design, Construction, and Performance. Taylor & Francis Group, London and New York.

19. Diamanti, N., & Redman, D. (2012). Field observations and numerical models of GPR response from vertical pavement cracks. Journal of Applied Geophysics, 81, 106-116.

20. FHWA Tech Brief (2003). Distress Identification Manual for the LTPP (Fourth Revised Edition). Chapter 3 Distress for Pavements With Continuously Reinforced Concrete Surfaces. Report No. FHWA-RD-03-031.

21. FHWA Tech Brief (2012). Continuously Reinforced Concrete Pavement Performance and Best Practices. Report No. FHWA-HIF-12-039.

22. FHWA Tech Brief (2013). Continuously Reinforced Concrete Pavement: Extending Service Life of Existing Pavements. Report No. FHWA-HIF-13-024

23. Folliard, K. J., & Prozzi, J. A. (2005). Early-age behavior of CRCP and its implications for long-term performance.

24. GDOT (2013). "Standard Specifications for the Construction of Transportation Systems" <http://www.dot.ga.gov/PartnerSmart/Business/Source/specs/DOT2013.pdf> (Accessed December 2016)

25. Gharaibeh, N., Darter, M., & Heckel, L. (1999). Field performance of continuously reinforced concrete pavement in Illinois. Transportation Research Record: Journal of the Transportation Research Board, (1684), 44-50.

26. Gulden, W. (1980). Evaluation of the Condition of the Continuous Reinforced Concrete Pavement Section on 1-95. Office of Materials and Research Pavement and Physical Research Branch.

27. GSSI (2003). TerraSIRch SIR System-3000 User's Manual.

28. GSSI (2006). GSSI Handbook For RADAR Inspection of Concrete.

29. GSSI (2016). Ground Penetrating Radar Explained. http://www.geophysical.com/whatisgpr.htm. Accessed January 2017.

30. Ha, S., Yeon, J., & Won, M. C. (2012). CRCP ME Design Guide (No. Product 0-5832-P1).

31. Highway Research Board (1973). Continuously Reinforced Concrete Pavement. National Cooperative Highway Research Program Synthesis of Highway Practice 16. Washington D.C.

32. IDOT (2005). Pavement Technology Advisory, Testing Pavement Friction, PTA-T3.

33. Impact Test Equipment (2017). Concrete Covermeter-Profometer Model 600. http://www.impact-test.co.uk/products/5496-concrete-covermeter-profometer-model-600/. Accessed October 2017.

34. Johnson C.E. (2016). An Investigation of Distress Found in Concrete and Asphalt Pavements for Georgia Forensic Guide Recommendation.

35. Kim, S. H. (2012). "Determination of Coefficient of Thermal Expansion for Portland Cement Concrete Pavements for MEPDG Implementation" GDOT No. 10-04.

36. Kohler, E., & Roesler, J. (2004). Active crack control for continuously reinforced concrete pavements. Transportation Research Record: Journal of the Transportation Research Board, (1900), 19-29.

37. Kohler, E. R., & Roesler, J. R. (2005). Crack width measurements in continuously reinforced concrete pavements. Journal of transportation engineering, 131(9), 645-652.

38. Kohler, E. R., & Roesler, J. R. (2006) Crack spacing and crack width investigation from experimental CRCP sections, International Journal of Pavement Engineering, 7:4, 331-340.

39. LaCourseiere, S.A., M.I. Darter, and S.A. Smiley, (1978). Structural Distress Mechanisms in Continuously Reinforced Concrete Pavement. Transportation Engineering Series No. 20, University of Illinois at Urbana-Champaign.

40. Lohonyai, A.J. (2015). To Engineer is Human. A Brief History of Ground Penetrating Radar. http://alohonyai.blogspot.com/2015/01/a-brief-history-of-ground-penetrating.html. Accessed January 2017.

41. Lokesh, V., Swamy, B. S., & Vijaya, S. (2014). Study on Soundness of Reinforced Concrete Structures by NDT Approach. International Journal & Research in Engineering and Technology. eISSN, 2319-1163.

42. McGhee, K. H. (1998). A Guide to Evaluating Pavement Distress Through the Use of Video Images. Virginia Department of Transportation, Maintenance Division.

43. Mihai, P., Gosav, I., & Rosca, B. (2010). Study on the Earthquake Action of Old Masonry Structures. Journal of Applied Sciences, 10(3), 157-165.

44. NCHRP Web Document 35 (2001). Rehabilitation Strategies for Highway Pavements, Appendix A Pavement Distress Types and Causes. http://onlinepubs.trb.org/Onlinepubs/nchrp/nchrp_w35-b.pdf. Accessed December 2016.

45. Penhall Technologies. Concrete Scanning and X-ray Using GPR. https://www.penhall.com/concrete-scanning-gpr/. Accessed January 2017.

46. Proceq. Profometer and Profoscope Concrete Cover Meter and Rebar Locators. https://www.proceq.com/compare/rebar-detection-and-cover-measurement/. Accessed July 2017.

47. Rada, G. R., Jones D.J., Harvey J.T., Senn K.A., & Thomas M. (2013). "Guide for Conducting Forensic Investigations of Highway Pavements." Transportation Research Board, Vol. 747.

48. Ren, D. (2015). Optimization of the Crack Pattern in Continuously Reinforced Concrete Pavements. doi:10.4233/uuid:599e8346-27d7-43e8-a67c-54f46ef03f76.

49. Roesler, J. R., Popovics, J. S., Ranchero, J. L., Mueller, M., & Lippert, D. (2005). Longitudinal cracking distress on continuously reinforced concrete pavements in Illinois. Journal of Performance of Constructed Facilities, 19(4), 331-338.

50. Selezneva O.I., D. Zollinger, M.Darter, (2001). Mechanistic Analysis of Factors Leading to Punchout Development for Improved CRCP design Procedures. Proceedings of the 7th International Conference on Concrete Pavements, p. 731-745.

51. Selezneva, O.I., (2002). Development of Mechanistic-Empirical Damage Assessment Procedures for CRC Pavements with Emphasis on Traffic Loading Characteristics. Ph.D. Dissertation, West Virginia University.

52. Sharma, S., & Das, A. (2008). Backcalculation of pavement layer moduli from falling weight deflectometer data using an artificial neural network. Canadian Journal of Civil Engineering, 35(1), 57-66.

53. Sivasubramanian, K., Jaya, K. P., & Neelemegam, M. (2013). Covermeter for identifying cover depth and rebar diameter in high strength concrete. International Journal of Civil and Structural Engineering, 3(3), 557.

54. Sub, Y. C., & McCullough, B. F. (1992). Early-Age Behavior of Continuously Reinforced Concrete Pavement and Calibration of the Failure Prediction Model in the CRCP-7 Program. Research Report 1244-3, Center for Transportation Research, The University of Texas at Austin.

55. Szymanik, B., Frankowski, P. K., Chady, T., & John Chelliah, C. R. A. (2016). Detection and Inspection of Steel Bars in Reinforced Concrete Structures Using Active Infrared Thermography with Microwave Excitation and Eddy Current Sensors. Sensors (Basel, Switzerland), 16(2), 234. http://doi.org/10.3390/s16020234.

56. Tsai, Y. J., & Wang, Z. (2014). Critical Assessment of I-85 CRCP Crack Spacing Patterns and Their Implications for Long-term Performance (No. FHWA-GA-14-1239).

57. Yoder, E. J., & Witczak, M. W. (1975). Principles of pavement design. John Wiley & Sons.

APPENDICES

Appendix A - Typical Section of SR6 North Bound Cobb County MP 0 to MP 1 Site

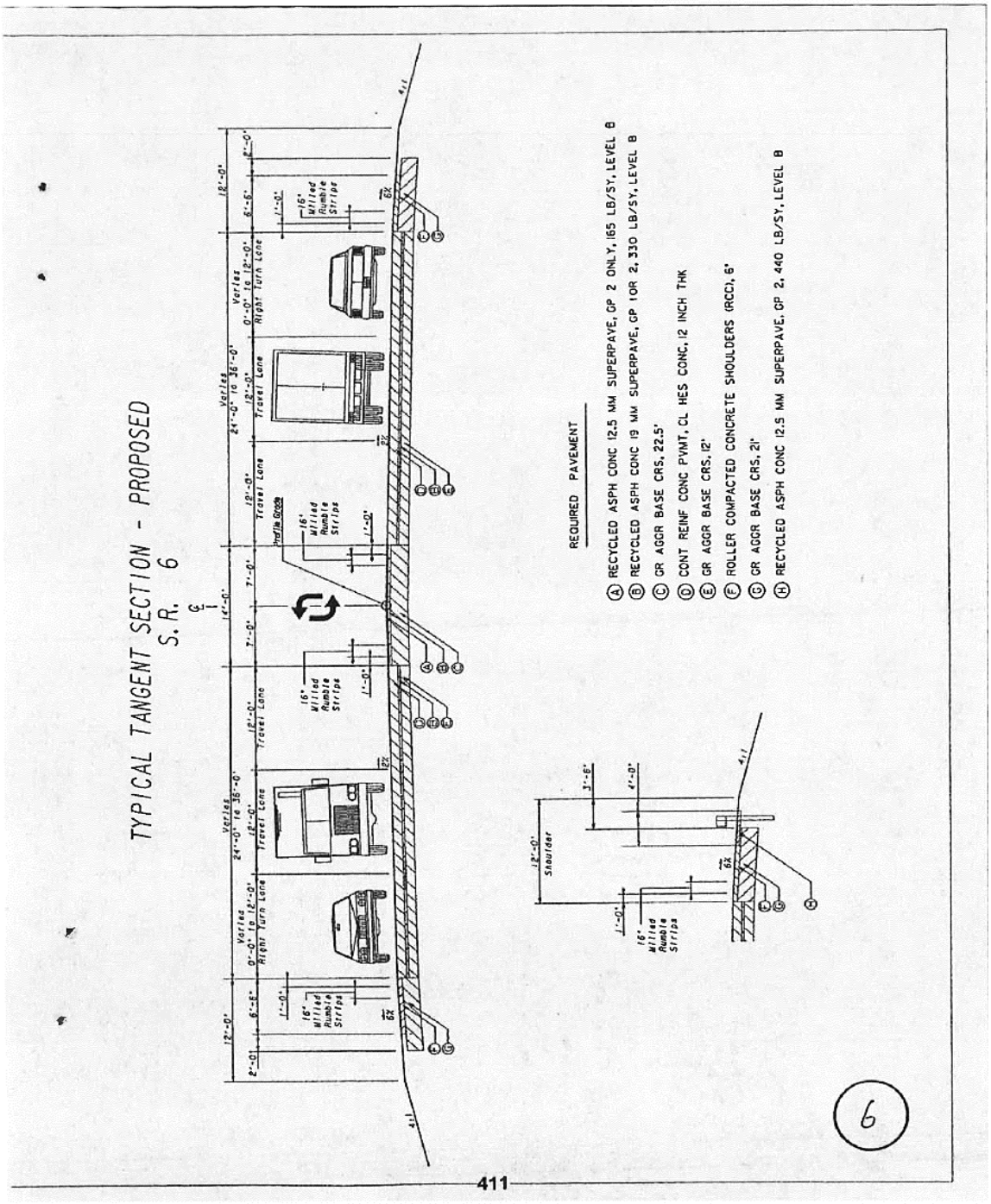

Appendix B - Typical Section of I-20 Ease Bound Haralson County MP 4 to MP 5 Site

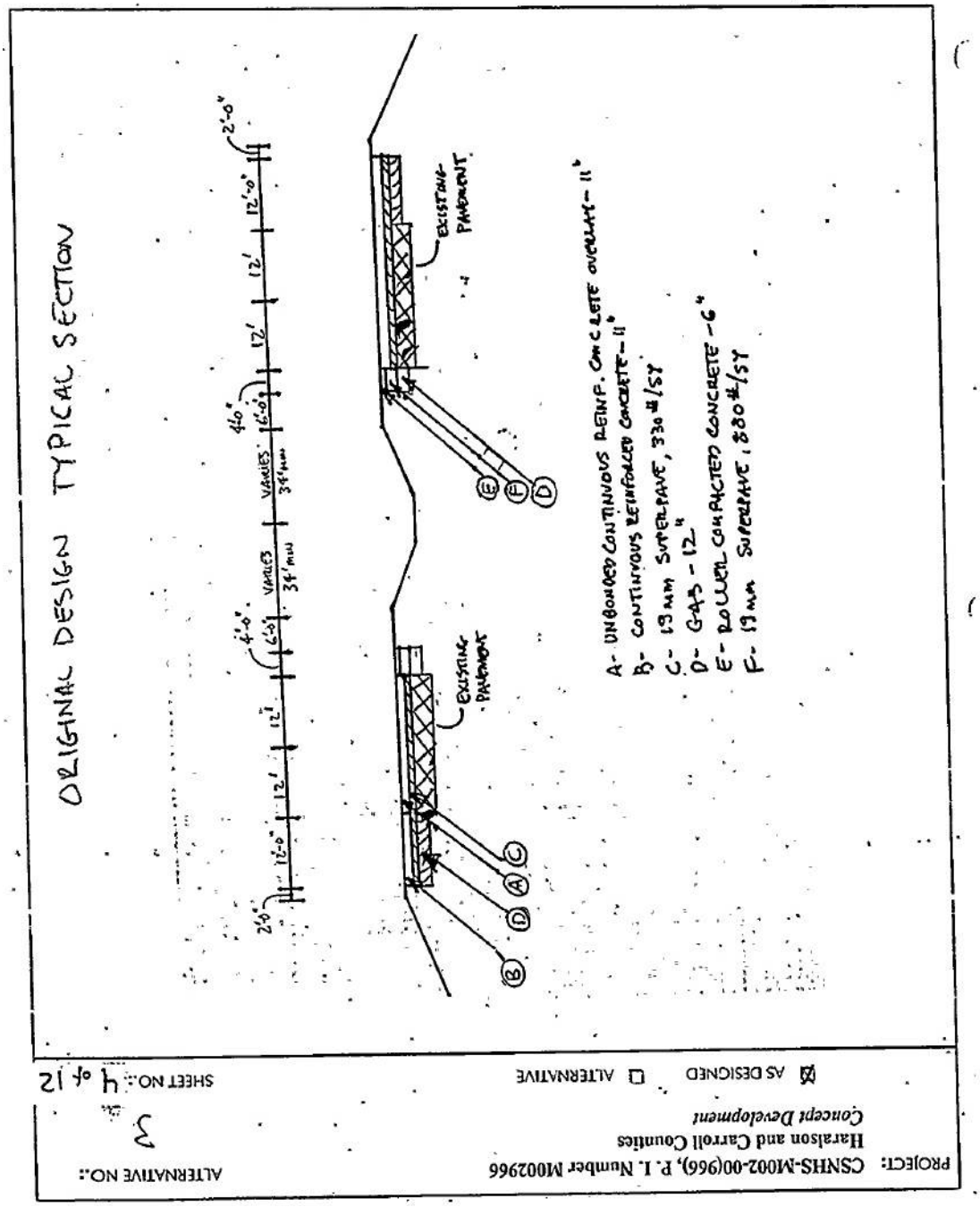

Appendix C - Typical Section of I-20 West Bound Carroll County MP 24 to MP 25 Site

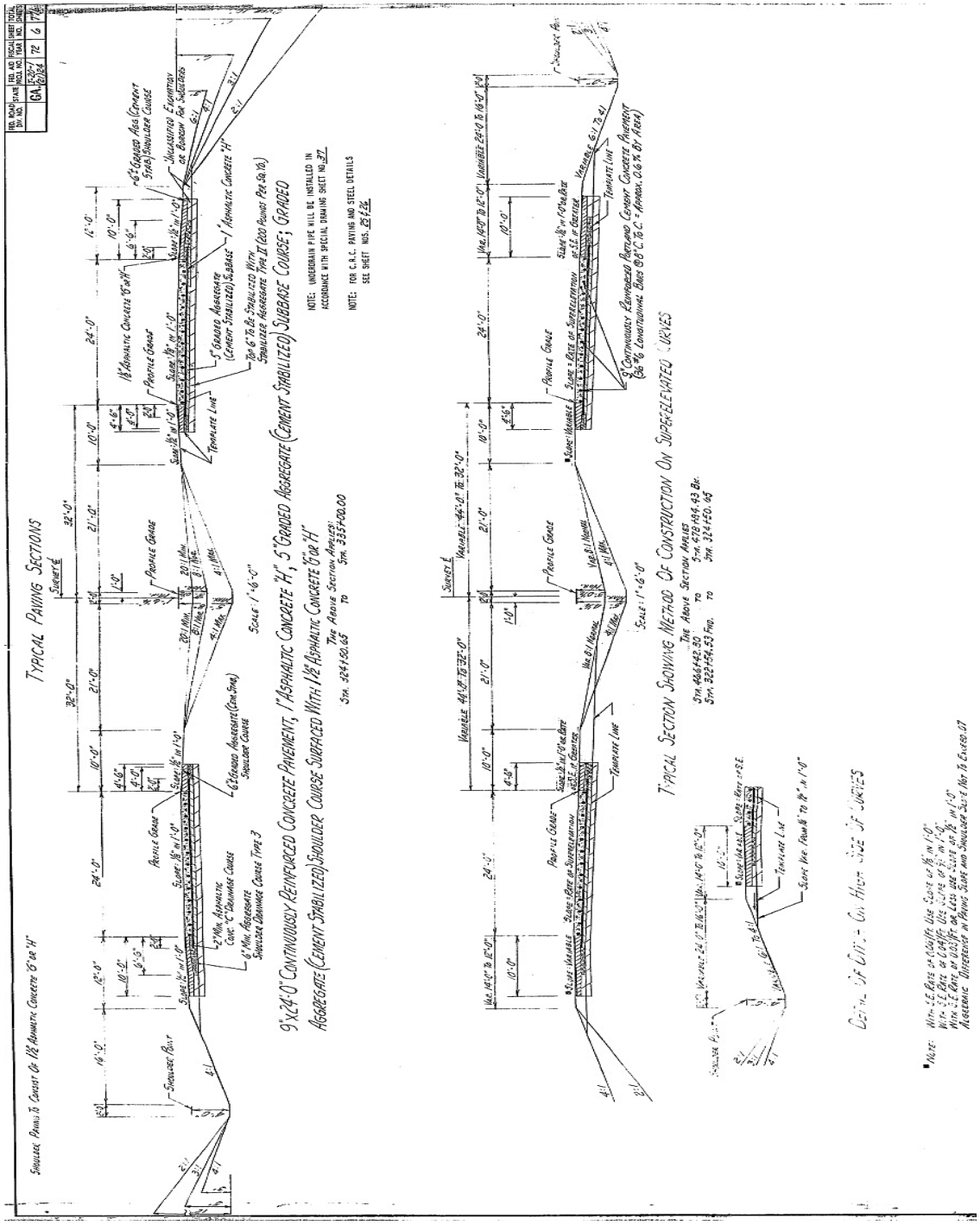

Appendix D - Typical Section of I-20 East Bound Newton County MP 92 to MP 93 Site

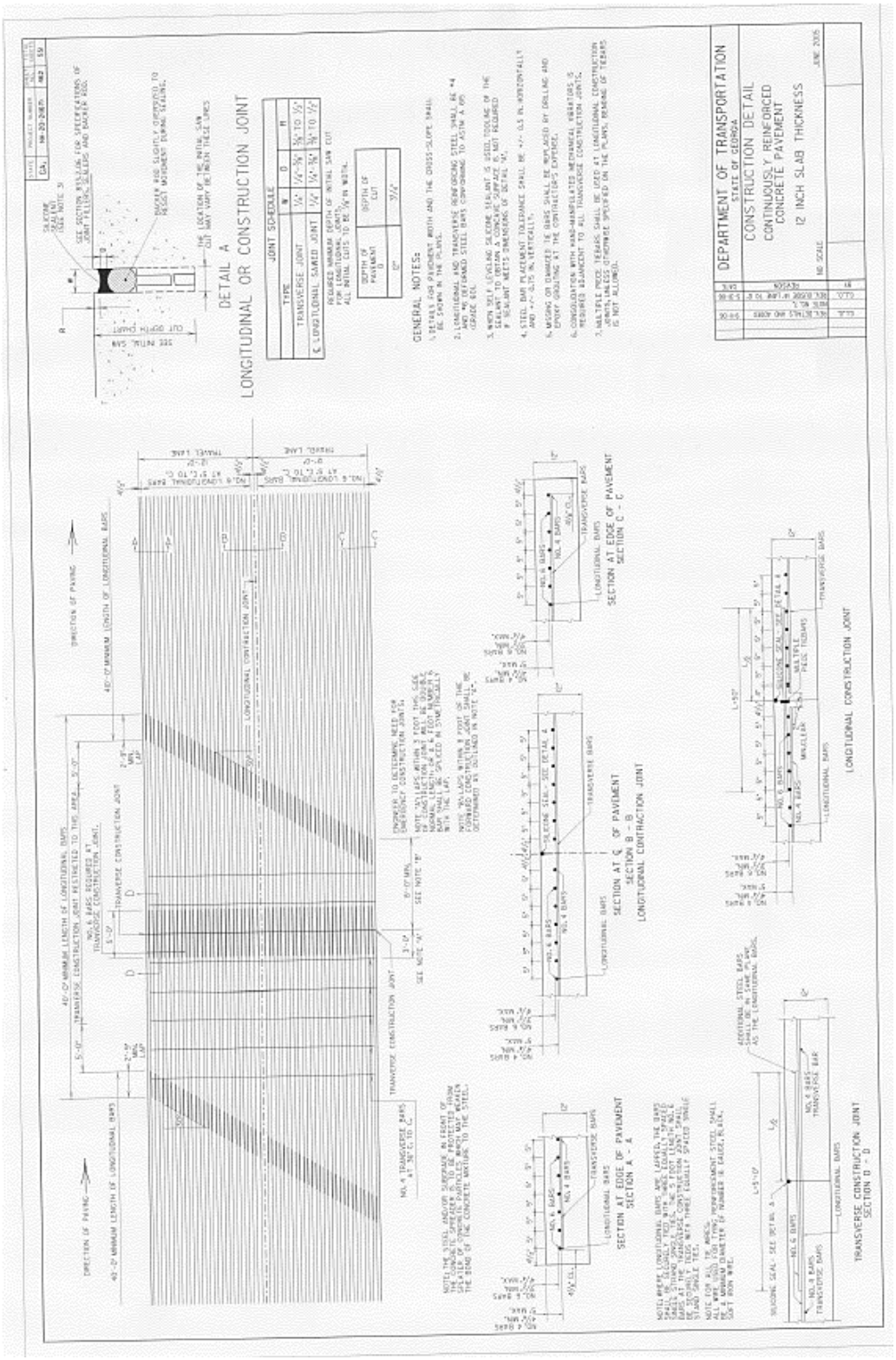

Appendix E - Typical Section of I-75 North Bound Cobb County MP 267 to MP 268 Site

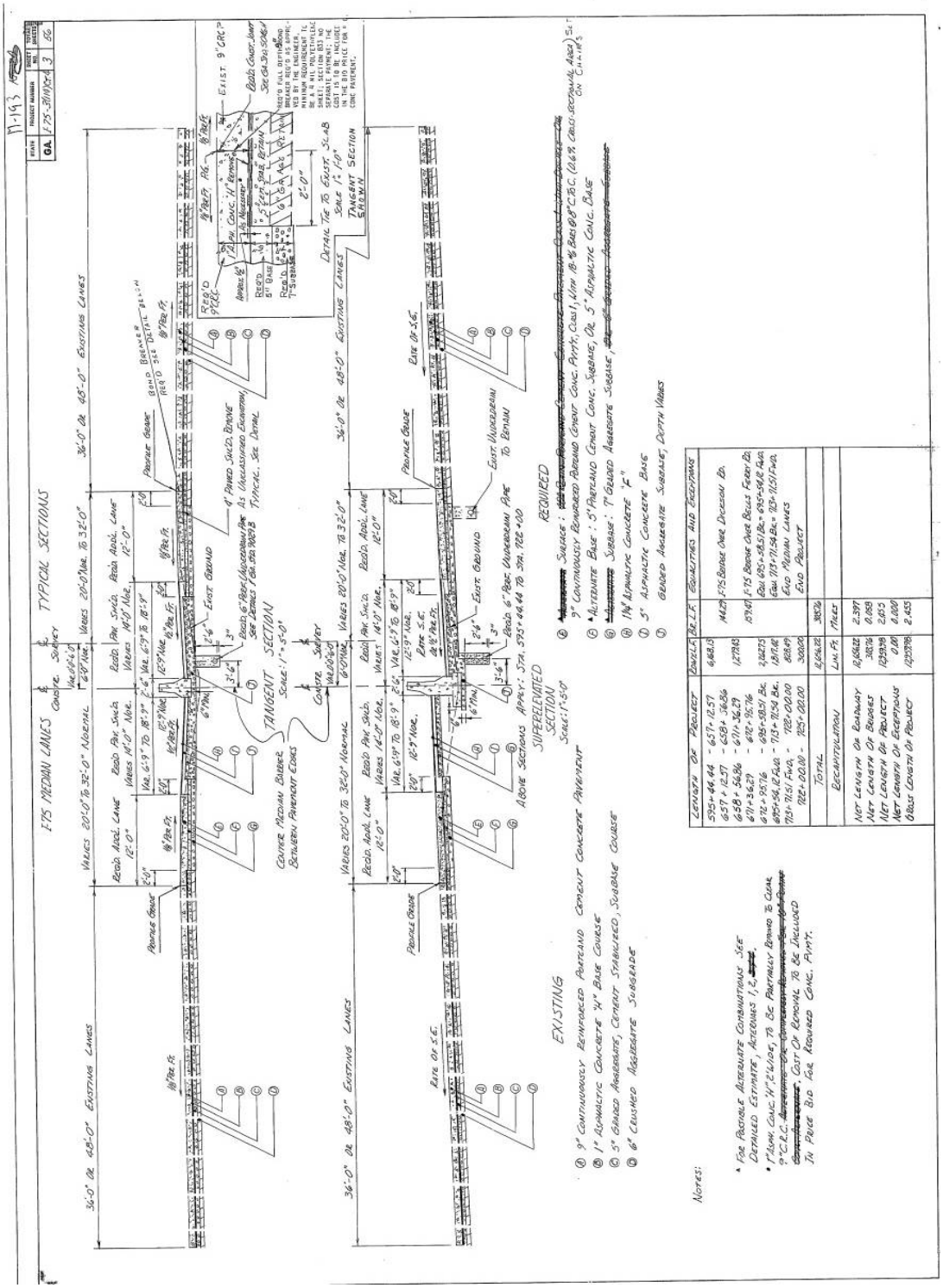

Appendix F - Typical Section of I-75 North Bound Tift County MP 57 to MP 58 Site

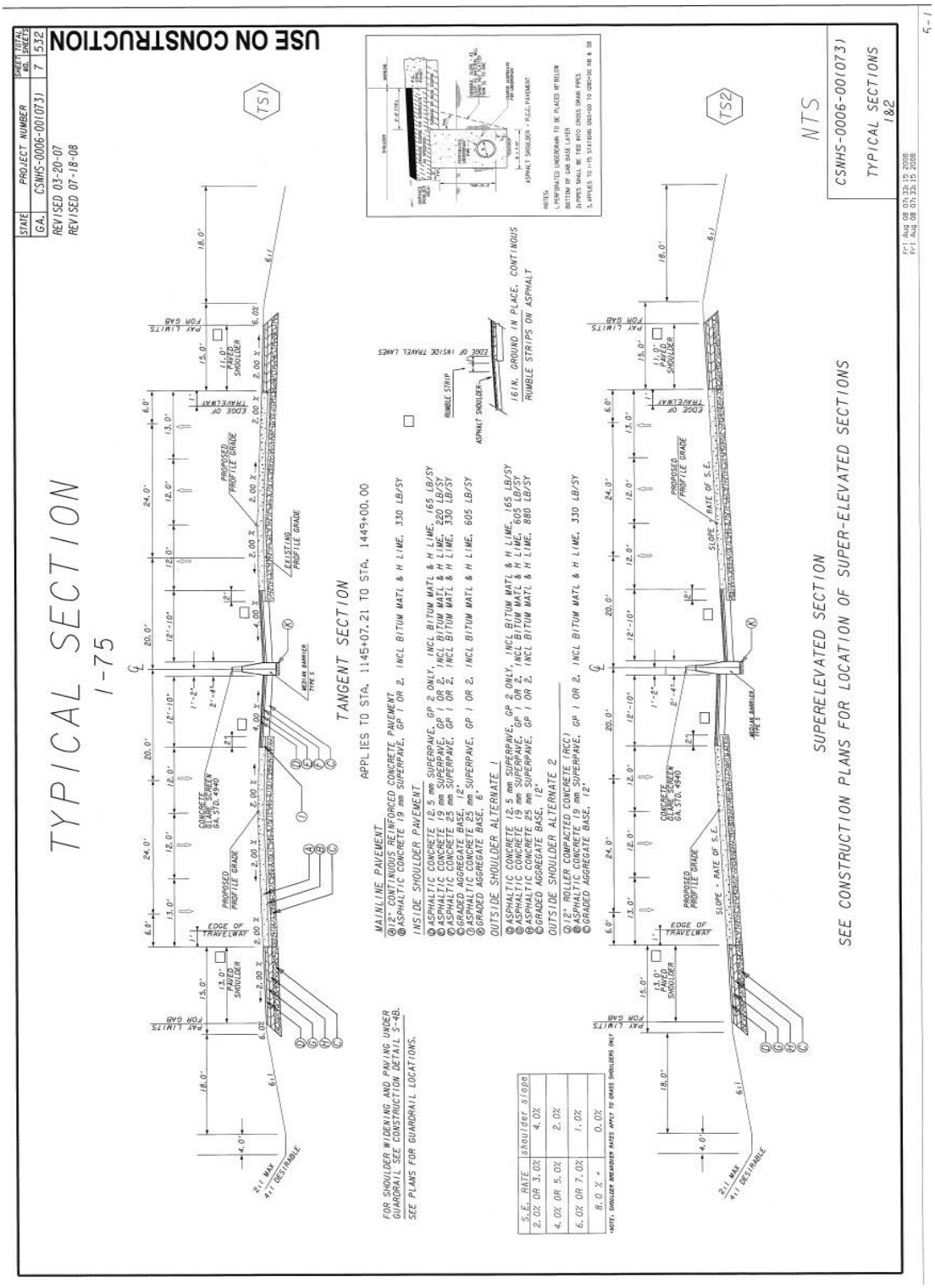

Appendix G - Summary Pavement Data Examined in Present Study

Selected Sites / NDT Results		*Site 1 SR6NBCMP0-1*	*Site 2 I20EBHMP4-5*	*Site 3 I20WBCMP24-25*	*Site 4 I20EBNMP92-93*	*Site 5 I75NBC MP267-268*	*Site 6 I75NBTMP57-58*
		SR-6 Cobb County	I-20Haralson County	I-20 Carroll County	I-20 Newton County	I-75 Cobb County	I-75 Tift County
Design Parameters	Site Condition	**Good**	**Good**	**Poor**	**Fair**	**Poor**	**Fair**
	Lane	Outside	Outside	Outside	Outside	Outside	Outside
	Age	12 (2005)	37 (1980)	45 (1972)	12 (2005)	32 (1985)	9 (2008)
	CRC Thck.(in)	12”	12”	8.70”	12”	10.25”	12”
	Longitudinal Rebar Size	#6	#6	#6	#6	#6	#6
	Spacing btw. Longt. Rebars (in)	5”	4” ~ 8”	8”	5”	5” ~ 9.5”	5”
	Transverse Rebar Size	#4	#6	-	#4	#4	#4
	Spacing between Trns. Rebars (in)	36”	23” ~ 46” (typical 39”)	-	36”	25” ~ 40” (typical 39”)	36” ~ 40” (typical 36”)
	Longitudinal Rebar Depth (in)	3.50”	4.25”	4.00”	4.00”	4.50	3.75”
	Transverse Rebar Depth (in)	4.50”	5.00”	-	4.75”	5.25	4.50”
Distress Assessment	Spacing btw. Single Transverse Cracks (ft.)	1’- 4’ (typical 1’)	1.6’~ 4.0 ‘ (typical 1.63’)	1’	1’- 10’ (typical 1’)	1.5’- 4.25’ (typical 3.25’)	1’~ 3’ (typical 1’)
	Spacing btw. Clusters of Cracks (ft.)	46’	24’	10’~ 20’	12’~ 60’ (typical 12’)	No Grouping (typical 1’)	6’~ 12’ (typical 6’)
	Transverse Crack width (in)	0.04” ~ 0.14” (typical 0.075”)	0.03” ~ 0.1” (typical 0.08”)	0.06” ~ 0.12” (typical 0.1”)	0.03” ~ 0.12” (typical 0.04”)	0.10” ~ 0.15” (typical 0.15”)	0.01” ~ 0.08” (typical 0.06”)
	Longitudinal Crack width (in)	-	-	-	0.01” ~ 0.08”	0.05”	0.06”
	Number of Punchouts / mile	0	0	10	0	0	0
ADT (2016)		37000	36400	67900	66300	21500	44600

Appendix H -- Forensic Investigation Procedures for GPR Evaluation of CRCPs

A. SCOPE

This test method describes the procedures for evaluating the performance of Continuously Reinforced Concrete Pavements (CRCPs) using the non-destructive test method – Ground Penetrating Radar (GPR). This document, together with the owner's manual and recommendations of the equipment manufacturers, delineates the procedures for the installation and calibration of equipment and the guidelines for conducting a proper survey of the pavement.

B. APPARATUS

The GPR technology is a non-destructive testing method used for structural assessment that allows for correlations between pavement distresses at certain locations with known pavement conditions. The GPR unit shall have hardware and software to create and store pavement information from each site. The methodology for collecting the required data from a site includes the following major components:

- An antenna having a capability of working with 1.5 GHz frequency for CRCP sections (TerraSIRch SIR System-3000)
- Pavement coring equipment
- Appropriate linear measuring devices and pavement marking instruments
- Manufacturer's instruction manual.

C. LIMITATIONS/RECOMMENDATIONS FOR SELECTING CRCP TEST SECTIONS

The CRCP sections under investigation shall be tested in 1.0mi (1.6km) lengths. Prior to conducting the GPR scanning of the pavement, at least one cored pavement specimen shall be taken from the start of the site section. The site section overall distance shall be divided into sub-segments as a function of cracking density and existence of other pavement distress

types such as punchouts. The sub-segments shall be tested as separate sections using the GPR over damaged and non-damaged areas in the transverse directions. In addition, the section from one sub-segment to the next sub-segment shall be examined using GPR in the longitudinal direction (traffic direction). The GPR scan in the longitudinal direction shall be performed on top of the wheel path. The GPR scan conducted in both longitudinal and transverse directions shall have the same alignment and remain linear from the beginning to ending points. Pavement profile shall not be surveyed when it is wet, as GPR equipment will yield inaccurate data under these conditions.

D. EQUIPMENT INSTALLATION PROCEDURE

1. Preliminary Preparations

   a) Prior to testing, the GPR unit's batteries must be fully charged with the antenna connected properly, and the main control unit checked.

   b) Unwanted items and metal pieces shall be removed from the pavement surface (if present).

   c) Establish all required preload setups including data collection parameters and filters the GPR unit. The steps for settings are as following:

      - Select the TerraSIRch Mode for the site investigation.
      - Select the frequency as 1.5/1.6 GHz antenna for concrete. Typical maximum depth scanned by GPR will be 1.5 ft. (50 cm).
      - Select the transmit rate (T_RATE) as 100 KHz.
      - Select the mode of distance-based data collection. This mode requires a survey wheel calibration which will be described in the next bullet.
      - Select 512 samples per scan for the use of 1.5 GHz frequency.

- Select 16- bits data format.
- Select 12-nS range for the recording of reflections from a single pulse.
- Select first the dielectric constant value as being between 5 and 8 for concrete materials. However, after calibration process of GPR, this value might change.
- Select the scan rate as 100 scans per second if the transmit rate is set to 100 KHz.
- Select the scan per unit of horizontal distance as 60 scans/foot or 5 scans/inch.
- Set the 2 gain points to neutralize effects of attenuation and make subtle sections more visible.
- Set the following filters to remove noise in the ground:
  - HP_IIR is set to 10 MHz.
  - LP_FIR is set to 3000 MHz.
  - HP_FIR is set to 250 MHz.

d) The survey wheel shall be calibrated to local conditions at each different site when distance-based data collection is used for testing. These steps should be followed:

- A measured line shall be prepared on the survey surface. A longer measured line will produce a more accurate survey wheel calibration.
- The calibrated distance taken from the measured line is entered into the GPR unit and the position of the antenna is set for the beginning of the line as front, center, or rear of the antenna.
- The antenna is moved along the length of the survey distance.
- Repeating this process several times and averaging of the results will produce a calibration of the survey wheel that will be more accurate.

2. Calibration Testing

a) Move GPR unit on the wheel path in the longitudinal direction to detect the location of transverse reinforcements.

b) Select one of the scanned transverse reinforcements on the GPR screen, move the GPR unit back over the selected reinforcement and mark the location of transverse reinforcement on the pavement.

c) Place the metal plate on the marked location of transverse reinforcement.

d) Move the GPR unit across the selected transverse reinforcement location again to confirm accuracy of the location of transverse reinforcement.

e) Scan the marked location in the transverse direction to detect the location of the longitudinal bars.

f) Select one of the scanned longitudinal reinforcements closest to the centerline of the lane and mark the location on the pavement. The depth value of the selected reinforcement shall be equal to or close to the depth taken from the construction drawings. The depth of longitudinal reinforcement shall be confirmed through destructive or non-destructive test methods.

g) If destructive methods of reinforcement depth confirmation are utilized, a core shall be taken at the marked location. If non-destructive methods of confirming the reinforcement depth are employed, the depth measurement shall be taken with a high degree of confidence.

h) The depth and size of longitudinal and transverse reinforcements and the layer thickness shall be confirmed and saved.

i) Move the GPR unit along the same transverse line from which the core was taken.

j) Calibrate the scanned depth value to the measured depth value on the GPR screen when you are on the selected location.

k) Save the new calibrated depth value, noting that the dielectric value might change from the previously entered value depending on the concrete material and depth calibration.

l) Save the new dielectric value and begin the site investigation.

E. SITE INVESTIGATION PROCEDURE

1. Prepare the equipment and required items needed to be used on the site as stated in D.1.
2. Calibrate equipment based on the information taken from destructive or non-destructive methods as illustrated in D.2.
3. Collect data using GPR in the longitudinal and transverse directions from each sub-segment.
4. Identify the location of transverse cracks and whether they form at the location of the transverse reinforcements.
5. Examine pavement condition throughout the 1.0mi (1.6km) site survey in terms of cracks, punchouts, patched areas, material problems, etc.
6. Perform a minimum of three sub-segments to investigate the site in greater detail.
7. Record the data and externally save using a compatible storage system (i.e., portable storage media, memory card, etc.)

F. POST-PROCESSING PROCEDURE

The selection of proper software compatible with the GPR model shall be used for post-processing. If required, the data taken by GPR may be calibrated with the software using the

location of the core secured from the site or from non-destructive testing. After calibration, reinforcement depths and other pavement characteristics shall be analyzed and interpreted.

G. CALCULATIONS

No calculations are required for this test.

H. REPORT

Report the summarized data and results obtained from a site investigation.

Appendix I - GDT

GDT for evaluating rebar depth/spacing/location and pavement layer thickness using a ground penetrating radar (GPR) device

A. Scope

For a complete list of GDTs, see the Table of Contents.

Use Method A to determine depth, location, and/or spacing of steel reinforcement in concrete pavements.

Use Method B to determine thickness of concrete pavement and sub-base layers.

Use Method C to determine thickness of asphalt concrete pavement and sub-base layers.

B. Apparatus

The apparatus consists of the following:

1. Ground Penetrating Radar (GPR) Device
2. GPR Manufacturer's Instruction Manual
3. Post-processing Software License and User's Guide

C. GPR Settings

Select parameters and preload setups recommended in the Manufacturer's Instruction Manual accompanying the unit. If a manual entry is required, the following parameter settings are recommended as a starting point for calibration:

> Note: An accurate estimation of dielectric values plays a key role in successful GPR data collection and processing. Furthermore, the ability of GPR to penetrate pavement layers depends on the frequency of the radar, which must be selected according to the Manufacturer's Instruction Manual.

1. Method A and Method B: Reinforcement Depth and Concrete Pavement Layer Thickness

a. Dielectric constant: 5-8 (for concrete)

b. Antenna frequency: 1-2 GHz

c. Transmit rate: 100 KHz

d. Sampling rate: 60 scans per foot (or 100 scans per second)

2. Method C: Asphalt Concrete Pavement Layer Thickness

a. Dielectric constant: 3-5 (for asphalt concrete)

b. Antenna frequency: 900 MHz

c. Transmit rate: 100 KHz

d. Sampling rate: 30 scans per foot (or 50 scans per second)

Note: Lower frequencies ranging between 100 MHz and 400 MHz are recommended to accurately measure the thickness of base/subbase layers. Approximately 15 scans per second are recommended for lower frequency antennas.

D. GPR Calibration

The survey (or travel) distance and rebar depth/pavement layer thickness must be calibrated in accordance with the Manufacturer's Instruction Manual. The calibration process involves comparing field readings against known standards to the nearest 0.06in (2mm).

1. Distance

The survey distance shall be calibrated based on the Manufacturer's Instruction Manual. A tape measure or a ruler should be used to establish the known distance.

2. Depth/Thickness

a. Method A: Calibrate the scanned depth using the procedures in the Manufacturer's Instruction Manual. The known standard depth is measured from a core. Alternatively, it

is determined by a rebar cover meter (e.g., profometer or pachometer).

b. Method B: Calibrate the thickness of concrete pavement and subbase layers. The known standard thickness is measured by taking a 4.00in (102mm) or 6.00in (152mm) diameter concrete pavement specimen with a drill core sample.

c. Method C: Calibrate the thickness of asphalt concrete pavement. The known standard thickness is measured by taking a 4.00in (102mm) or 6.00in (152mm) diameter asphalt pavement specimen with a drill core sample.

Note: The success of GPR calibration/operation depends on the operator's knowledge of which GPR device he/she is operating and background knowledge of the technology. GPR uses high-frequency radio waves and operates by transmitting pulses of electromagnetic energy into the pavement layers using an antenna or multiple antennas attached to a GPR device. These pulses are reflected back to the antenna with time and amplitude which is correlated to dielectric discontinuities in the pavement materials such as reinforcing steel, air, concrete, soil, and asphalt concrete. The reflection is recorded to form a series of pulses or the radar signal. The signal contains a record of the thicknesses of layers within a pavement section.

E. GPR Operation

Note: GPR data shall be collected when the pavement surface is NOT wet or moist. The data collection must be conducted within the recommended operating temperature in the Manufacturer's Instruction Manual.

1. To operate the GPR unit, follow the procedures shown in the Manufacturer's Instruction Manual accompanying the unit.

2. Move the GPR unit on the wheel path in the longitudinal (or traffic) direction.

Note: Continuous data collection over a 1.0mi (1.6km) pavement segment is highly recommended for detection of thickness variation over distance and transverse rebar spacing/depth/location.

3. Collect data using the GPR unit in the longitudinal (or traffic) direction along the center line of a lane.

4. Collect data using the GPR unit in the transverse (or perpendicular to traffic) direction.

Note: More than 3 transverse-direction scans are recommended over areas with and without distress to review cross-sectional profiles and measure longitudinal rebar spacing/depth/location.

5. Save the collected data.

F. Post-processing of Scanned Data

A post-processing software program compatible with the stored file format shall be used. Simple basic post-processing steps which are recommended in the post-processing software user's guide should be applied to the collected dataset. Basic data processing should leave the original dataset intact such that it does not distort the information. It should be recognized that excessive filtering could drastically alter the overall dataset. Basic data processing generally involves the following three steps:

1. Define the pavement surface level

2. Apply background removal filtering

3. Generate a radargram or a display of the processed data.

G. Interpretation of Radargrams

When using a GPR unit, radiowaves are sent into the ground and are reflected by buried objects below the ground. A receiver antenna detects and records the time taken for signals to be reflected back to the surface, which can then be used to determine the depth to the reflective object.

The radargram is a measure of the reflection amplitudes and the travel time that the reflections take. It represents a surveyed length along the x-axis, and the y-axis representing depth. Such data display is central to data processing that closely approximates an image of the subsurface including anomalies and discontinuities in their proper spatial positions. The three types of radargrams (or displays of the GRP data) include:

a. one-dimensional trace

b. two-dimensional cross-sectional images

c. three-dimensional topographic display

A one-dimensional trace does not have very much importance until several traces are placed side-by-side to produce a 2-D cross-sectional image, or placed in a 3-D view. The following procedure shall be used to interpret a 2D radargram (with a surveyed length along the x-axis and the depth in the y-axis):

1. Method A: A peak hyperbolic amplitude coincides with the GPR measurement directly above each reinforcing bar (or dowel) in reinforced concrete (or jointed plain) pavement sections. Rebar spacing is determined by evaluating the distance between peak hyperbolic reflections. The rebar depth is measured from the pavement surface to the peak hyperbolic reflection(s).

2. Method B and Method C: The thickness of pavement and subbase layers shall be determined at various locations along the surveyed length of road. For a successful interpretation of radargrams, it is important to recognize that the reflection signal of air gaps between pavement and sub-base layers is significantly different from that of standard pavement and sub-base material layers. Such sub-vertical discontinuities in GRP reflection is captured in a radargram in order to determine the thickness of each layer in a pavement section.

H. Calculations

No calculations are required for this test.

I. Report

Report a radargram (or 1D oscilloscopes, 2D cross-sectional displays, and/or 3D topographic plots of the processed data) and record the reinforcement location/depth/spacing and pavement/sub-base layer thickness obtained from Section G.